A metabolomics investigation of a nanogold drug vehicle on experimental animals

S Bartlett

orcid.org 0000-0002-8426-0832

Dissertation submitted in fulfilment of the requirements for the degree *Masters of Science in Biochemistry* at the North-West University

Supervisor:	Dr JZ Lindeque
Co-supervisor:	Prof CJ Reinecke
Assistant supervisor:	Prof AF Grobler

Graduation May 2019
21077258

Acknowledgements

First and foremost, all praise is directed towards my Heavenly Father God. All I am privileged to experience in this life is through His grace and perfect love. Almighty God – it is only because of You and for You.

Gratitude beyond words for my family and friends, who have encouraged and offered support before I could even ask for it. To my parents and all my insane, intolerable and yet incredible siblings whose prayers have carried me through. A special thank you to Henrietta Victor – the best mother and woman to have ever lived!

Heartfelt gratitude towards my leaders and my mentors, without whom this document would have surely never seen the light!

- Dr Zander Lindeque – insightful and brilliant. There is never a time when you don`t have a solution to an obstacle. Thank you for offering up your time whenever I come knocking. The amount of work, knowledge and guidance you have provided is invaluable. I was fortunate to have you as my main supervisor
- Prof Carools Reinecke – excellent academic. Thank you for guiding this project into existence and acquiring funding and expert advice whenever it was needed. If not for you – I may not even have continued on with a MSc degree and I owe you for that. That one phone call changed the course I was on and I am very thankful.
- Prof Anne Grobler – a phenomenal woman of science! I appreciate all the effort put in and all the resources made available to me by you.
- I`d like to acknowledge that this project was birthed as a joint initiative of the DST Preclinical platform and the national (TIA) metabolomics platform, which unlocked many opportunities and possibilities.
- Last, but surely not least, sincere gratitude towards Professor Lodewyk Jacobus (Japie) Mienie, who is not only an outstanding biochemist but an excellent mentor in all aspects of life. Furthermore, providing many of the original images in this document. Thank you to both you and your beautiful wife Ansie – you know how much you are appreciated.

I`d like to acknowledge the Centre for Human Metabolomics (CHM), for assisting in my professional upbringing, being the place where I was introduced to metabolomics and all the gadgets that go with it. Also thankful for the use of instrumentation and the knowledgeable staff who were always willing to lend a hand. To my former colleagues at PLIEM and NBS – I have learned a great deal of being an analyst committed to precision and quality from all of you. You remain my friends always.

To Mrs M van Reenen – thankful for the assistance and advice in the bio statistical analysis of the data. You greatly aided in reliable results.

(This study forms part of another research project for which a PhD was awarded to Dr Clinton Rambanapasi at the Faculty of Health Sciences, North West University (PhD thesis titled: *An assessment of the biodistribution, biopersistence and toxicity of gold nanoparticles)*.

There were some collaboration with Dr Rambanapasi in various ways, which included employing the same group of rats for our respective studies, thus minimising the amount of rats used to comply with ethics.

Dr Clinton Rambanapasi – it was a privilege to work together with the commencement of this project. Thank you for the synthesis of the nanogold particles and your collaboration on this project overall. I believe your future endeavours will be truly blessed.

To the knowledgeable staff at the NWU-Vivarium – I give thanks and credit for the exceptional housing and care of the experimental animals.

Herewith also an acknowledgement to the National Research Foundation (NRF), an establishment that recognises potential and ensures the growth thereof, to not only benefit the country but the scientific community as a whole. I am full of gratitude for the great financial aid I have received to be able to complete this study (Grant no: 89748).

"Gold is a treasure and one who possesses it, would succeed in helping souls into paradise…"

-Christopher Columbus-

"There is gold, and an abundance of jewels;

But the lips of knowledge are a more precious thing."

-Proverbs 20:15-

Abstract

Nanotechnology has increasingly received attention the last few decades and the term refers to the categories of applied science and technology, where the combining key subject is the study of matter in scales of 1 to 100 nm and the designing of devices within that size range. Gold nanoparticles have especially drawn massive scientific attention; the reasons being that these particles exhibit high chemical stability and unique optical properties. Furthermore, gold nanoparticles can be easily synthesised and modified, while providing great potential for a drug delivery vehicle. There is however a gap in current research with regards to the safety and effect of these particles, especially in the field of metabolomics. This study thus aimed to provide a more comprehensive view of the effect of gold nanoparticles on the metabolome, by implementing an animal model. Two groups of Sprague-Dawley rats were monitored: one control group and one treatment group. The control group received a 0.9% saline solution and the treatment group received a solution of gold nanoparticles dispersed in citrate (90µg/500µl). Urine was collected at different time points over the course of 48 hours. The study utilised three different, but effective, platforms popular within the field of metabolomics, namely 1-dimensional Nuclear Magnetic Resonance (^{1}H-NMR) spectroscopy, Liquid Chromatography Mass Spectrometry and Gas-chromatography Time-Of-Flight Mass Spectrometry (GC-TOF/MS). Urine samples were analysed via these platforms using both untargeted and targeted metabolomics approaches, investigating an array of metabolites (including amino acids, acylcarnitines and organic acids). The data was subjected to bio-statistical analysis to identify the relevant changes in metabolite levels and produce a full list of significant compounds affected by the intervention of gold nanoparticles. The significant metabolites brought forth evidence of possible perturbation within the pathways of energy metabolism as well as carbon- and amino acid metabolism. The results were found to produce a similar profile to that of many heavy metals, in the sense that binding with sulphur-containing molecules occurred readily and consequently inhibiting the function of several proteins and enzymes. The most prominent findings were linked to the enzyme dehydrogenase family and the thiol-rich compounds of the amino acid pathways, which are often associated with a phenotype similar to heavy metal poisoning. Therefore, it is reasoned as is in the case of other heavy metals, that gold (even in nanoform) possesses a high affinity for sulphur-containing compounds and will promptly replace these bonds, by displacing the original ion.

***Key terms**: Gold nanoparticles, drug delivery vehicle, metabolomics, Nuclear Magnetic Resonance (^{1}H-NMR) spectroscopy, Liquid Chromatography Mass Spectrometry and Gas-chromatography Time-Of-Flight Mass Spectrometry (GC-TOF/MS*

Table of contents

Lists:

List of figures

List of tables

List of equations:

List of abbreviations

α–KGDH	alpha ketoglutarate dehydrogenase
µl	Microliter(s)
2-OH-isovaleric acid	2-hydroxy-isovaleric acid
AdoHcy	S-adenosylhomocysteine
AdoMet	S-adenosylmethionine
ANOVA	Analysis of Variance
ATP	Adenosine Triphosphate
Au	Symbol for element Gold
Aβ	Amyloid Beta
BCAA	Branched Chain Amino Acid
BCKD	αlpha-Ketoacid dehydrogenase
BHMT	Betaine homocysteine methyltransferase
BSTFA	N,O bis(trimethylsilyl) trifluoroacetamide
Caco-2	Human colorectal adenocarcinoma cells that differentiate
CBS	Cystathionine β- synthase
CID	Collision Induced Dissociation
CO_2	Carbon dioxide
CoA	Coenzyme A
CTH	Cystathionine deficiency
D	Effect size
DLS	Dynamic Light Scattering
DMSA	Dimercaptosuccinic acid
DNA	Deoxyribonucleic acid
EI	Electron Impact
ESI	Electronspray Ionisation
FASII	Fatty Acid Synthesis type II
FC	Fractional Concentration
FDA	Food and Drug Administration
FDR	False Detection Rate
GABA	Gamma Amino Butyric Acid
GC/MS	Gas Chromatography Mass Spectrometry
GC-FID/MS	Gas Chromatography Mass Spectrometry coupled with a Flame Ionisation Detector
GC-TOF/MS	Gas Chromatography Time-of-Flight Mass Spectrometry
GLY	Glycine
GNMT	Glycine N-methyltransferase
GNPs	Gold Nanoparticles
GSH	Glutathione synthesis
H_2O_2	Hydrogen peroxide
$HAuCl_4$	Chloroauric acid
Hcy	Homocysteine
HO	Hydroxyl radical
HPLC	High Pressure Liquid Chromatography
Hz	Hertz
IS	Internal Standard
LC/MS	Liquid Chromatography Mass Spectrometry
LC-MS/MS	Liquid Chromatography Tandem Mass Spectrometry
LC-QQQ/MS	Liquid Chromatography Triple Quadrupole Mass Spectrometry
LSPR	Localised Surface Plasmon Resonance
m/z	mass-to-charge ratio
MAT	Methionine adenosyltransferase
miRNAs	MicroRNA
ML	MicroLab

List of abbreviations (continued)

MOX	Methoxyamine hydrochloride
MRC-5	Medical Research Council cell train 5
MRM	Multiple Reaction Monitoring
MS	Mass Spectrometry
MSTUS	MS Total Useful Signal
MSUD	Maple Syrup Urinary Disease
MTHFR	Methyltetrahydrofolate reductase
MTs	Methyltransferase
N	Normal concentration / Normality
$Na_3C_6H_5O_7$	Sodium Citrate
$NaBH_4$	Sodium borohydride
NADPH	Nicotinamide Adenine Dinucleotide Phosphate Hydrogen
NH_4	Ammonium
NISTII	Compound Library
NKCT1	Protein toxin from Indian Cobra Venom
NMR	Nuclear Magnetic Resonance
NTNU	Norwegian University of Science
O^{2-}	Superoxide radical
PEG	Poly (ethanolglycol)
ppm	parts per million
psi	Pressure per Square Inch
QC	Quality Control
RA	Rheumatoid Arthritis
RNA	Ribonucleic acid
ROS	Reactive Oxygen Species
rpm	revolutions per minute
SAH	S-adenosylhomocysteine
SAHH	S-adenosylhomocysteine hydrolase deficiency
SAMe	S-adenosylmethionine
SD	Sprague Dawley
SER	Serine
SHMT	Serine hydroxymethyltransferase
S-MTHF	Methyltetrahydrofolate
TCZ	Tocilizumab
TEM	Transmission Electron Microscopy
TMCS	Trimethylsilyl chlorosilane
TOAB	Tetraoctylammoniumbromide
TUS	Total Useful Signal
TXI	Triple resonance inverse
UPLC	Ultra Performance Liquid Chromatography
UV/Vis	Ultraviolet-Visible Spectroscopy
V	Volts

Chapter 1: Introduction

Nanoparticle-technology has been considered a “hot topic” in recent years, in many different fields of science. Gold nanoparticles (GNPs) or nanogold particles, often referred to as simply “nanogold”, have been of interest especially in the healthcare industry as a possible platform for drug delivery. There has been some light shed on the properties and consequently the almost endless possibility of applications of GNPs, but less so with regards to their safety. Nanogold has already been successfully implemented in therapies for various diseases, including Rheumatoid Arthritis (RA) and cancer. There are nanodrugs currently available that are FDA-approved (Pillay, 2014) and it is for this reason that nanomaterial safety is important within the researching community at this time. Existing literature with regards to this is not comprehensive and at times contradictory (Alkilany & Murphy, 2010).

Research regarding the effect of nanogold on the metabolism of living organisms is lacking and since the metabolome offers the closest relation to the phenotype (Bathe *et al.* 2014) it seems that a great need in the current literature will be met by launching a metabolic investigation on the overall effect of nanogold on the metabolism.

This study comprised of substantial analytical work and an in-depth analysis of the data obtained with the administration of nanogold to experimental animals. An international prize has been awarded for the presentation of this study in 2017 (See Annexure D).

Chapter 2 focuses on existing literature with regards to nanoparticle-technology, more specifically nanogold particles and their properties and role as a possible drug delivery tool. The chapter gives an overview of the principles of the methods and instrumentation used and elaborates on the study design. It also states clearly the aims and objectives of the study.

Chapter 3 comprises of all the methods and materials employed to achieve the aims. The chapter concludes with the statistical protocols that the data was subjected to.

Chapter 4 contains the data obtained from the analytical work discussed in chapter 3 and highlights the significant findings, followed by a full discussion of the effect on the metabolism.

Chapter 5 concludes the findings by summarising the overall effect of nanogold on the metabolism as found with this study and proceeds to generate a hypothesis. The chapter ends with a brief discussion on pitfalls of the study and the prospect of future studies.

Chapter 2: Literature Review

2.1 Nanoparticle-technology:

Nanoparticle-technology has rapidly become popular in the fields of chemistry, physics and biochemistry. The term nanotechnology refers to the categories of applied science and technology, where the combining key subject is the study of matter in scales of 1 to 100 nm and the designing of devices within that size range. Nanotechnology is often perceived as only an extension of existing sciences into the nanoform (Official website of the United States National Nanotechnology Initiative, accessed 2018). This new trend or interest in nanotechnology originated from a renewal in the field of colloidal science, along with a propagation of new analytical methods and instruments.

Nanoparticles (or nanoclusters or nanopowders) can be defined as particles "having one or more dimensions in the order of 100 nm or less" (Dreher, 2004). Nanoparticles have quite a long history, despite the general idea being that they are a discovery of the modern age. The use of these fine particles date back to as far as the 9th century, when they were used by the artisans in Mesopotamia to produce the gleaming effect on pots. Even today, pottery recovered from the Middle Ages possess an unequivocal gold or copper glaze (Vithya *et al.* 2011).

Nanogold particles have especially drawn massive scientific attention, the reasons being that these particles exhibit a potential for high chemical stability and unique optical properties (Khan *et al.* 2017). Nanogold particles can be synthesised with ease, which makes it even more appealing to use for various applications, namely chemical sensing, biological imaging, and drug delivery (Yeh *et al.* 2011). Furthermore, it was believed that the element gold is not metabolised by the body and has even been a part of culinary treats for the wealthy for decades. This could have birthed the concept of a gold vehicle, which could potentially then serve as a carrier for drugs to a target site (Dreaden *et al.* 2012). Compounds containing gold have been used effectively in medical areas as anti-inflammatory agents in the treatment of rheumatoid arthritis such as the medicines Aurofin® and Tauredon® (Mascarenhas *et al.* 1972). Nanogold particles are making headlines with recent advances in the detection and treatment of cancer, since nanoscale gold particles exhibit a great possibility to act as photothermal therapy agents (Huang et.al; 2010). Even though bulk gold is generally accepted to be chemically inert and harmless, it should be noted that nanogold deviates from bulk gold almost in every aspect but chemical makeup. Thus, knowing that bulk materials differ from their nanoforms, it can be expected that nanogold particles display a degree of toxicity, even though gold at a larger scale is viewed as "safe".

2.2 Properties of nanogold:

There are several differences between bulk gold and gold particles at nanoscale, of which the most notable is the different colours. Nanogold mixtures consisting of sub-20nm particles are usually red or pink when in solution. The colour of the particles may also appear blue, green or brown as their size change (Yeh *et.al*; 2012). As the size decreases to nanoscope, the properties of the material change leading to a different physical appearance. The colours emerge as a consequence of conduction band electrons in the metallic structure that interact with the electric field vector of the incident light (Koole *et al.* 2014).

Seeing the link between colour and size, it is thus possible to determine the size of these metallic nanoparticles with spectrophotometry. Moreover, spectrophotometers can be used to hint toward the structure and scattering patterns of nanoparticles (Tomaszewska *et al.* 2013). Nanoparticles with diameter between 1-100 nm possess a unique optical absorption that correlates to the oscillation of surface electrons, called the Localised Surface Plasmon Resonance (LSPR). LSPR is by definition resonant oscillation of conduction electrons at an interface between negative and positive permittivity material submitted by incident light (Yeh et.al; 2008). This is the foundation for common tools that measure adsorption of material onto planar metal surfaces (gold/silver) or evidently the surfaces of metal nanoparticles. The reactive surface of nanogold makes it applicable for *in vivo* molecular imaging (Sperling *et al.* 2008). With this reactive surface, these particles also possess an affinity towards ligands, which bind to the surface of nanogold particles and alter the chemical properties thereof. This event is one of the reasons why nanogold particles act as a delivery vehicle in many pharmaceutical applications so efficiently.

It is evident that a large variance in physicochemical properties of these particles can occur and is therefore essential that particles are sufficiently characterised. Characterisation is traditionally done by UV/Vis spectrometry, transmission electron microscopy (TEM) and dynamic light scattering (DLS) (Lindeque *et al.* 2018).

2.3 Application of nanotechnology in drug delivery:

Drug delivery refers to the manner or process in which a pharmaceutical substance is administered into an organism to obtain a therapeutic effect or relief (Tiwari *et al.* 2012). Traditionally the drug delivery system supports the adsorption of the respective drug across a biological membrane. Examples of the conventional methods include oral ingestion or intravascular injection, where the medicine is distributed throughout the body via systemic blood circulation. Difficulties arose with this, due to the fact that only a small percentage of the drug reaches the affected organ. Consequently, the researching community started to address this problem by finding ways to target the specific areas that need treatment. Targeted delivery seeks to focus the therapeutic agents in the tissues of interest, while lowering the amount of the drug in other areas of the body. In other words, “targeted delivery” encompasses delivery of medication to a patient in a way that elevates the concentration of the drug in certain parts of the body relative to others. It is also known as “smart drug delivery” (Lui *et al.* 2016). This relatively new way of thinking regarding drug delivery platforms aims for a prolonged, localised, targeted and protected drug interaction with diseased tissue. The advantages of targeted drug delivery are decreased frequency of doses, less side-effects and lower fluctuation in circulating drug levels. The use of nanoparticles as a method of drug delivery is becoming notable seeing that their characteristic physicochemical properties allow them to be promising platforms for this (Yeh *et al.* 2012).

Nano-enabled drug delivery systems contain qualities that may increase solubility and improve biodistribution of drugs. There are a number of properties that allow the nanoparticle to be a potentially successful drug delivery tool in various biomedical and industrial applications. One particular quality is their impressive surface to volume ratio. This, together with its optical properties (e.g. fluorescence) becomes a function of the particle width (Huang *et al.* 2010).

The size of the nanoparticle is the main property that can potentially enable it to pass through the biological barriers in the human body. It may even open the possibility of delivering drugs across the blood brain barrier, being then an effective tool for neurological treatment (Saraiva *et al.* 2016).

Various substances have been explored to coat (functionalise) nanoparticles, these include albumin, gelatine, phospholipids and different polymers of a more chemical disposition. It is apparent in these studies that there is a correlation between the interaction with cells and possible toxicity and the actual composition of the nanoparticle formulation (De Jong *et al.* 2008). The motivation for researching nanotechnology with the goal of applying it to medicine stem from the considerable improvement in different fields it would lead to.

The general aim in researching nanotechnology is to eventually obtain more specific targeting, biocompatibility and the faster development of new treatments. In order to achieve this, the main focus point today is to ensure minimisation of toxicity, while preserving the remedial properties.

One of the greatest reasons for use of nanogold in drug delivery is the probability of medicine attached to the molecule, being metabolised slower and consequently having an extended lifetime within the body, thus increasing the efficacy of the remedial consequence. However, the threat exists that any molecule attached to the nanoparticle could be displaced almost immediately when administered due to the higher affinity of other compounds, such as thiols (Gao *et al.* 2012) toward the particles, and this should be investigated.

Nanogold vehicles, if found to be harmless enough, could play an extraordinary therapeutic role in many diseases, of which the following section showcases popular examples.

2.3.1 Nanogold as part of the treatment to combat cancer:

i) Nanogold affects the protein form

Different proteins recognise different cells and this causes a dilemma in today's cancer treatments. Healthy cells are similar to cancer cells and consequently destroyed by chemotherapy, due to the fact that the protein/drug cannot distinguish between healthy and cancerous cells.

However, the surrounding area of a cancer cell is slightly more acidic and these cells tend to be more permeable, thus if a protein could be altered using nanogold particles, in such a way that it recognises cancer, based on these properties, medicine would then be able to only target sick cells. This will by all accounts be a tremendous breakthrough in cancer treatment, with chemotherapy being delivered to the cancerous cells alone (Jain *et al.* 2012). A patient's normal cells would stay intact to further combat symptoms and have an overall better prognosis.

ii) Gold particles can act as light-activated heaters which can highlight cancer and aid in the destruction of the cells:

The work of Professor Mostafa El-Sayed (Georgia Tech School for Chemistry and Biochemistry) has provided great insight into the early detection and improved treatment of all types of cancer (Huang and El-Sayed, 2010). In his research, existing and new theories, regarding how nanogold structures react with light, were put to the test. With the use of dark-field imaging, an illuminating distinction could be made between cancerous and normal cells, through antibodies clinging to the abnormal cell surfaces and the scattering of light emanating from the gold particles. Additionally, during these experiments, it was discovered that the metal properties of the nanoparticles enable them to serve as light-activated heaters, which were utilised for destruction of these cells. This was done, by aiming lasers of visible light at the cells and destroying the cancer selectively, with significantly less force and intensity, than traditional treatment procedures (El-Sayed *et al.* 2008).

In photodynamic cancer therapy, light-excitable photosensitisers are used to increase energy in the oxygen molecules in surrounding tissue, which in turn leads to higher levels of reactive oxygen species (ROS). ROS is directly related to the aging and death of nearby cells. Thus, in this event will be responsible for the necrosis and apoptosis of cancerous cells.

Nanogold promote special ways of killing tumours (Kodiha *et al.* 2015). They can cause cell death not only by their association with ROS, but also by photo thermal ablation and mechanical damage, along with optimal concentration of localised medication (drug delivery).

2.3.2 Gold as treatment for Alzheimer's disease:

Professor Wilhelm Glomm (Ugelstad Laboratory at the NTNU) has stated that the proteins in Alzheimer-patients (specifically amyloid-βeta or *Aβ* protein) tend to cling together to form plaque, which leads to decreased signal transmission from the brain. A study at NTNU was thus aimed at creating tiny clusters of gold inside the proteins, which will result in proteins spreading out and refolding themselves (Lystvet, 2013). The protein can be manipulated in such a way that it dissolves the plaque and removes it from the body. Individually the protein is not harmful and theoretically the nanogold particles are not toxic, but there is a lack in knowledge about the potentially harmful effects that may occur when you combine them.

A study published in *Nanoletters* by Kogan et.al. (2006) dealt with functionalised gold particles that selectively attached to the *Aβ* protein and after being exposed to radiation, decimated the aggregate.

2.3.3 Gold nanoparticles as treatment for Rheumatoid Arthritis:

Gold nanoparticles have successfully been implemented in treating Rheumatoid Arthritis (RA) by (Lee *et al.* 2014) by forming a nanogold-TCZ complex. This complex is formed with both hyaluronate and tocilizumab (TCZ). Interleukin-6 is involved in the pathogenesis of RA and TCZ is an immunosuppressive drug that inhibits the interleukin-6 receptor. Therefore by binding TCZ and hyaluronate, a very powerful complex emerges which protects the cartilages against the damage from the arthritic disease, thanks to the lubricant effects of the hyaluronate. In combination with the properties from the nanoparticles, this complex is stable and directed to become an efficient delivery tool for the treatment and relief of RA.

2.3.4. Previous findings surrounding gold nanoparticle-safety and metabolomics:

Many of the literature involving the use of nanogold point to successful outcomes and emphasise the treatment delivery potential thereof, however as Gerber *et al.* (2013) states: “But in contrast to the multitude of studies that addressed the clinical use of gold nanoparticles, only little is known about the potential toxicological effects such as induction of inflammatory immune responses, possible apoptotic cell death or developmental growth inhibition in embryos.”.

That said, it is not difficult to find studies focusing on the toxicological properties of nanogold, which put a large question mark next to the use of nanogold in therapy.

It was seen that nanogold exerts toxic effects in MRC-5 lung fibroblasts related to oxidative damage (despite up regulated antioxidants and stress responses) (Li *et al.* 2010). In a more recent study where the reaction to nanogold by Caco-2 cells was researched, with regards to cellular uptake, RNA expression and cytotoxicity, the only positive finding was the increase in glutathione metabolism. This was concluded to be due to the metal binding that occurs. It was established that high concentrations of nanogold (of the smaller scale, such as 5 nm gold nanoparticles) would cause differences in the levels of metals and selenium and also then lead to the activation of oxidative stress signalling pathways (Bajak *et al.* 2015).

In contrast, the effect of nanogold on microRNA (miRNAs) was studied and by Huang *et al*. (2015), who declared that no cytotoxicity was detected after treating the cells with nanogold for 1, 4 and 8 hours respectively. Albeit, they did add that many of the miRNAs were not expressed uniformly and the mitochondria and energy metabolism were affected (Huang *et al.* 2015). Toxic studies were also conducted and it was concluded that nanogold conjugation increased antiarthritic activity, along with reduction of NKCT1 toxicity.

Conde *et al.* (2014) evaluated gold nanoparticles for signs of genotoxicity and cell toxicity, via an “antisense nanogold beacon” with which the blocking gene expression of colorectal cancer was tested. The proteomic effects of this nanobeacon with regards to cancer cell exposure were also investigated and in both cases the authors found no noteworthy toxicity.

Choi *et al.* (2010), assessed the role of size and surface charge on gold nanoparticles by monitoring zebrafish embryos, which resulted in embryo deaths, due to apoptotic cell death directly linked to nanogold, along with other morphological effects such as extremely small and under pigmented eyes. A zebrafish model was also implemented by Troung *et al.* (2013) who confirmed the above findings by narrowing in on how surface functionalisation and charge of gold nanoparticles affect *in vivo* molecular responses.

Overall, all these authors concluded that surface functionalisation of nanogold affects the biological responses on the phenotype and on molecular level. Hence, the link between metabolic changes and particle morphology, size, charge and coating remain important gaps worth studying.

Studies surrounding protein and DNA with regards to nano safety have been explored to a considerable degree, yet the effects on the metabolome remain to be unclear and partially highlighted.

The following literature includes some studies done concerning metabolomics and gold nanoparticles:

Lasagne-Reeves *et al*. (2010) published results of renal toxicity in mice due to the grouping of nanogold in the kidneys. Creatinine and urea concentrations were determined, for these metabolites are normally associated with kidney function and renal failure. Unfortunately, no other metabolites were considered and thus, the study does not provide a comprehensive account of the effects of nanogold on the metabolome (Lasagne-Reeves *et al.* 2010). In the same year, Cho *et al.* reported that PEG-coated particles of sizes 4nm and 13nm were responsible for the activation of metabolic enzymes in the liver. The research did not include any detection of metabolites however. Furthermore in 2012 a paper was published by Wang *et al*. on the metabolic effect of 15 nm gold nanoparticles and the energy metabolism of Drosophila larvae. RNA and proteins were analysed to assess any change in lipid levels and concluded that lipid levels increased whilst stress response levels remained low (Wang *et al.* 2012).

Research was conducted on human skin after 24 hour therapy with nanogold of various sizes, ranging from 10 to 60 nm and no notable absorption was observed and consequently no change in NADPH levels of the epidermis (Liu *et al.* 2012).

Gioria *et al.* (2015) approached the assessment of nanogold effects from a combined proteomic and metabolomics perspective. The study involved exposing Caco-2-cells to 5 and 30nm particles respectively, which led to cell apoptosis. The study highlighted various affected biological pathways. The same metabolites were altered with exposure to both particle sizes, however the changes observed with the 5nm particles were more prominent. The highlighted pathways included amino acid metabolism (with significant metabolites: glycine, glutathione, L-leucine, L-isoleucine), carbohydrate metabolism (with elevated propionylcarnitine), glutamate metabolism (changes in carboxylic acid levels) and the electron transport chain (altered concentrations of beta-guanidinopropionic acid and trimethylamine-N-oxide), along with several disturbances within the proteome. The authors concluded that these perturbations at protein and metabolic level were due to intracellular accumulation of nanogold.

Lindeque *et al.* (2018) investigated the depletion of metabolites in HepG2 cells with nanogold treatment, where nanogold particles were capped with different coatings (namely citrate, poly-sodiumsterene sulfunate and poly-vinylpyrrolidone).

The study concluded that a strong possibility of metabolite binding to the nanoparticles exist, as an overall depletion of metabolites was observed regardless of particle coating.

The metabolic effects of three surface modified gold nanorods were analysed in cancer and non-cancer cells, by employing the metabolomic methods of Nuclear Magnetic Resonance (NMR) and Gas Chromatography Mass Spectrometry coupled with a Flame Ionisation Detector (GC-FID/MS). Cytotoxicity was observed with noticeable disruptions to the cell metabolisms, affecting the energy pathways, choline metabolism, hexosamine biosynthesis and also inducing oxidative stress.

2.4 Methods of synthesis of nanogold particles:

Few methods for the synthesis of nanoparticles exist and in this document only the two most relevant will be discussed.

2.4.1 The Turkevich-Frens method:

The Turkevich method is an endothermic process, also known as citrate reduction, for it involves the reduction of chloroauric acid ($HAuCl_4$), by the addition of sodium citrate ($Na_3C_6H_5O_7$) in water to reduce the Au^{3+}-ion (Turkevich *et al*., 1951). The citrate serves as the reducing agent, while coating the particle. The method was first published by J.Turkevich in 1951 and improved by G. Frens about two decades later. Frens refined the Turkevich method by concluding the relationship between concentration of sodium citrate and particle size (Frens, 1972).

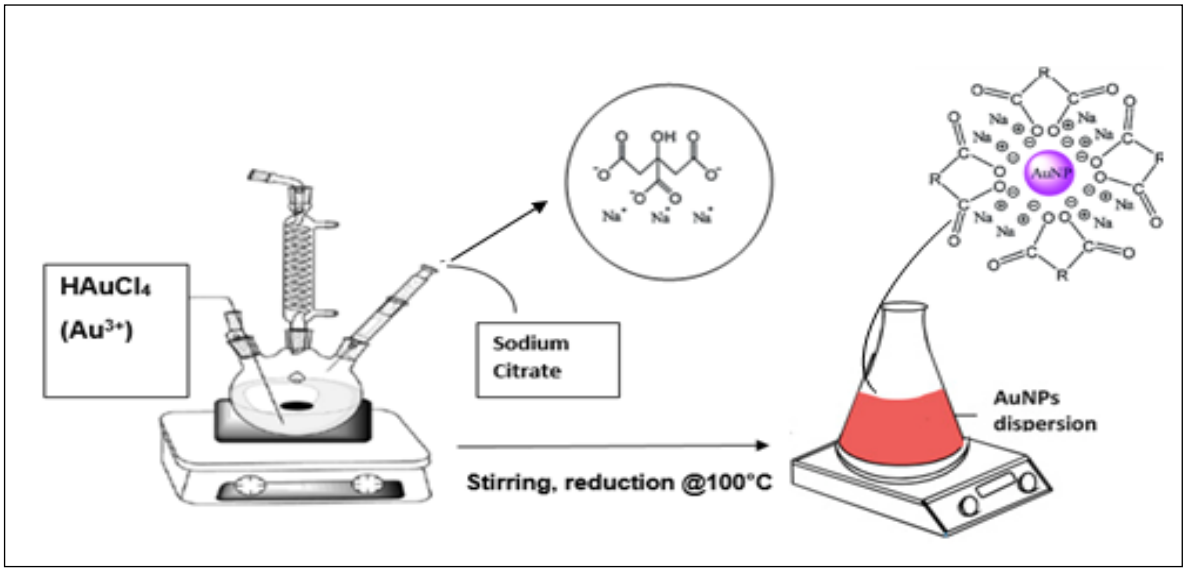

Figure 2.1: A depiction of the Turkevich-Frens method, also known as citrate reduction. This image was inspired by multiple sources: Herizchi *et al.* 2014, Imbraguglio *et al.* 2013 and Zhao *et al.* 2013

The concentration of sodium citrate is inversely proportional to the size of the particles, for instance if larger particles are required then a lower concentration of citrate should be used, in doing so smaller particles will aggregate into larger ones for there would be less reducing agent available.

It is important to synthesize nanoparticles of uniform size and shape, for different properties accompany the different sizes and forms of nanoparticles, which could therefore affect the biological system differently. To successfully achieve the correct size during synthesis, the basic principle of fractional concentration (FC) of citrate should be understood. With regards to citrate reduction, one can adjust the size of the forming nanoparticle by utilizing the ratio of the $HAuCl_4$ (aq) to the citrate (Brust *et al.* 1994).

The particular particle size and diameter of choice can be produced by calculating its corresponding FC of citrate, which is added during the synthesis. A negative linear relationship exists between the citrate`s fractional concentration and the size of the gold nanoparticle, as can be seen from the graph in Figure 2.3.

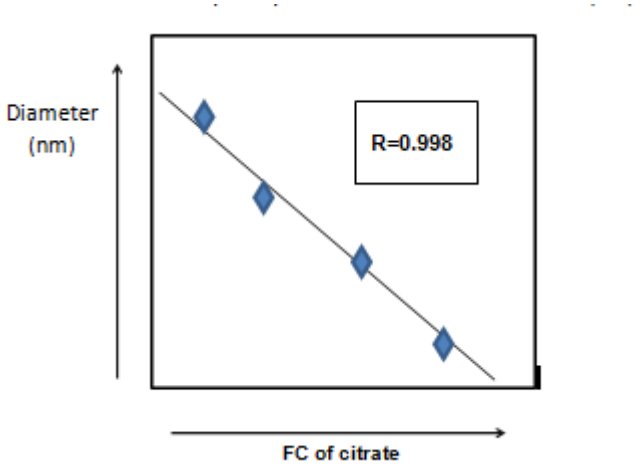

Figure 2.2: The diameter of the produced nanogold is dependent on the ratio between the $HAuCl_4$ and the amount of citrate added. Adapted from Gosh *et al.* 2011.

The equation below is used for the FC-calculation and makes use of the concentrations of the reducing agent and the reagent providing the Au-ion.

Equation 2.1: The fractional concentration (FC) is given by the relationship between the concentration of the citrate and the sum of concentrations of citrate and chloroauric acid.

$$Fractional\ concentration\ (FC)\ of\ citrate = \frac{[citrate]}{[citrate] + [HAuCl4]}$$

2.4.2 The Brust-Schiffrin method:

The Brust-Schiffrin synthesis requires two organic liquids, for instance water and toluene, which are not miscible. This involves the reaction of tetraoctylammonium bromide (TOAB) and chloroauric acid along with the immiscible organic solutions. Stirring these reagents rapidly forms an emulsion which is then reduced with sodium borohydride ($NaBH_4$) to form gold nanoparticles. The size of particles produced is naturally smaller due to the increased reducing ability of $NaBH_4$.

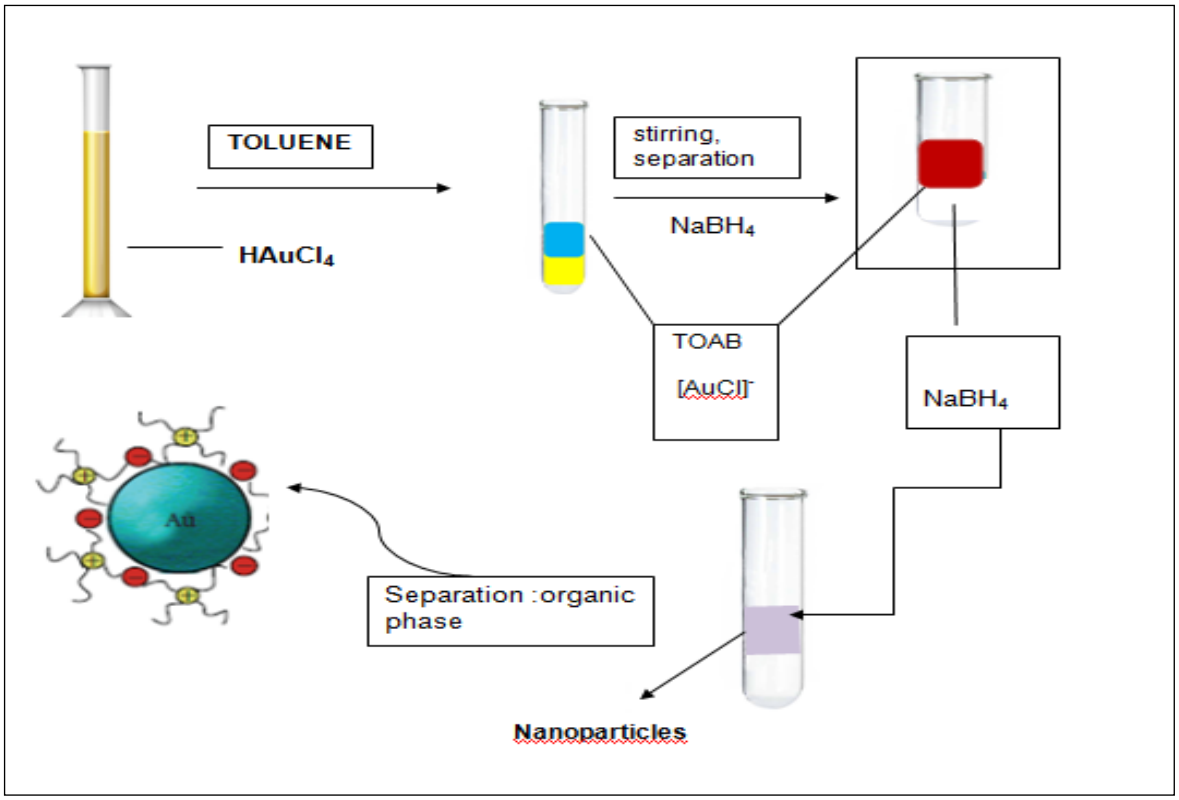

Figure 2.3: A depiction of the Brust-Schiffrin method, adapted from Calandra *et al.* 2010.

2.4.3 Separation as a means for sample clean up:

After synthesis and functionalisation of the gold nanoparticles, the suspension still contains large amounts of unreacted ligand (like citrate). It is therefore important to separate the particles from the unreacted reagents before using. In analysing the overall effect of any substance on a system, it is of the utmost importance to limit the variables, the external or environmental influences and any other factors that could produce insignificant findings.

To achieve a simplified, but significant conclusion it is necessary to perform separation techniques and sample clean up, to distinguish between toxic or non-toxic consequence due to nanogold and irrelevant or coincidental effects. Gold nanoparticles are separated based on size and morphology (Hanauer *et al.* 2007) and usually by centrifugation or gel electrophoresis.

i) Centrifugation:

To exclude particles of width that are not of interest, the solution can be centrifuged @ 2000 x g for 45 minutes. The pellet can then be resuspended in a buffer or deionised water, depending on the specific protocol for nanogold in the study.

A more complex type of centrifugation, namely the sucrose gradient centrifugation, is also used to successfully separate nanogold particles (Wilson and Walker, 2010) via a gradient of density and size. The larger and denser particles accumulate at the bottom of the tube.

ii) Gel electrophoresis:

Nanogold particles can be separated with gel electrophoresis, by coating the particles with appropriately charged polymers. The result is then confirmed with transmission electron microscopy (TEM). The advantage with gel electrophoresis is the ability to conduct multiple runs on one gel, thus being time and cost effective, in comparison to other separation methods including centrifugation, HPLC and size-exclusion chromatography (Hanauer *et al.* 2007).

2.5 Metabolomics:

“Metabolomics”, though the latest discipline in the world of “-omics”, is not a novel branch of science and is multidisciplinary whilst focusing on the coinciding systematic determination of metabolite levels in the metabolome and the correlating changes due to stimuli (Trivedi *et al.* 2017). The metabolome refers to the entire collection of metabolites - the small chemical intermediates and products of metabolism. Metabolites are the end products of processes within a biological system and their concentration is a direct indication of how the system reacts to any genetic or environmental changes. As proteins make up the proteome, so do a particular set of metabolites equal that metabolome.

The consequence of altering even a single gene within the system is not necessarily limited to one biochemical pathway. It is also possible that the metabolites belonging to one pathway be elevated when another seemingly related pathway has been altered.

This is due to pleiotropic effects. Therefore, a wide-ranging analysis of all metabolites is needed. Such an approach involves the identification and quantification of all the metabolites and thus, unveils the metabolome of the system of interest and is then by all accounts a metabolomics study. Metabolomics approaches utilise well designed sample preparation methods and analytical techniques to achieve non-exclusion of any metabolites and must also include plans to identify unfamiliar products.

The phenotype usually presents the first signs of perturbations and illness and is the reason why omics exist, the reason for investigations into metabolomics: for the metabolome gives “a snapshot of the functional phenotype of disease” (Bathe *et al.* 2014). Data from the metabolome characterised some of the metabolic perturbations that accompany certain disease, such as colorectal cancer.

The phenotype is capable of modifying the genotype and any consequential events. The figure below illustrates the relationship between the phenotype and the omics (See Figure 2.4)

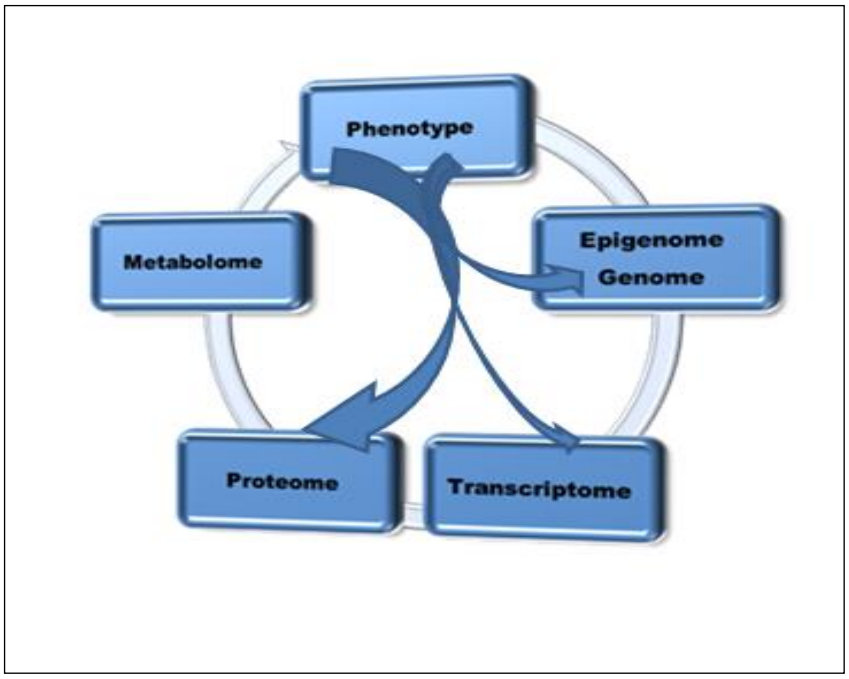

Figure 2.4 An illustration of how the phenotype links to the different disciplines in the omics. According to Bathe *et al.* 2014 the metabolome is the closest molecular representation to the functional phenotype. (Figure adapted from Bathe *et al.* 2014.)

Both the proteome and metabolome best reflect the phenotype, however though it is possible to measure the end products of the proteome, the measurement of specific protein function is made difficult by the presence of other proteins. It is not yet possible to measure every protein and fragments thereof and existing knowledge surrounding protein function is still catalectic. On these grounds, accurate conclusions in terms of the phenotype cannot be derived from the proteome alone.

According to Bathe *et al*. (2014), in the study of colorectal cancer, the most suitable reflection of the tumour phenotype, would be the metabolome.

All functions of biological nature within the body is dependent on metabolic function. Since nanogold particles have been gaining attention in various categories of the biological sciences, many studies have been centred on their cytotoxicity. Some of these studies indicate an effect of the particles on the biological system, but none have compiled a full metabolic profile or give extensive views on the metabolites that accumulate in either biofluids or tissues.

2.5.1 Metabolomics approaches:

Metabolic targeting equals the quantification of only a small number of known compounds, whereas profiling has to do with the quantification of most known metabolites under specific conditions. This combination of approaches of metabolomics analysis has proven to be a valid resource for researching and expanding the knowledge of the effects of various substances and pathogen-interaction on the phenotype. In other words, metabolomic analysis is the most promising and valid path to understanding metabolism and predicting novel pathways and in this case, understanding the metabolic pathway of nanogold.

There are usually two roads to follow when utilising metabolomics for any study, which is (i) an untargeted or (ii) a targeted approach (refer to Figure 2.5).

Untargeted metabolomics aims to comprehensively measure all the ions in a sample, including chemical unknowns, i.e. with this approach all metabolites within a certain mass range are registered.

On the other hand, targeted metabolomics deals with the measurement of only a small subset of defined and known metabolites, which have been previously characterised and annotated (Roberts *et al.* 2012). For generating a hypothesis an untargeted approach should be implemented, which requires instruments that are able to detect a great range of metabolites (like non-scanning time-of-flight instruments). Consequently, this approach renders an extensive dataset, which is then sorted via multivariate statistical processes. Targeted metabolomics is hypothesis-driven and focuses on the analysis of certain metabolites of interest, in order to test a hypothesis, elaborate on existing findings or establish a biomarker. For this approach less expensive instrumentation is sufficient, but sample preparation is more complex than that of an untargeted method.

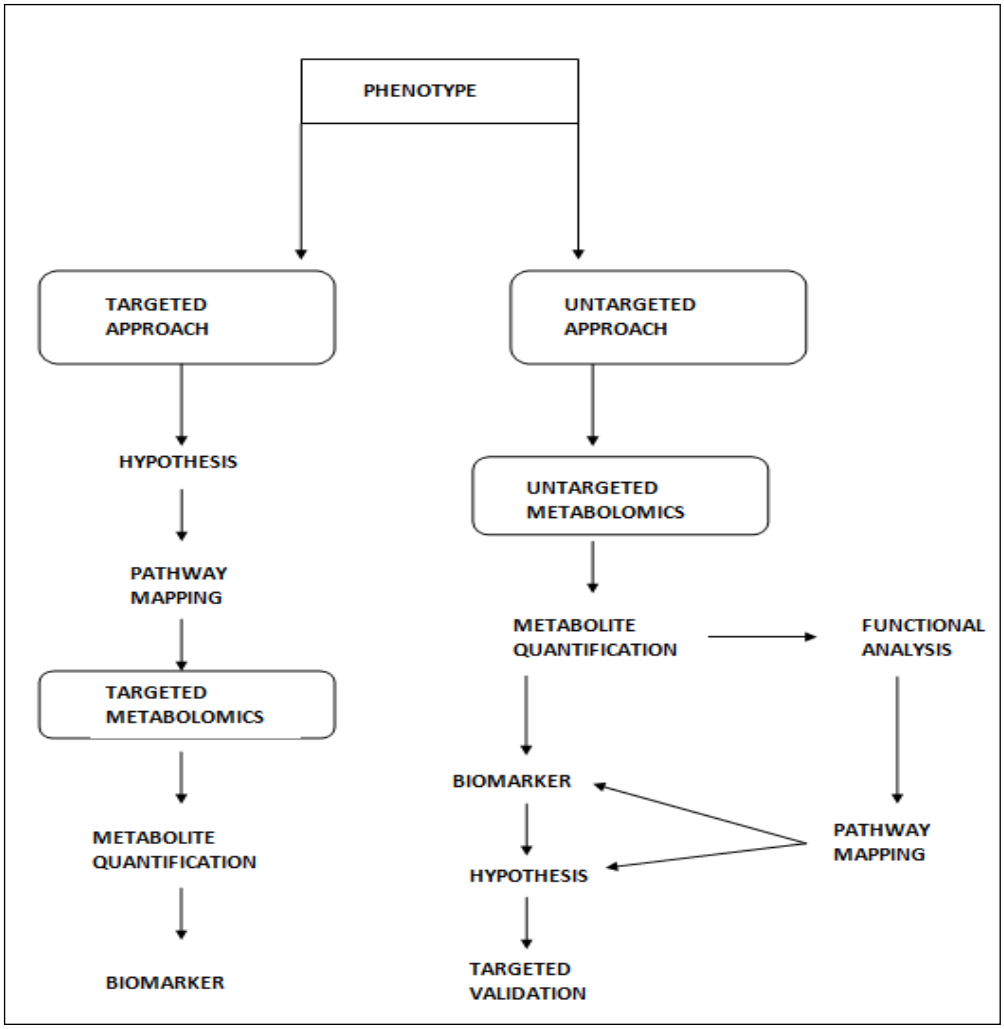

Figure 2.5: A schematic representation (adapted from: Dang *et al.* 2016) depicting the workflow of an untargeted approach versus that of a targeted design. Biomarkers are used to either confirm or generate a hypothesis.

2.5.2 Metabolomics tools (instrumentation):

The process of metabolic profiling encompasses the measurement of metabolites and their intermediates that mirror the responses to genetic alterations, pathophysiological and physiological changes and other stimuli (Clarke *et al.* 2008). The metabolite profile usually obtained from either urine, serum or biological tissue extract offers a platform to understand the metabolic phenotype, in that it accentuates potential biomarkers and mechanisms linked to toxicology and pathology. This was a key message in Clarke *et al*. (2008), where it was also stated that metabolomics in conjunction with other omics is the approach to be opted for when dealing with hindrances in preclinical drug development.

An all-inclusive spectrum of metabolites can be produced by the metabolic profiling “tools”, which are mainly nuclear magnetic resonance (NMR) and mass spectrometry (MS). According to Clarke *et al.* (2008), both approaches can be directed in such a manner that it generates an untargeted profile, however MS is better equipped for targeted profiling.

Ideally, MS is done along with NMR to optimise the level of identifying and quantifying as much of the metabolome as possible.

The metabolome can be investigated by means of Gas- and Liquid Chromatography coupled with Mass Spectrometry and NMR methods. Cajka *et al.* (2015) had done citation research and reported that Mass Spectrometry dominates in metabolomics studies compared to NMR in a ratio 5:2 in 2016. However, a more recent study (Bingol, 2018) reported great progress on NMR methods and specifically an increase in the popularity of the hybrid MS/NMR approach. At this time, there is no single analytical technique that is able to find all the metabolites within a sample, due to large diversity in chemical structures (Roessner *et al.* 2009) and since the different metabolites detected by one instrument is not necessarily detected by the other, these methods complement each other.

2.5.2.1 Gas Chromatography Mass Spectrometry (GC/MS):

This analytical technique as the name entails, requires the sample and the mobile phase to be gaseous. It is usually used when analysing less polar, volatile compounds (Agilent Technologies, 2014).

However, with the help of derivatisation agents, GC is also commonly used to analyse small polar compounds like organic -, amino - and fatty acids (commonly referred to as primary metabolites). An advantage of the GC/MS is that it effectively separates compounds of similar structure due to its high resolution separation. It is also fairly less expensive than LC/MS (Agilent, 2014), but it requires greater sample preparation. Overall, it remains one of the most useful methods to analyse metabolic variation and has been referenced countless times in the metabolomics literature.

2.5.2.2 Liquid Chromatography Mass Spectrometry (LC/MS):

LC/MS is ideally suited for non-volatile compounds (Agilent Technologies, 2014). A larger variety of biochemical compounds can be measured by LC/MS (such as complex sugars and amino acids) when switching between positive and negative ionisation, normal- and reverse phase chromatography, and different ionisation technologies. While LC-MS is very useful for untargeted analyses, it unfortunately comes with more post-analysis problems than GC-MS. The biggest pitfall in LC-MS metabolomics is the accurate identification of the detected compounds.

Unlike EI mass spectra, ESI or CID spectra are less reproducible, especially between instruments (Halket *et al.* 2004). For this reason, it appears that LC-MS is more often used in a targeted manner. Moreover, derivatisation is often necessary to aid in distinguishable retention times and fragmentation patterns; of which butylation is a popular method.

To obtain the most comprehensive detection of metabolites, it is best to combine GC-MS and LC-MS/MS. Organic acids are effectively quantified via GC-analysis, however LC-MS/MS can measure amino/nitrogen- containing compounds (acylcarnitines and amino acids) far better than GC/MS is able to. This was confirmed in a study by Kanani *et al.* (2008), when the researchers showed that analysis of amino-containing compounds with a GC/MS led to the distortion of final results. Thus, it is ideal to have a hybrid-approach and rather analyse amino acids and acylcarnitines with LC-MS/MS and then combine the profile gathered from the GC/MS analysis for a more complete view of the accumulated analytes.

2.5.2.3 Nuclear Magnetic Resonance (NMR) Spectroscopy:

In NMR spectroscopy, the proton spectrum of each sample is examined and structural information on analytes is easily acquired. It is an effective application in metabolomics with regards to cost and time, due to its less extensive sample preparation. The technique is able to detect hundreds of metabolites in various tissue and biofluids, but it is less sensitive than the classic chromatographic methods. The reason being difficulty with identification, due to the overlap of chemical shifts of metabolites (Schnackenberg *et al.* 2012). This complexity that occurs can be opposed to some extent by the standard data-handling software, with which parts of the spectrum is magnified and evaluated at a higher resolution (Clarke *et al.* 2008). The peak area is directly proportional to concentration and many other useful aspects of the sample can be rapidly determined with ease, such as the creatinine value of a urine sample.

As can be seen from Table 2.1, there are advantages and disadvantages to both the NMR and MS methods. The NMR does overall prove to be the most advantageous, with its non-destructive character, robustness and less straining sample preparation, but MS does however still consist of the more elaborate database, compared to those currently available for NMR and therefore the combination of the techniques is currently the best option to obtain the most comprehensive metabolic picture.

Table 2.1: Adapted from Weckwerth (2007). This table summarises the advantages and weaknesses of NMR and MS methods with regards to metabolomic profiling.

	MS	**NMR**
Detection limits	Picomolar	Low micromolar, nanomolar
Scope of metabolite detection	Possible problem with chromatographic separation, thus usually needs a more targeted approach, lack of ionisation, but ability to detect positive and negative ions-gives extra information.	If metabolite contains a hydrogen atom, it will be detected, unless concentration is very low and/or protein binding causes marked line broadening.
Sample handling	Whole sample analysed in one measurement.	Differs for each class of metabolite, usually extraction in a suitable solvent is necessary.
Sample volume	Low microliter range	200-400µl, but with microcoils = 5-10µl
Sample recovery	Destructive, but small sample volumes lost	Non-destructive
Sample preparation	Can be substantial	Minimal
Ease of molecular identification	Difficult, often only the molecular ion is available and extra experiment is required (routine tandem-MS), GC-MS has better retention times and a more thorough database	High, due to database and analysis of 1D and 2D spectra
Time of basic data collection	10 min (UPLC)	5min
Precision	5% intraday and interday is now common without prior chromatography	1-5%
Instrument robustness	Low	High
Availability of databases	Comprehensive databases available	Not comprehensive yet, but increasing, more and more libraries becoming freely available online

2.6 Problem statement:

Nanogold might revolutionise healthcare, yet there lies a gap in the knowledge of these fine particles with regards to safety as a drug delivery vehicle. Although nanogold provides a great amount of promise as a drug delivery tool, numerous toxic effects have also been reported. Most of these reports focus only on physiological level while others focus on DNA and protein interaction. However the effects thereof on the metabolic profile remains largely understudied, especially *in vivo*. Also, time-related effects of these particles under pre-clinical conditions still remain to be elucidated. The study will thus attempt to answer the following questions:

1. What is the overall effect of nanogold on the metabolome of rodents?
2. Which metabolic pathways are affected by nanogold (from a systemic point of view)?
3. Can the metabolic changes be related to toxicity?

2.7 Aims and objectives:

The overall aim is to assess the validity of nanogold as a potential drug delivery tool, by evaluating the exometabolome of experimental animals, focusing on any toxic consequence.

Objectives for this study include:

1. Fine tuning of existing protocols, to achieve optimal precision.
2. Nanogold administration to rodents (SD-rats) and collection of urine samples at different time points.
3. Multiplatform metabolomic analysis of the urine samples
4. Biological and toxicological evaluation of results which is preceded by data processing via various statistical methods.

2.8 Study design:

It is still unclear whether gold nanoparticles affect metabolic processes *in vivo*, and which pathways or compound classes are involved. In order to elucidate the effect of gold nanoparticles on the metabolome, and to highlight the pathways of interest, an untargeted metabolomics study approach (which is hypothesis generating) was selected. The study was designed in such a manner as to characterise the effect of nanogold on the exometabolome (urine metabolome) of rodents over time. Figure 2.6 offers a schematic overview of the experimental design.

Three complementary analytical platforms were selected to extend the profiling coverage and included GCTOF/MS, LC-MS/MS and ^{1}H-NMR, which will be discussed in detail in Chapter 3. These three platforms complement each other well in the sense that one supplies an array of results, while the others provide more specific information. Together these three methods lower the risk of missing any significant analyte and ensure the aims and objectives of the study are met. A repeatability study was performed to corroborate the GC-MS protocol employed, considering that most pitfalls and setbacks were experienced with this part of the analytical work. The repeatability study also serves as proof of analytical precision (See Annexure A).

^{1}H-NMR is ideally suited to yield a broad overview of metabolites within a matrix and therefore give an untargeted picture of the analytes of interest. This platform coupled with two targeted methods ensures a more complete view of the effect of nanogold. NMR sketches the outline of the image, while GCTOF/MS and LC QQQ-MS colours it in by zooming in on the known metabolites of note.

The targeted analyses comprise of organic acid extraction and analysis on GCTOF/MS, and amino acid and acylcarnitine analyses on LC QQQ-MS with multiple reaction monitoring (MRM). Organic acid analysis has been at the heart of metabolomics, being that most compounds are converted to organic acid form, along with amino acids and acylcarnitines for their role in the primary metabolism. It is therefore the focus of this design as to bring forth a comprehensive and detailed image of the nanogold effect on the metabolism overall.

An animal model of Sprague-Dawley (SD) rats was selected. The purpose of using an animal model lies in its definition: an animal is used in research of human-related issues (biology and disease), without the risk of involving actual human beings or harming them in any way (Hau, 2008).

By using Sprague Dawley (SD) rats, we can study the possible toxic effects (or otherwise) of gold nanoparticles and the accumulation of metabolites in urine of the body, since the rat metabolism displays a significant resemblance to that of the human. Sprague Dawley rats are the most common of animals used in animal testing and were selected for use in this study as well. It is a breed of albino rat and its main advantage being its ease of handling and calmness.

Although tissue specific (endometabolome) analyses could be valuable, we decided to collect urine samples in this study due to the ease and non-invasive procedure for collection. Moreover, seeing the systemic nature of urine (exometabolome), it is also capable of providing extensive information on the metabolic pathways that could possibly be affected by nanogold; and unlike the snapshot-look of blood, urine carry information of metabolic changes that occurred minutes or even hours prior of collection. Despite this advantage of urine, it was also decided to collect samples in a time base manner: a baseline sample (T0) of all participating rats followed by three collection points (T1, T2, T3) after administration of the nanogold.

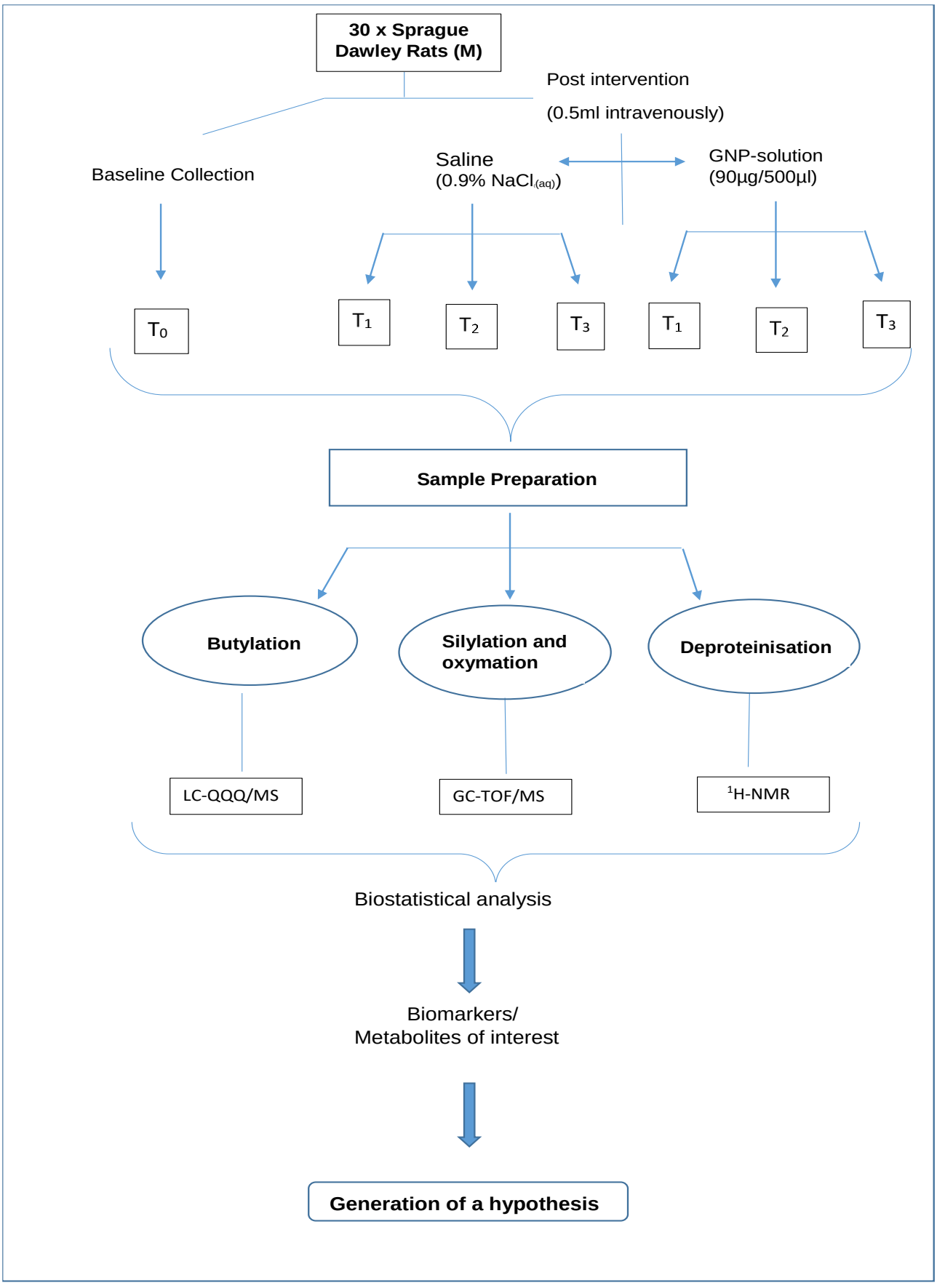

Figure 2.6: A visual representation of the experimental design.This figure gives an overview of the protocols of the study and clear directions to achieve the aim

Chapter 3: Materials and methods

3.1 Synthesis of nanogold particles: Turkevich-Frens Method

The particles used in this study was synthesised and characterised by Dr Clinton Rambanapasi at the Faculty of Health Sciences, North-West University via an adapted Turkevich-Frens method (Rambanapasi, 2015). The product formed had a distinct wine-red colour, indicating the formation of particles within the order of 14nm.

Characterisation of these particles were done by obtaining the UV/Vis absorption spectra to determine concentration, transmission electron spectroscopy (TEM) to determine morphology and size distribution and dynamic light scattering (DLS) to derive the hydrodynamic particle size and to confirm the expected negative zeta potential due to the citrate coating.

A detailed description of the processes mentioned and the corresponding results can be found in Annexure B.

3.2 Experimental animals:

Vertebrate animals are protected by law in South Africa (Animals Protection Act No.71 of 1962) and thus it is an offence to kill or hinder the welfare of an animal for any scientific purpose without justification. The justification for use of experimental animals is formally validated through a process of ethical review. The Medical Research Centre's guidelines were followed in obtaining a unique ethic approval number from AnimCare.

The NWU approval for this study is: NWU-00029-14-A5. This ethical application therefore encloses both this study and that of Dr Clinton Rambanapasi and was obtained preceding any experimental work.

The animals were housed at the Vivarium, a state-of-the-art animal testing facility linked to the DST Pre-clinical Platform at the NWU and all caretaking and handling were done by accredited staff in a controlled environment.

A total of thirty male SD rats were initially bred for the purpose of this study, approximately of the age 8-10 weeks with weight averaging between 250-300g per rat. The animals were housed, nourished and monitored by qualified staff at the DST/NWU/PCDDP Vivarium (Potchefstroom, South Africa) and kept individually in metabolic cages as to assist in the collection of urine.

The rats were kept under standard environmental conditions with *ad libitum* access to food and water.

The rats were divided into two groups (control: n = 12; treated: n = 18) and injected intravenously in the tail vein with 500µl volume of either a citrate-capped nanogold solution (90µg/500µl) or equal volume of saline solution (0.9% NaCl).

3.3 Sample collection and storage:

Urine was collected individually from each rat by use of metabolic cages. This was done over the course of two days at different time points, where the first day of collections were only to establish baseline data. The baseline collections are represented in this document by T0 (initial collection after rats were placed in the metabolic cages) and the collections after treatment are represented by T1, T2 and T3 (equal to 4 hrs, 8 hrs and 24 hrs respectively after administration). The rats were closely monitored to detect difference in appearance or behaviour that might be indicative of a harmful side-effect. All samples were stored at -80ºC.

3.4 ^{1}H-NMR analysis:

3.4.1 Sample preparation:

A volume of 500µl of each sample was aliquoted and 1500µl of cold acetonitrile added. The urine to acetonitrile ratio was 1:3. The mixture was then kept on ice for 10 minutes, followed by centrifugation for another 10 minutes at 12000 g, 4ºC. The supernatant was transferred to new eppendorf tubes, followed by a drying step under nitrogen. The samples were then re-dissolved in 500µl of water and loaded onto the NMR instrument.

3.4.2 Instrumentation:

The analysis was performed on a Bruker Avance III HD NMR spectrometer fitted with a triple-resonance inverse (TXI) ^{1}H (^{15}N, ^{13}C) probe head and x, y, z gradient coils. ^{1}H spectra were received as 128 transients in 32 K data points with a spectra width of 6002 Hz. The water resonance was pre-saturated by single-frequency irradiation, with an excitation pulse of 8 microseconds, all the while keeping the temperature of the samples at 27℃.

3.4.3 Data pre-processing:

Pre-processing of NMR spectral data was done using the Bruker Topspin software (Ellinger *et al.* 2013). Automatic shimming on the deuterium signal of the sample was done. This was followed by a baseline and phase correction and an automatic Fourier transformation. Each sample was scanned 256 times, with run time totalling to 15 minutes per sample. A scan for one-dimensional (1D) ^{1}H-NMR analysis involves a 90° excitation pulse that lasts 8 microseconds and a delay of 4 seconds.

Further processing of the data was performed with Bruker Amix software (Ellinger *et al.* 2013). Traditionally, NMR spectra is sorted into buckets (0.02 spectral bins) between the interval of 0.5 - 10 ppm, ignoring the area of the water peak, which then in this study yielded a data matrix of 452 bins with spectral density data. This data is then used for metabolite identification and confirmation with Bruker pH 7.0 spectral libraries of pure compounds, producing results of level 1 identification.

3.5 LC-MS/MS analysis:

3.5.1 Sample preparation:

Centrifugation @ 6000 rpm of all samples were done prior to other sample preparation, to ensure debris-free aliquots. A sample volume of 10µl was then transferred into a GC-vial, followed by the addition of 250µl of stable isotope mixture into each vial. The isotope mixture consisted of arginine, citrulline, glycine, lysine, glutamic acid, isoleucine, phenylalanine, valine, methionine, acetylcarnitine, free carnitine, isovalerylcarnitine, propionylcarnitine, octanoylcarnitine, decanoylcarnitine, dodecanoylcarnitine, tetra-decanoylcarnitine, hexadecanoyl carnitine and octadecanoyl carnitine. All samples were then dried under a controlled stream of nitrogen (N_2) gas. All samples underwent butylation and were thus derivatised with 300µl butanolic-HCl (3N), after which all samples were incubated at 50℃ for 60 min.

Samples were then left to cool down, before undergoing another drying process with nitrogen at 37℃. The dried samples were then reconstituted in a 100µl mixture of equal volumes of acetonitrile and water, before being transferred into vials with inserts and loaded onto the LC-MS/MS instrument.

3.5.2 Instrumentation and MS conditions:

An Agilent 6410 LC-MS/MS (QQQ) system with a 1200 series auto sampling unit was employed for the liquid chromatography analysis.

Each batch consisted of a randomised requisition list, which included baseline, control and treated samples with a QC sample at every 10th position on the sampling rack. The method was set-up to inject 1µl of sample, followed by gradient of solvent flow. The mobile phase A was a mixture of 0.1% formic acid in water and B was 0.1% formic acid in acetonitrile. The gradient for the programmed flow of the mobile phases can be found in Table 3.1. The column used was a C18 Zorbax SB-Aq Agilent product with dimensions: 150mm x 2.1mm x 3.5µm and the temperature thereof was 30ºC throughout the analysis and conditioned for 10 minutes after each run.

The gas temperature of the ESI was 300ºC at all times, with a nitrogen flow rate of 7.5l/min. A capillary voltage of 3500V was used along with the pressure of the nebuliser remaining at 30psi.

Table 3.1: Gradient programming for mobile phases used to separate acylcarnitines and butylated amino acids.

Flow rate (ml/min)	Mobile phase A (%)	Mobile phase B (%)	Time (min)
0.2	95	5	0
0.2	95	5	1
0.2	82	18	5
0.2	82	18	8
0.3	0	100	15
0.3	0	100	20
0.2	95	5	23

A protocol of Multiple Reaction Monitoring (MRM) was implemented where the parent mass of compound is specified for MS/MS fragmentation and then expressly monitored for a single ion. Table 3.2 consists of all the transitions of the butylated amino acids and acylcarnitines that were detected. MRM excludes unnecessary ions by higher criteria of parent and daughter ion match and in doing so, ensures higher sensitivity and accuracy of the compounds within the sample.

Table 3.2: MRM transitions of the butylated amino acids and acylcarnitines and corresponding isotopes.

	Compound Name	Precursor Ion	Product Ion	Dwell	Fragmentor	Collision Energy
Window 1	Homocystine	381.2	192.1	45	98	8
	3-Nitro-Tyrosine	283.1	181.1	45	98	12
	Citrulline_IS	236.2	74.1	45	89	32
	Arginine_IS	235.2	74.3	45	103	32
	Citrulline	232.2	70.1	45	89	32
	Arginine	231.2	70.1	45	103	32
	C0_IS	221.2	103.1	45	103	16
	C0	218	103	45	103	16
	Histidine	212.1	110.1	45	89	16
	Lysine_IS	207.2	88.1	45	89	20
	Lysine	203.2	84.1	45	89	20
	Glutamine	203.1	84.1	45	89	20
	Homocysteine	192.1	90.1	45	161	12
	Ornithine	189.2	70.2	45	69	20
	Asparagine	189.1	144.1	45	89	8
	Pyroglutamic acid	186	84.1	45	103	16
	Cysteine	178.1	76	45	185	16
	Threonine	176	74.2	45	84	12
	Proline	172.1	70.2	45	94	20
	Serine	162	60.1	45	79	12
	GABA	160.1	87.1	45	79	8
	Alanine	146.1	90.1	45	79	4
	Glycine_IS	134.1	78.2	45	65	4
	Glycine	132.1	76.1	45	65	4
	C18_IS	487.5	85.1	45	160	36
	C18	484	85.1	45	155	36
	C16_IS	459.4	85.1	45	152	32
	C16	456.4	85.1	45	152	32
	C14_IS	431.4	84.9	45	150	44
	C14	428.4	85.1	45	150	28
	C12_IS	403.3	85.1	45	117	32
	C12	400.3	85	45	117	32
	Homocystine	381.2	192.1	45	98	8
	C10_IS	375.3	85.1	45	122	24
	C10	372.3	85	45	122	24
	Cystine	353	130	45	118	16
	C8_IS	347.2	85.2	45	105	24
	C8	344.3	85.1	45	123	24
	Cystathionine	335.2	190.1	45	97	13
	C6	316	85.1	45	113	20
	C5_IS	311.2	85	45	140	20

Table 3.2 (continued):

	Precursor Ion	Product Ion	Dwell	Fragmentor	Collision Energy	Compound Name
	C5	302.2	85.1	45	128	20
	C4_IS	291.2	160.9	45	108	20
	C4	288.2	85.1	45	108	20
	C3_IS	277.2	85	45	128	20
	C3	274.1	85.1	45	128	20
	Glutamic acid_IS	265	89.1	45	89	24
	C2_IS	263.2	85	45	95	20
	Tryptophan	261.2	159.1	45	94	16
	C2	260.2	85	45	108	20
	Glutamic acid	260.2	84.1	45	89	24
	Aspartic acid 2BE	246.2	144.1	45	98	8
	Tyrosine	238.2	136.1	45	94	12
	Phenylalanine_IS	227.2	125.1	45	108	16
	Phenylalanine	222.2	120.1	45	108	16
	C0_IS	221.2	103.1	45	103	16
	C0	218	103	45	103	16
	Methionine_IS	209.1	107.2	45	94	8
	Methionine	206.1	104.1	45	94	8
	Isoleucine_IS	198.2	96.2	45	89	8
	Leucine_Isoleucine	188.2	86.2	45	89	8
	Creatine	188	90.1	45	89	16
	Pyroglutamic acid	186	84.1	45	103	16
	Valine_IS	182.2	80.2	45	89	12
	Valine	174.2	72.2	45	89	12

3.5.3 Data pre-processing:

Peaks were detected and integrated via the Mass Hunter Qualitative Analysis software. A data matrix of integrated peak areas of all compounds was formed. The data was normalised with MSTUS (Warrack *et al.* 2009) to account for sample dilution. Isotopes were used to identify the retention time of all target compounds.

3.6 GCTOF/MS analysis:

3.6.1 Sample preparation:

3.6.1.1 The optimised automated extraction process:

Creatinine determination of each sample was done during ^{1}H-NMR analysis prior to being loaded onto the MicroLab (ML) autosampler from Hamilton Technologies.

The automated method developed by Phiri (2017) was used in this study. The sample numbers and corresponding creatinine values were entered into Microsoft Excel. This sheet was used in the Hamilton software to calculate the volume of sample required for extraction based upon the mmol/l concentration of creatinine in each urine sample. Saline was used to top-up sample volumes to a total of 500µl. A volume of 23µl internal standard (3-phenylbutyric acid) was added to the vials, followed by acidification with 50µl of 5N HCl. Thereafter, 200µl of acetonitrile was pipetted into the samples and mixed thoroughly. The channel aspirated 300µl of the upper phase and dispensed it with high pressure and speed. Six hundred microliters of ethyl acetate was then added to the vials via the automated hand, followed by a 4-step mixing process. The software then allowed for each sample to have a waiting period of 5 minutes, followed by the transfer of 600µl of the upper phase to a second vial. This extraction step is repeated, with 700µl transfer of the top phase.

A final extraction with ethyl acetate is then performed as a guarantee of a complete organic acid extraction, followed by a last transfer of the same amount of the upper phase. The total extraction volume was 1600µl.

To remove residual water from the samples, another mixing step was performed in the second vials with anhydrous sodium sulphate (added manually before extraction). The dried extract was then subjected to a controlled stream of nitrogen gas in order for the solvents to evaporate. This concluded the automated extraction protocol.

3.6.1.2 Derivatization:

The samples were derivatised with a 50µl mixture of Methoxyamine hydrochloride (MOX) followed by incubation at 50℃ for one hour. Thereafter silylation was done with 100µl of BSTFA/TMCS (99:1) and again incubated for an hour. After samples cooled down to room temperature, transferring of samples into appropriate vials with inserts, by using an Agilent manual glass syringe. The samples were then loaded onto the GCTOF/MS where 1µl of the each sample was injected for analysis. All batches were randomised beforehand to include samples from different collection time points and a QC sample was inserted after every 10 samples.

3.6.2 Instrumentation and MS conditions:

The GC-MS analysis was carried out on GC-TOF/MS system, manufactured by Agilent (7890A GC unit coupled with a Leco Pegasus HT TOFMS and Agilent 7693 autosampler). The column used was a RXi-1MS column with dimensions of 30m x 320µm x 0.25µm, supplied by Restek. 1 µl of sample was injected with 1:10 split. The carrier gas, hydrogen, flowed at a constant rate of 2.5ml/minute. The front inlet temperature during each injection was 250ºC. The GC oven was programmed to start at a temperature of 80ºC for 1 minute, followed by a gradual and steady increase by 8ºC every minute until 150ºC, then was elevated again to 230ºC at a rate of 10ºC per minute and finally increased by 18ºC per minute up to 300ºC. The temperature remained at 300ºC for a minute before decreasing to its initial temperature. The temperature of the source was constant at 200ºC. The temperature of the transfer line remained 225ºC. Electron impact ionisation (EI) was executed at -70V for fragmentation of compounds. Data was acquired t 20 spectra/second (50-950m/z) after a 115s solvent delay.

3.6.3 Data pre- processing:

Software from Leco called ChromaTOF was implemented for data extraction. A baseline “spanning” tracking method was employed to remove the baseline and “noise” was eliminated by using a baseline offset of 1. The software also performed an automatic smoothing of the chromatograms. Detection of peaks were done by using a predicted peak width of 3 seconds and a signal-to-noise ratio of 20.

The commercial library NIST11 and an in-house library was used to identify the compounds. Identification could only occur once there was a spectral match of 80% similarity between the compound and library. A data matrix was then created by aligning of peaks through an additional software package called Statistical Compare. The data were also normalised with MSTUS; albeit, standard creatinine and internal standard normalisation was compared and presented in Appendix C.

3.7 Statistical Analysis across the platforms:

The data matrices acquired from each analytical platform were processed separately. Firstly the matrices were evaluated to detect any drifts during analysis or within-batch effects. Thereafter being approved for further statistical analysis, a supervised zero and QC-filter was applied. Any compound not reliably measured was eliminated (a CV > 50% was used), as well as any elements that were not present in all samples of at least one experimental group. The data was transformed by use of a generalised log function. The NMR data was used to provide an overview of the metabolic changes over time and was processed with two-way ANOVA (for independent factors). This will be elaborated on in Chapter 4. Thereafter the NMR, GC and LC data were blocked to focus on the differences between treated and control rats at each time point. Student's t-test ($p < 0.05$) and effect size ($d > 0.8$) were used to identify the metabolites that differed significantly between the groups at each time point. Volcano plots of the t-test and effect size values were created to visualize the results of each time point and analytical platform.

Chapter 4: Results and discussion

4.1 Data quality:

To ensure the quality and validity of data, certain measures were taken prior and during sample preparation and analysis, which included data processing procedures focused on quality assurance. Sample preparation thus included the addition of quality control (QC) samples that were frequently analysed throughout the batches. These QC samples underwent the exact protocol of preparation and analysis as the other samples in the batch.

The QC samples more or less produced the same spectral intensities regardless of time or position. However, the concentration of some metabolites decreased with time due to conversions; and therefore a pre-statistical intervention (QC filter) was performed to remove such unreliable compounds from the data. There were no bothersome batch effects observed across any of the three platforms and therefore there was no need to perform any batch corrections. All the batches generated reproducible and comparable peaks and no visible drift in retention times was noted (Figure 4.1 and 4.3). All instrumentation used were maintained, conditioned and calibrated according to a regular in-house schedule, which further promoted high quality data. In this section, a few representative spectra of each platform (Figures 4.2, 4.4 and 4.5) have been added to illustrate the quality and reliability of data obtained.

i) LC-QQQ/MS Spectra:

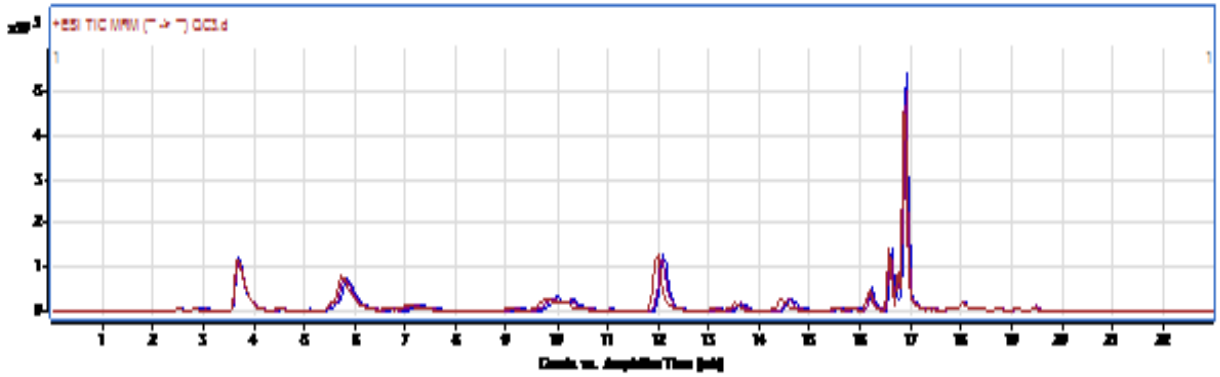

Figure 4.1: A chromatogram of the QC samples used during the LC-MS/MS analysis that have been superimposed, verifying the method precision.

The chromatogram in Figure 4.1 displays the superimposed peaks of all the QC samples that were analysed on the LC-QQQ/MS instrument, highlighting the excellent precision and repeatable nature of the method.

A QC sample also validates the practical knowledge, skill and precision of the analyst, ensuring uniformity during the experimental work of the study. A repeatability study (Annexure A) however establishes this prior to the commencement of experimental work.

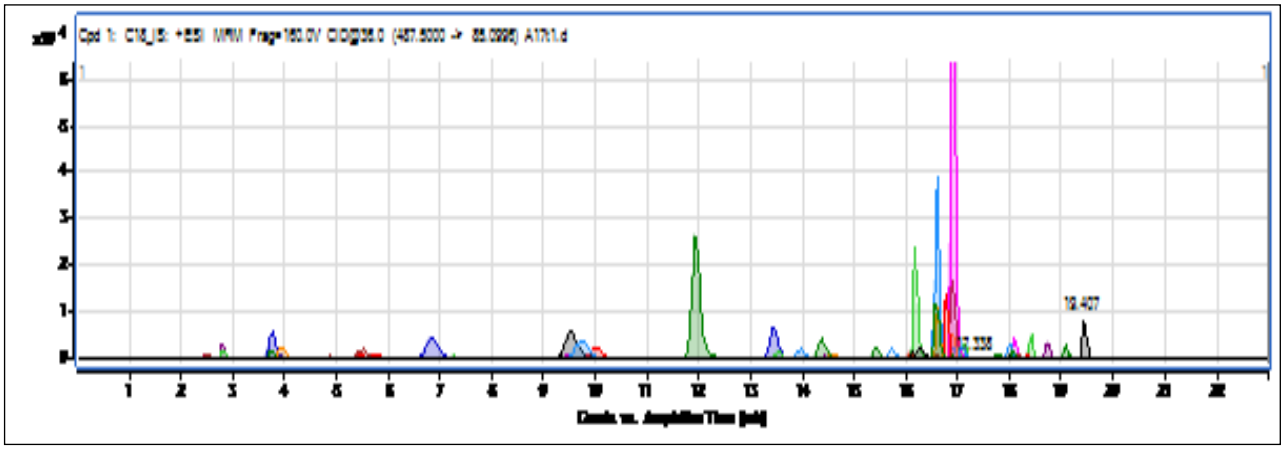

Figure 4.2: A chromatogram of a representative sample, displaying the separation of amino acids and acylcarnitines on the LC-MS/MS.

The chromatogram in Figure 4.2 serves as a sample chromatogram to illustrate the separate detection of the target amino acids and acylcarnitines with the LC-MS/MS instrument. The added chromatography gives superior results to direct infusion as less interference (more selectivity) is found for compounds of similar (or nearly similar) masses (Lin *et al.* 2010) such as lysine and glutamine (Table 3.2).

ii) GC-TOF/MS spectra

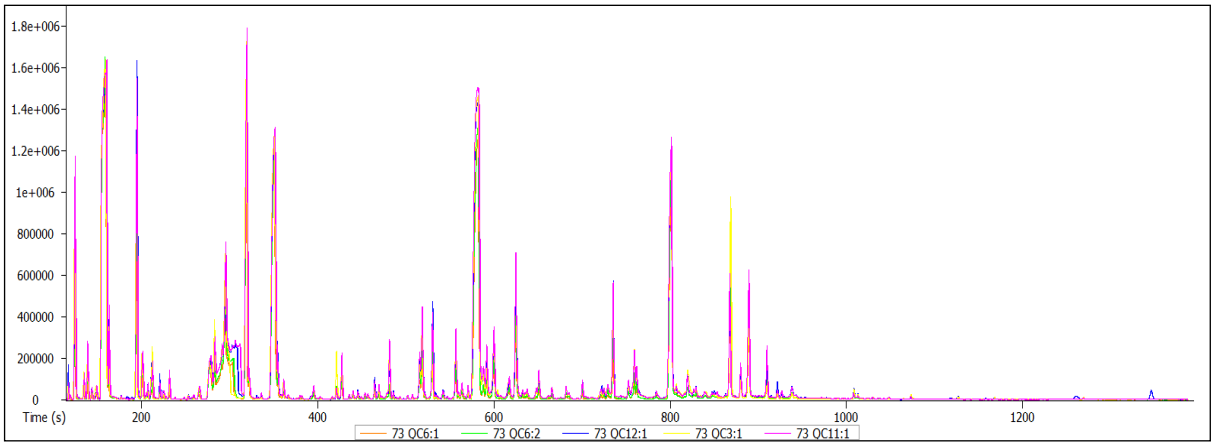

Figure 4.3: A chromatogram of the QC samples used during the GCTOF/MS analysis that have been superimposed, verifying method precision.

As in Figure 4.1, the good repeatability and precision of the GCTOF/MS analysis is showcased in Figure 4.3, by superimposition of QC peaks. Expectedly, some peaks of this untargeted analysis were not stable throughout the batches and were subsequently removed from the data. The chromatogram given in Figure 4.4 serves a sample of the superior chromatographic resolution (and peak intensities) obtained with the use of hydrogen as carrier gas for GCTOF/MS analysis (Verezele, 1964).

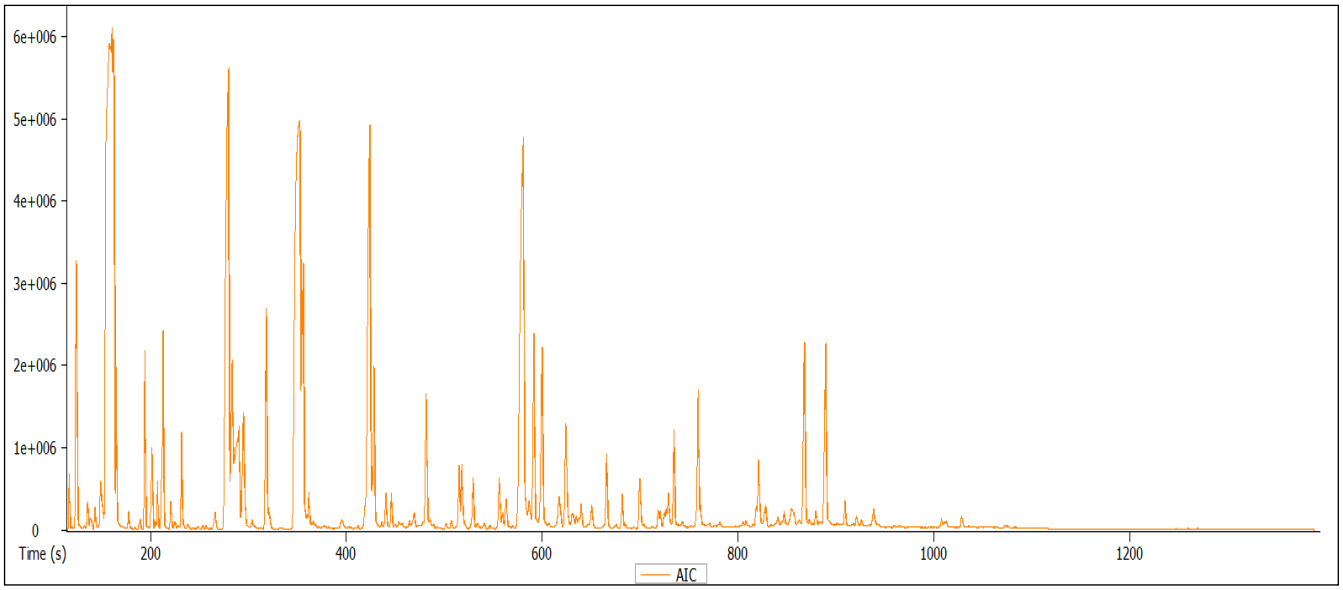

Figure 4.4: A representation of a GCTOF/MS chromatogram of an exemplar sample.

ii) ^{1}H-NMR spectra

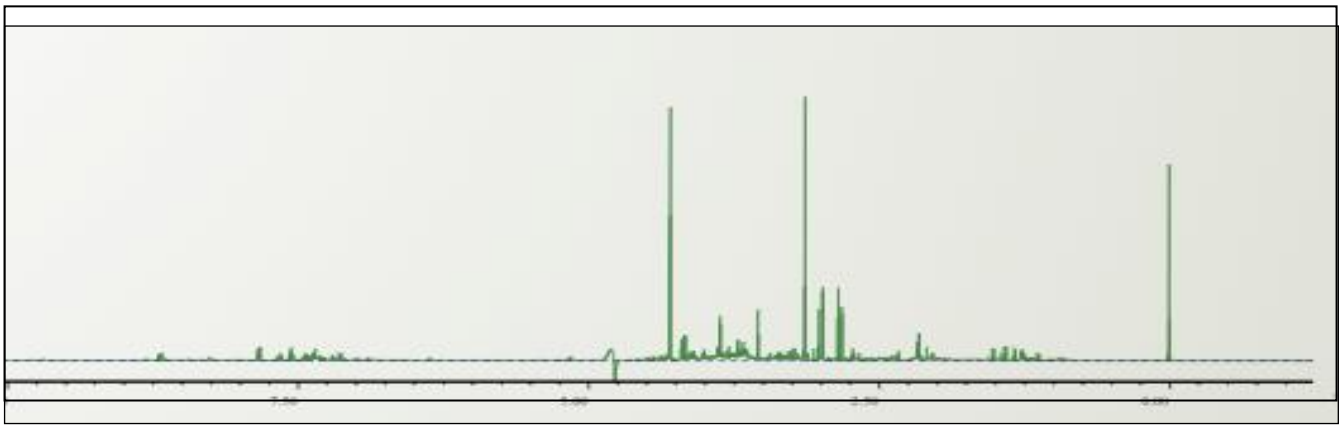

Figure 4.5: A representation of spectra obtained from the ^{1}H-NMR method.

The NMR spectra is comparatively unbiased, due to its robust and global assessment of the metabolome. The samples remain largely chemically unchanged, due to minimal sample preparation. The peak intensities and separation were of a high quality and identification was done with a higher confidence than with the MS methods.

Normalisation play an important role in the quality of the data as it guarantee that data acquired from different samples are comparable. Normalisation usually involves re-scaling data in order for the unit range to be uniform and eliminates redundancy of data. The GC-MS and LC-MS/MS data were normalised with Total "useful" signal (TUS) normalisation (Warrack *et al.* 2009) and was preferred over normalisation to creatinine as it is known that nanogold can influence renal function (Abdelhalim *et al.* 2011). Nevertheless, a comparison of TUS and creatinine normalisation was performed for the sake of completion and are presented in Appendix C.

Similar normalisation was used for the NMR data, albeit with a slight modification. NMR has a relatively large dynamic range, especially regarding the higher concentrations and is able to detect compounds in the high mg/l range. It is then understandable that variance in one or two extremely high peaks (abundant compounds) could influence the total signal significantly, which can resultantly skew the downstream results. Hence, the *median signal* was determined for each sample and used to normalise the NMR data (Scholz & Selbig, 2007; Steuer *et al.* 2007).

The analytical outliers across all platforms were pronounced and easily visually identified with the use of heatmaps and eliminated (data not shown). The data from the NMR analysis did not produce any significant outliers. However, several outliers were identified and eliminated from the GC-TOF/MS data. This is most probably due to the fact that samples from the NMR analysis were re-used for the organic acid extraction, which could have affected the extraction process.
It is believed that the pH was kept from being lowered due to the buffer added during NMR sample preparation. The limited sample volumes, as mentioned before, created this need to re-use samples and due to the non-destructive nature of the NMR analysis, it seemed viable.

4.2 Statistical overview: ^{1}H-NMR

The data obtained in this study consisted of two factors namely treatment and time. Based on this design, it would be appropriate to use a mixed-model two-way ANOVA method (for time series data). However, one of the key limitations of this study is the limited volume of urine acquired for certain rats at different time points. Consequently, it was not possible to provide metabolic profiles of all the samples, resulting in incomplete time series data.

Hence, standard two-way ANOVA (two independent factors or between subjects mode) was used to obtain an overview of the NMR data and thus metabolic changes (over time), where after the NMR, GC and LC data were analysed in a blocked manner (Xu and Goodacre, 2012) as described in the previous chapter.

The Venn diagram in Figure 4.6 summarises the influence of the two factors on the metabolite levels detected in the urine. This figure shows that the levels of 2 features were significantly altered by the treatment irrespective of time. It also shows that the levels of 21 features changed over time irrespective of treatment, while 105 features were unaffected. The two metabolites altered were unknowns and were therefore not studied any further.

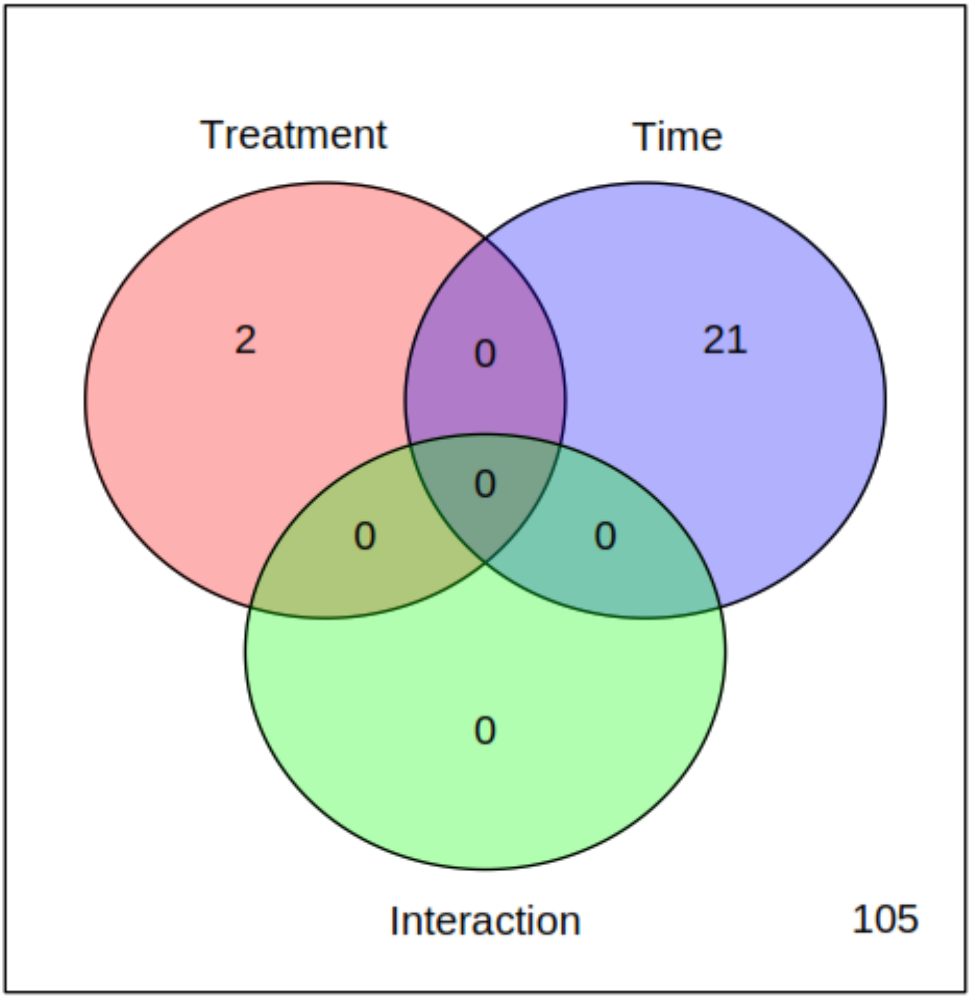

Figure 4.6: A Venn diagram summarizing the two-way ANOVA results.

The main reason for the large time-related effect is the inclusion of the baseline (T0) time point in the data. Since most metabolite concentrations changed after the intervention (box plots Figure 4.7), it is clear that time had the largest effect on the data.

This result then supports the decision to explore the differences for each time point in a blocked manner to simplify the observed differences. Time related changes were also visible in the control rats as the stress of the saline injection influenced the exometabolome (which warrants the inclusion of a control group).

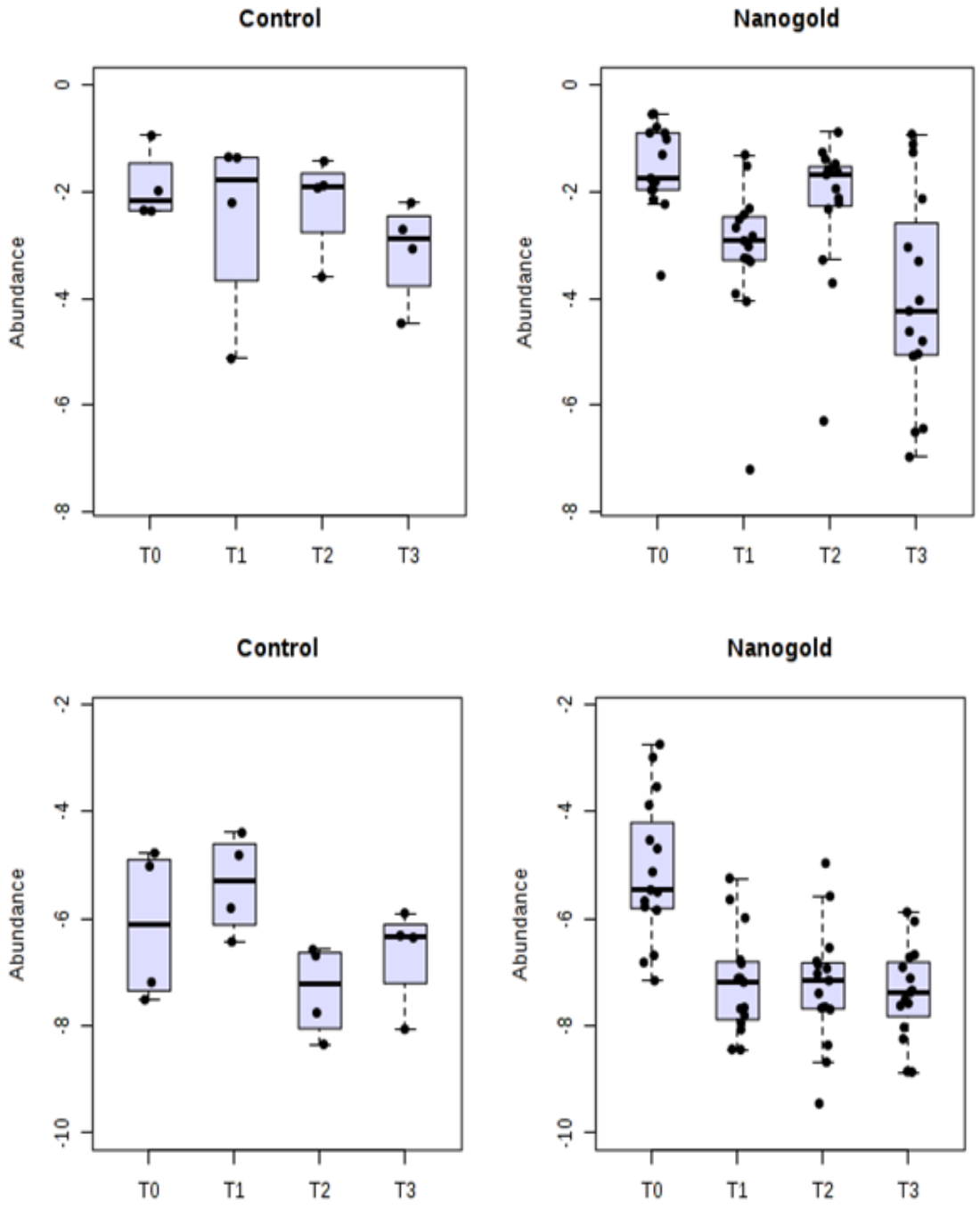

Figure 4.7: Box plots illustrating the significance of the first time point after intervention, where the y-axis carries normalised, log transformed values. These box plots have been selected to be included in the dissertation as representative figures, illustrating the largest difference occurred between T1 and the other timepoints for most analytes.

4.3 Metabolic changes over time (Statistical blocking):

Significant metabolic differences between the control and nanogold treated rats at each time point were identified with univariate stats (specifically Student's t-test and effect size). Volcano plots of all the comparisons are shown in Figure 4.8 and 4.9. The compounds that differed markedly between the groups are summarised in Table 4.1. Volcano plots are scatter plots that visualise differences in large datasets quite quickly (Seifuddin *et al.* 2013). These plots have become increasingly popular in omics studies, since it highlights the most meaningful changes. The x-axis carries the magnitude of a statistical signal, while the y-axis emphasises the significance of that statistical signal. The two statistical components weighed against one another in Figure 4.7 is effect size and the p value. A volcano plot from each time group was obtained, apart from the GC-MS data of T2 (where too few control samples remained).

A visible observation in the volcano plots is the relatively large differences found in metabolites levels at T1 - the first collection after nanogold treatment.

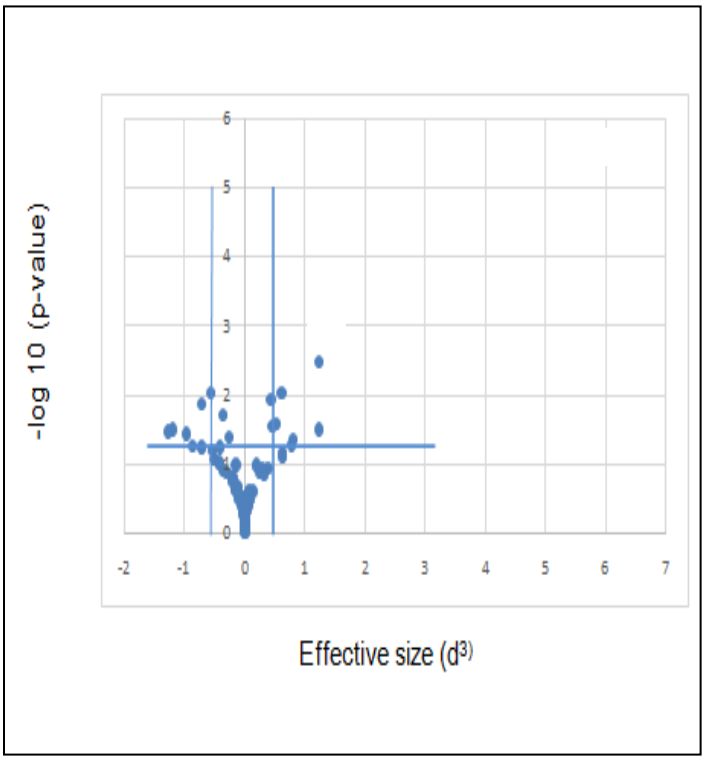

A

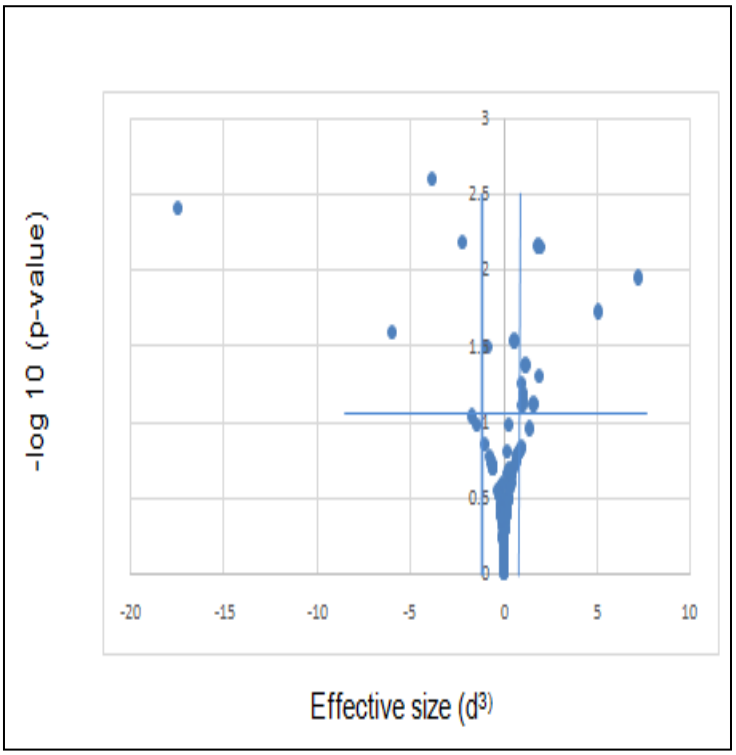

B

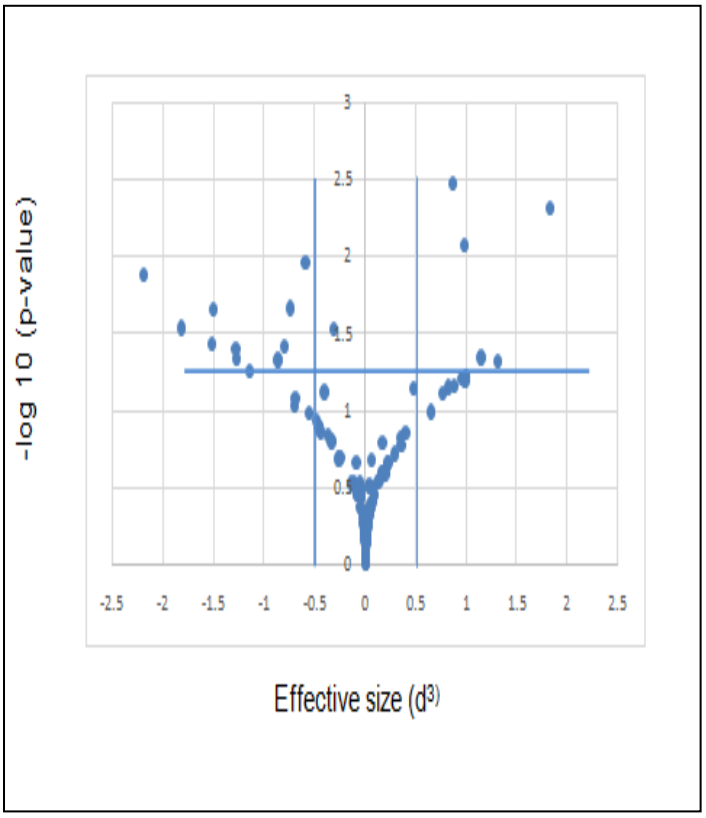

C

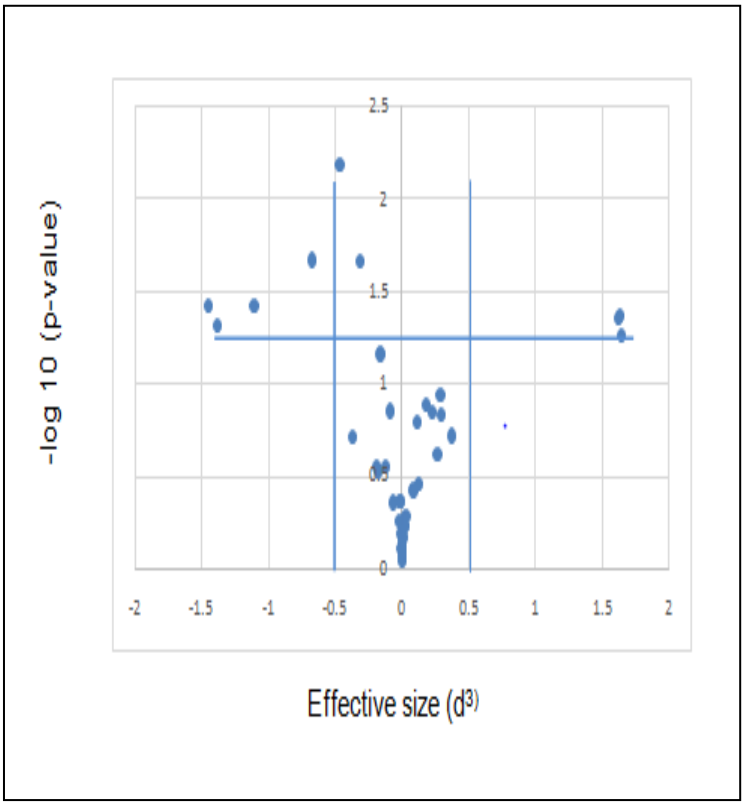

D

Figure 4.8: Volcano plots illustrating the most significant changes at each time point across all platforms as the p-value (-log 10) is depicted as a function of the cubed effect size (d^3). Plot A, B and C show the significant changes found during the NMR analysis of treated rats and control group rats at time points T1, T2 and T3 respectively. Plot D displays the differences obtained during LC-QQQ/MS of time points T1.

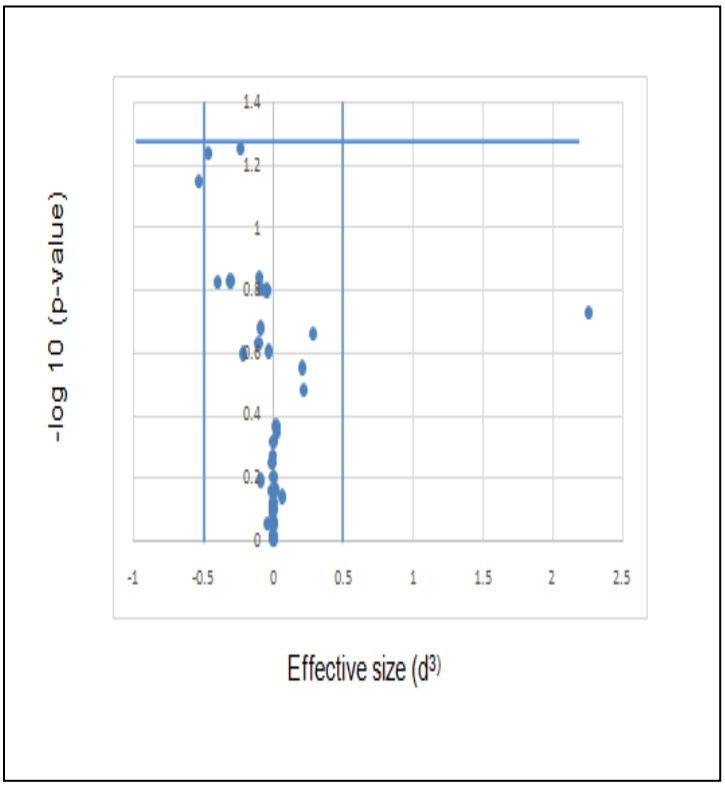

E

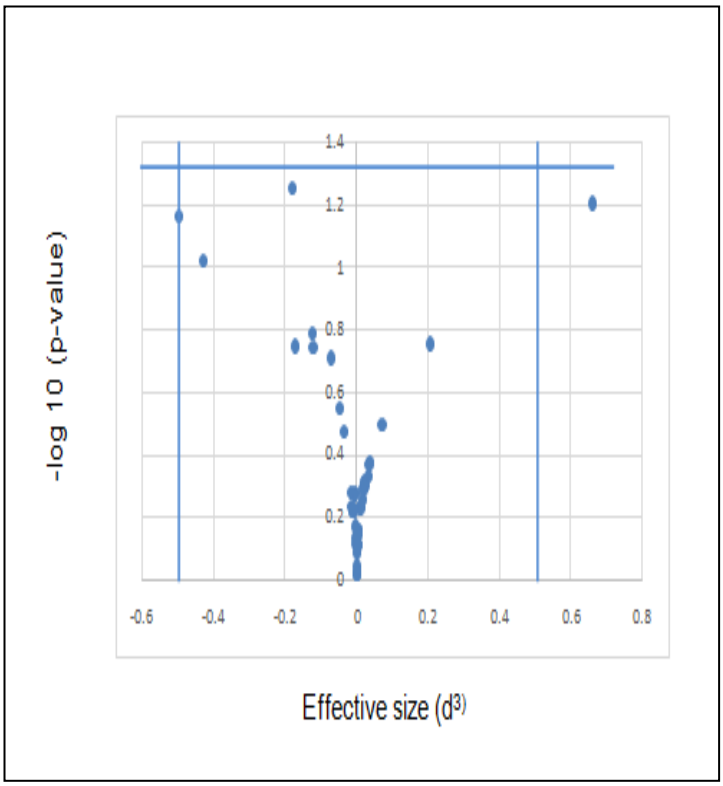

F

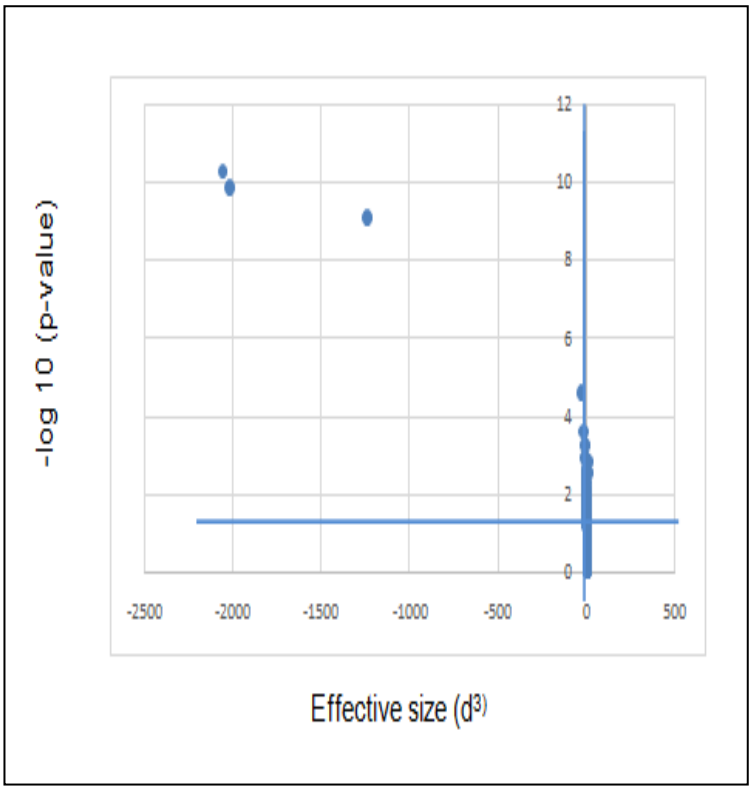

G

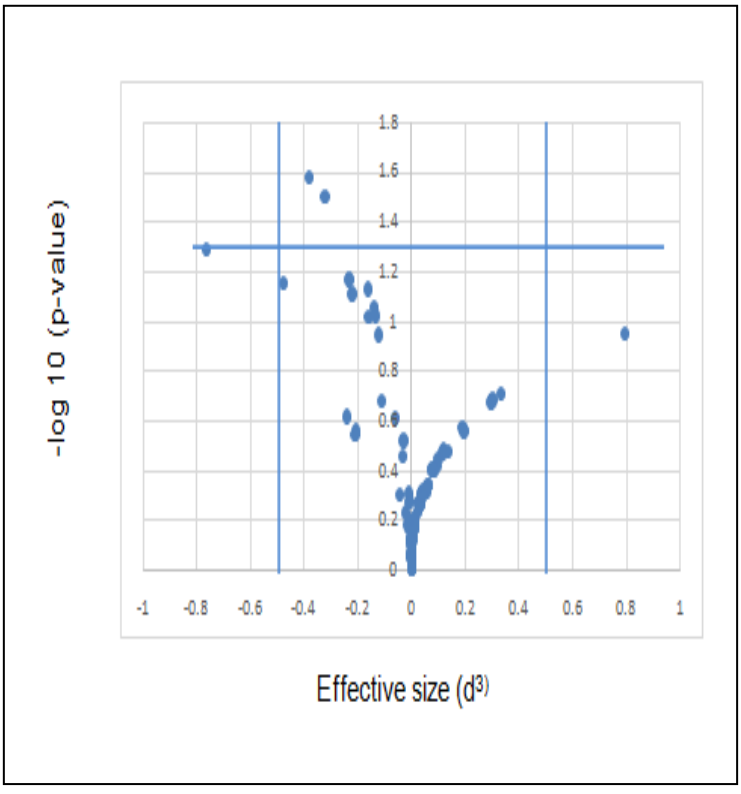

H

Figure 4.9: Volcano plots illustrating the most significant changes at each time point across all platforms as the p-value (-log 10) is depicted as a function of the cubed effect size (d^3). Plot E and F display the differences obtained during LC-QQQ/MS of time points T2 and T3. Plot G and H illustrate the volcano plots from GC-TOF/MS data of time points T1 and T3.

Table 4.1: A table comprising of all the metabolites that were deemed statistically significant with the main decision resting upon a p-value of less than 0.05, categorised according to time of collection.

Metabolite	**ID Level [a]**	**Analytical platform**	**Direction of change [b]**	**Raw p [c]**	**FDR-corrected p[d]**	**d [e]**
T1						
Norvaline	3	GC-TOF/MS	↓	**<0.001**	**<0.001**	**12.72**
Methylmalonic acid	1	GC-TOF/MS	↓	**<0.001**	**<0.001**	**12.64**
Methylmaleic acid	3	GC-TOF/MS	↓	**<0.001**	**<0.001**	**10.75**
2-Ketoglutaric acid	1	GC-TOF/MS	↓	**<0.001**	**0.001**	**3.27**
Succinylacetone	3	GC-TOF/MS	↓	**<0.001**	**0.007**	**2.67**
Unknown		GC-TOF/MS	↓	**0.001**	**0.024**	**2.17**
Hydrocinnamic acid	3	GC-TOF/MS	↓	**0.001**	**0.023**	**2.13**
Pipecolic acid	3	GC-TOF/MS	↓	**0.003**	**0.032**	**1.82**
1-Monopalmitin	3	GC-TOF/MS	↓	**0.003**	**0.030**	**1.82**
Carballylic acid	3	GC-TOF/MS	↓	**0.004**	**0.033**	**1.80**
Unknown		GC-TOF/MS	↓	**0.005**	**0.037**	**1.77**
Alloxanoic acid	3	GC-TOF/MS	↓	**0.004**	**0.034**	**1.77**
p-Coumaric acid	3	GC-TOF/MS	↓	**0.004**	**0.033**	**1.77**
2-Desoxy-inososе	3	GC-TOF/MS	↓	**0.006**	**0.038**	**1.77**
Succinic acid	1	GC-TOF/MS	↓	**0.003**	**0.034**	**1.73**
Unknown		GC-TOF/MS	↓	**0.006**	**0.037**	**1.72**
Vanillic acid	3	GC-TOF/MS	↓	**0.007**	**0.041**	**1.70**
2-Hydroxyglutaric acid	1	GC-TOF/MS	↓	**0.004**	**0.035**	**1.66**

Table 4.1 Continued

Metabolite T1	**ID Level [a]**	**Analytical platform**	**Direction of change [b]**	**Raw p [c]**	**FDR-corrected p[d]**	**d [e]**
Aminocaproic acid	3	GC-TOF/MS	↓	**0.010**	**0.049**	**1.56**
Fumaric acid	1	GC-TOF/MS	↓	**0.008**	**0.044**	**1.47**
Suberic acid	3	GC-TOF/MS	↓	**0.009**	**0.049**	**1.42**
Ritalinic acid	3	GC-TOF/MS	↓	**0.010**	**0.048**	**1.39**
Valeric acid	3	GC-TOF/MS	↓	0.012	0.055	1.34
3-Methyladipic acid	3	GC-TOF/MS	↓	0.012	0.053	1.33
Citrulline	3	GC-TOF/MS	↓	0.012	0.053	1.33
Aconitic acid	1	GC-TOF/MS	↓	0.013	0.052	1.32
Methionine	1	LC-QQQ	↑	0.055	0.237	1.18
Unknown		GC-TOF/MS	↓	0.015	0.058	1.48
4-Hydroxyphenylethanol	3	GC-TOF/MS	↑	0.025	0.080	1.32
Oxalic acid	1	GC-TOF/MS	↓	0.025	0.081	1.32
Adipic acid	1	GC-TOF/MS	↓	0.015	0.059	1.27
4-Decenedioic-Acid	2	GC-TOF/MS	↓	0.015	0.058	1.27
Ferulic acid	3	GC-TOF/MS	↓	0.017	0.063	1.22
Malonic acid	1	GC-TOF/MS	↓	0.031	0.093	1.22
Methyl succinic acid	1	GC-TOF/MS	↓	0.019	0.067	1.20
2-Hydroxyadipic acid	3	GC-TOF/MS	↓	0.033	0.095	1.20
Citric acid	1	GC-TOF/MS	↓	0.020	0.068	1.18

Table 4.1 Continued

Metabolite T1	**ID Level [a]**	**Analytical platform**	**Direction of change [b]**	**Raw p [c]**	**FDR-corrected p[d]**	**d [e]**
Erythronic acid (lactone)	3	GC-TOF/MS	↓	0.035	0.100	1.18
Tyrosine	1	LC-QQQ	↑	0.044	0.247	1.18
N-Acetylglutamic acid	3	GC-TOF/MS	↓	0.038	0.101	1.15
Ethylmalonate	1	GC-TOF/MS	↓	0.037	0.104	1.15
Unknown		GC-TOF/MS	↓	0.039	0.101	1.13
2-Furanacrylic acid	3	GC-TOF/MS	↓	0.039	0.102	1.13
Octanoylcarnitine	1	LC-QQQ	↓	0.038	0.294	1.13
Isocitric acid	3	GC-TOF/MS	↓	0.041	0.104	1.12
3Z-Hexenedioic acid	2	GC-TOF/MS	↓	0.042	0.103	1.12
Acetylcarnitine	1	LC-QQQ	↓	0.049	0.238	1.11
2,3-Dihydroxybutanoic acid	3	GC-TOF/MS	↓	0.042	0.102	1.11
Pyruglutamate	1	GC-TOF/MS	↓	0.027	0.085	1.09
Unknown5		NMR	↓	0.034	0.325	1.08
3-Methylglutaconic acid	1	GC-TOF/MS	↓	0.047	0.107	1.07
Valine	1	NMR,LC-QQQ	↑	0.003	0.140	1.07
LACTIC-ACID	1	GC-TOF/MS	↑	0.044	0.105	1.07
2-Keto-isovaleric acid	3	GC-TOF/MS	↓	0.048	0.106	1.06
Senecioic acid	3	GC-TOF/MS	↓	0.049	0.106	1.06
Glutaric acid	1	GC-TOF/MS	↓	0.038	0.102	1.01

Table 4.1 Continued

Metabolite T1	**ID Level [a]**	**Analytical platform**	**Direction of change [b]**	**Raw p [c]**	**FDR-corrected p[d]**	**d [e]**
Urea	1	NMR	↓	0.037	0.325	0.99
Pimelic-Acid	1	GC-TOF/MS	↓	0.044	0.104	0.96
Unknown		NMR	↓	0.014	0.247	0.89
TMAO	1	NMR	↓	0.009	0.288	0.83
Hexanoylcarnitine	1	LC-QQQ	↓	0.006	0.251	0.78
Allantoin	1	NMR	↓	0.020	0.306	0.72
Arginine	1	LC-QQQ	↓	0.021	0.278	0.68
2-OH-isovaleric acid		NMR	↑	<0.001	<0.001	1.81
Unknown1		NMR	↑	0.001	0.072	1.09
Choline	1	NMR	↑	0.032	0.361	1.07
Unknown4		NMR	↓	0.032	0.332	1.06
3-Nitro-Tyrosine	1	LC-QQQ	↓	0.038	0.367	1.03
Alanine	1	NMR, LC-QQQ	↑	0.045	0.352	0.93
Propionylcarnitine	1	LC-QQQ	↓	0.021	0.415	0.88
Unknown3		NMR	↑	0.029	0.359	0.77
Unknown6		NMR	↓	0.042	0.346	0.64

Table 4.1 Continued

Metabolite	ID Level [a]	Analytical platform	Direction of change [b]	Raw p [c]	FDR-corrected p[d]	d [e]
T2						
Unknown		NMR	↓	0.004	0.247	2.60
Dimethylamine	1	NMR	↑	0.011	0.235	1.93
Valine	1	NMR	↓	0.002	0.316	1.57
N-methylhydantoin	1	NMR	↑	0.007	0.178	1.25
Unknown		NMR	↑	0.007	0.219	1.23
Unknown		NMR	↑	0.042	0.487	1.05
Unknown		NMR	↓	0.032	0.400	0.97
Unknown		NMR	↑	0.029	0.410	0.83
T3						
Unknown		NMR	↓	0.013	0.327	1.30
Unknown		NMR	↓	0.029	0.459	1.22
Unknown		NMR	↑	0.005	0.299	1.22
Indoxy sulfate	1	NMR	↓	0.022	0.399	1.15
Unknown		NMR	↑	0.047	0.372	1.10
Unknown		NMR	↓	0.040	0.421	1.09
Unknown		NMR	↓	0.045	0.411	1.09
Citric acid	1	NMR	↑	0.045	0.436	1.05
Creatinine	1	NMR	↓	0.047	0.394	0.96
2-ketoglutaric acid	1	NMR	↑	0.003	0.419	0.95
Unknown		NMR	↓	0.038	0.442	0.93
Unknown		NMR	↓	0.021	0.450	0.91
Allantoin	1	NMR	↓	0.011	0.337	0.84
Glyceric acid	3	GC-TOF/MS	↓	0.027	2.289	0.72
Erythronic acid (lactone)	3	GC-TOF/MS	↓	0.032	1.366	0.69
Valine	1	NMR	↓	0.030	0.417	0.68

[a] Identity confidence level according Schymanski *et al.*, 2014; [b] Direction according to effect size (where positive sign indicates that analyte concentration was higher in that time group);
[c] Raw p-value (Student`s t-test p-value); [d] False detection rate (FDR) correcting for multiple testing;
[e] Effect size (d-value)

4.4 Metabolic specific discussion:

After thorough reflection on the results obtained, evidence of perturbation with nanogold intervention is clear. The extent of these effects on the metabolism however will be discussed in this section. Throughout this section several figures have been added to aid in illustrating the various metabolic pathways, their relevant compounds and the processes involved. All these figures have been specially compiled with assistance from Professor Lodewyk Jacobus Mienie (associate Professor in Biochemistry: Human Metabolomics at North-West University, Potchefstroom, South Africa). Figure 4.10 gives a comprehensive view on the affected metabolites and overall metabolism involved. These processes occur within the cells of different tissue and organs and will be discussed in more detail as the chapter progresses.

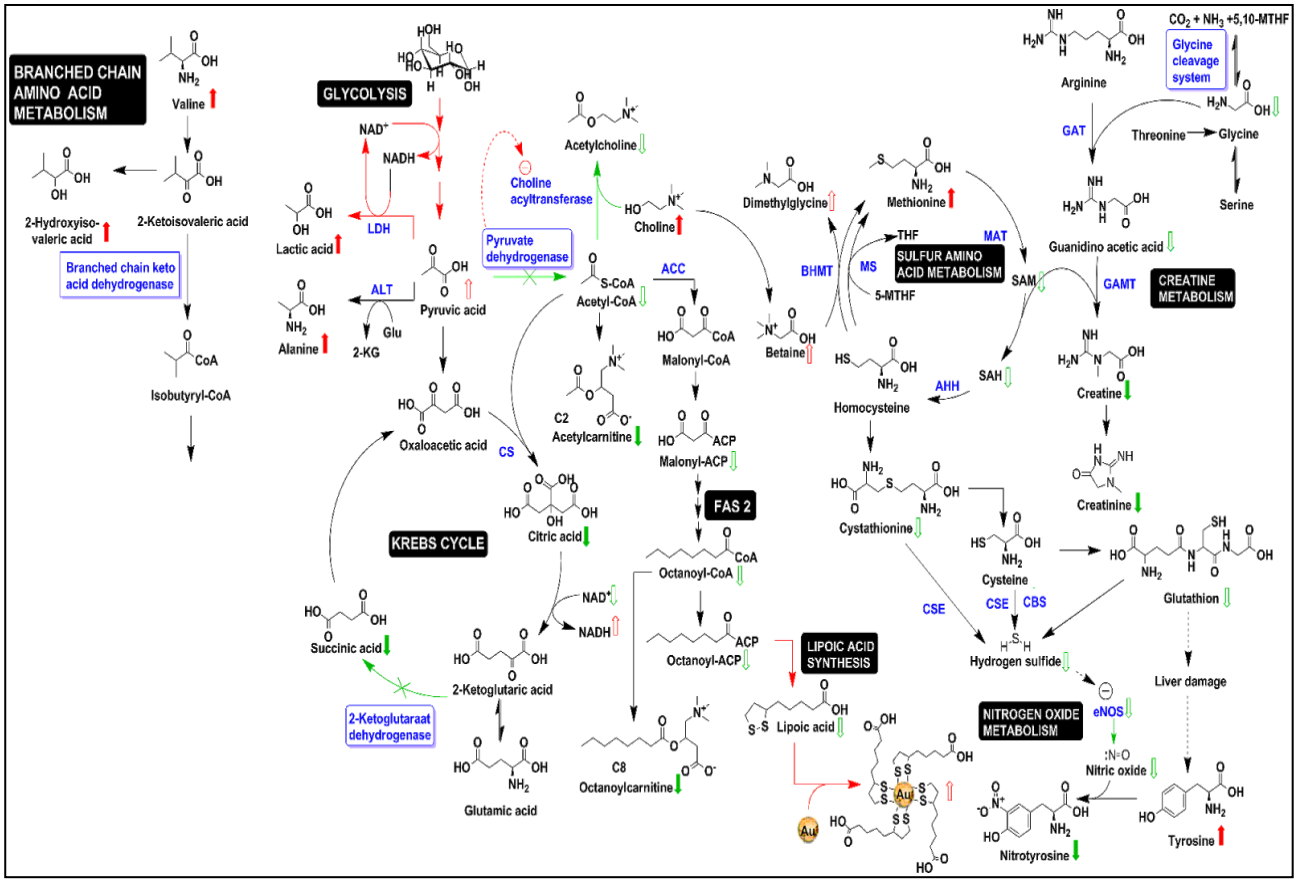

Figure 4.10: An overview of the metabolism involved with nanogold intervention, indicating the change in levels of metabolites.

4.4.1 Energy metabolism: The affected pathways (Glycolysis, Krebs-cycle)

From the list of urinary metabolites that were significantly different between the experimental groups, it seems that the treatment affected energy metabolism. The main metabolites of note associated with the energy metabolism are alanine and lactic acid, both of which were significantly elevated immediately (4h) after nanogold intervention. Both these compounds are formed from pyruvate via alanine transaminase and lactic dehydrogenase, respectively (Stromme *et al.* 1976). The concentration of both these metabolites is proportional to that of pyruvate. Elevated concentrations of pyruvate, alanine and lactic acid is often present with inborn errors of metabolism, of which the most widely known are: the pyruvate carboxylase defect (Habarou *et al.* 2015), multiple carboxylase (biotin) defect, pyruvate dehydrogenase defect (Brown *et al.* 1994), multiple 2-ketoacid dehydrogenase (also known as thiamine and lipoic acid defect or thiamine responsive maple syrup urinary disease –MSUD) (Blackburn *et al.* 2017), electron transport chain defects and anoxia (Haas *et al.* 2008). The pyruvate dehydrogenase (most commonly linked to severely increased lactic acid) is a complex consisting of three parts namely, E1, E2 and E3 (Hrycyna, 2009). The E2 component make use of the thiol - rich, lipoic acid, to function which in return is sensitive to heavy metal poisoning. Figure 4.11 provides a schematic representation of the energy metabolism, pathways affected (glycolysis, Krebs-cycle and their intermediates) and the association with the electron transport chain.

While this result hints to possible disturbance of the electron transport chain, some of the other metabolites in Table 4.1 contradict this notion. All the Krebs-cycle intermediates were initially lower after treatment, which included acetylcarnitine (a reflection of acetyl-CoA), citrate, isocitrate, aconitate, 2-ketoglutarate (and related 2-hydroglutarate), succinate, and fumarate. An inhibition of the electron transport chain would lead to the accumulation of NADH and subsequent accumulation of Krebs-cycle intermediates due to the dehydrogenase reactions in the pathway. Since this was not observed (for T1 at least), it can be reasoned that the immediate upstream enzyme (pyruvate dehydrogenase) could be involved. A secondary entry point for pyruvate into the Krebs cycle is pyruvate carboxylase but again, the lower intermediates (especially fumarate) do not support this fully. Moreover, if the Krebs cycle is not functioning at full capacity, then energy levels could be affected which would mean that the energy dependent pyruvate carboxylase reaction is hindered (Engelking, 2010).

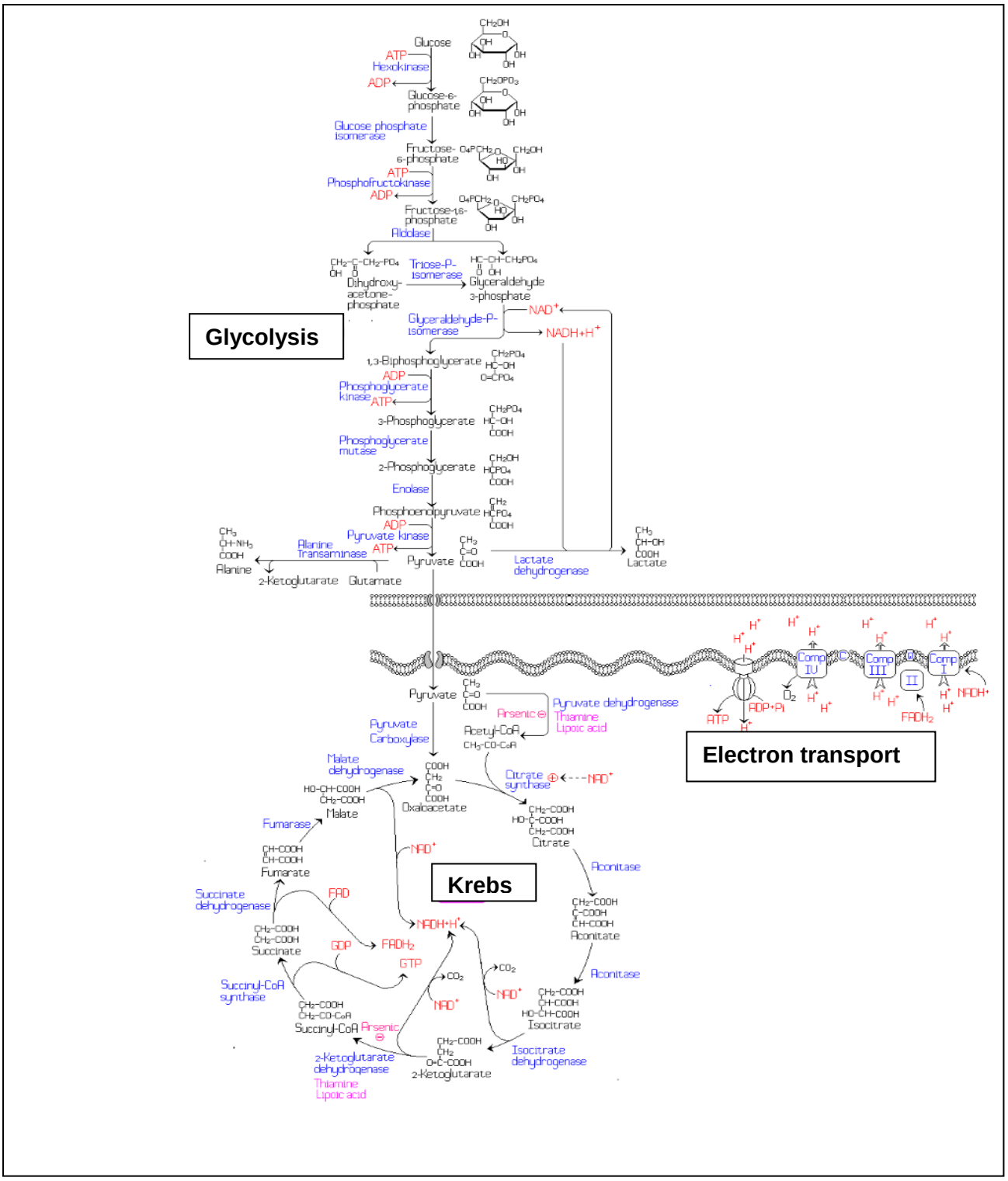

Figure 4.11: A schematic of the energy metabolism, pathways affected (glycolysis, Krebs-cycle and their intermediates) and the association with the electron transport chain

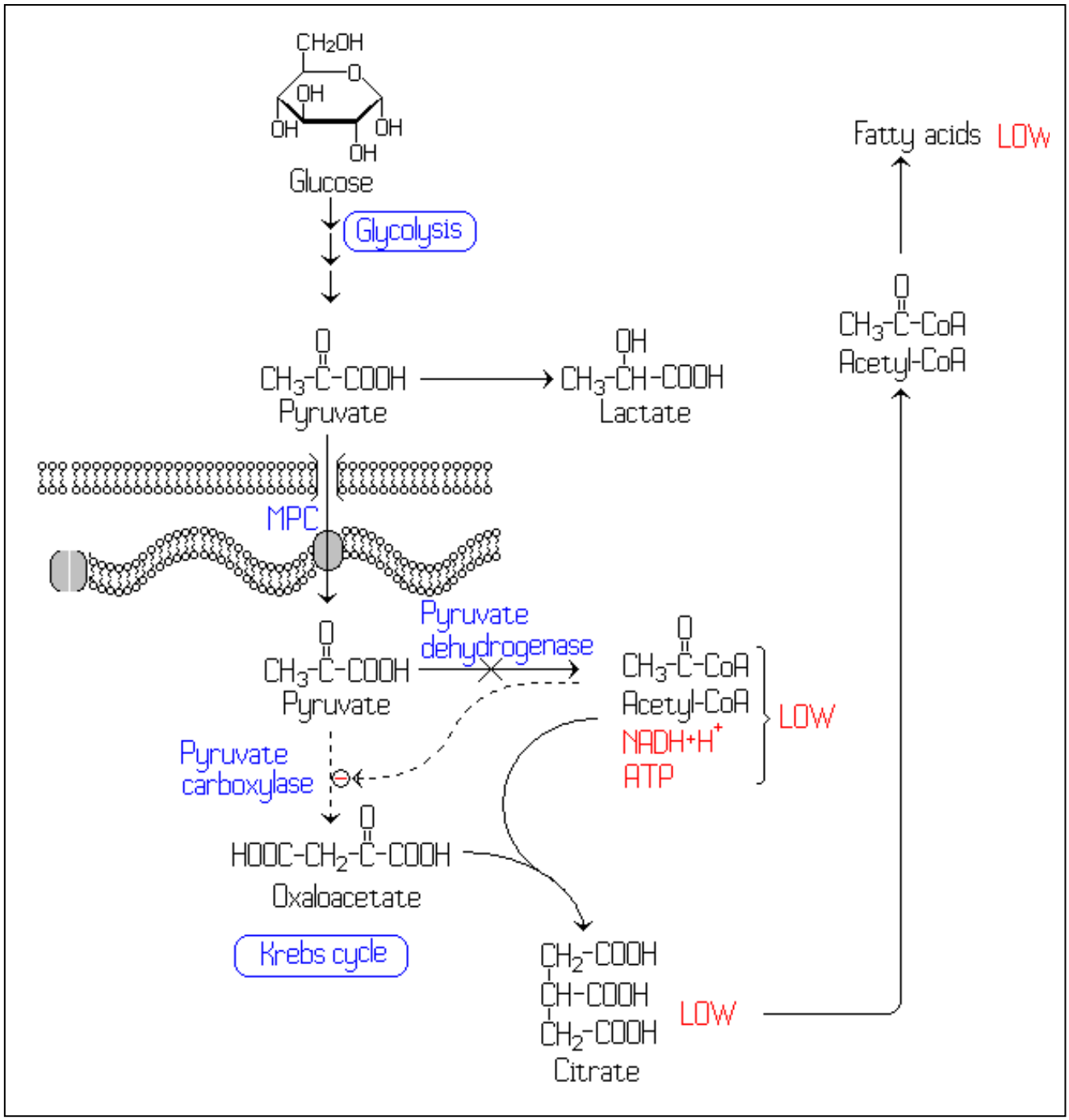

Figure 4.12: A closer view of the effect of an inhibition of the pyruvate dehydrogenase complex.

As mentioned and illustrated in Figure 4.12, the pattern of change in metabolites observed with nanogold administration can partially be ascribed to the decreased activity of pyruvate dehydrogenase, which is supported by the lowered levels of 2-ketoglutaric acid and citrate. 2-Ketoglutaric acid (also known as α-Ketoglutarate) is oxidatively decarboxylated by the α-ketoglutarate dehydrogenase (α-KGDH) to succinyl-CoA. This sets off the production of CO_2 and NADH within the second TCA cycle. The enzyme complex is comparable to that of pyruvate dehydrogenase in its mechanism of action and protein makeup (Oregon State University, 2008).

A deficiency in α-KGDH is characterised by increased excretion of α-ketoglutarate and citrate (Kohlschütter *et al.* 1982), as seen at timepoint T3. An inhibition of lipoic acid often leads to α-ketoglutarate deficiency and is also often linked to arsenic poisoning (Mayr *et al.* 2014).

These findings point to the possible effect of nanogold on the activity of pyruvate dehydrogenase α-ketoglutarate dehydrogenase. Both of these enzymes are multiprotein acyl-CoA forming dehydrogenase enzymes with co-factors of thiamine and lipoic acid.

4.4.2. Branched chain amino acid metabolism:

Valine, 2-Ketisovaleric acid and 2-OH-isovaleric acid (2-hydroxy-isovaleric acid) are all biomarkers for metabolic defects along the branched chain amino acid metabolism (BCAA). Elevated levels of valine and 2-hydroxy-isovaleric acid and decreased levels of 3-methylglutaconic acid, propionylcarnitine and methylmalonic acid were detected after nanogold intervention, which provides proof that BCAA metabolism was affected to some extent by nanogold intervention. It is likely a consequence of lower ATP production which leads to the stimulation of proteolytic metabolism. 2-Hydroxy-isovaleric acid is usually characteristically elevated and is regarded as the most sensitive biomarker for the inhibition of a branched chain 2-ketoacid dehydrogenase activity; and with the elevated levels found after nanogold intervention of both valine and 2-hydroxy-isovaleric acid, it can be hypothesised that the 2- keto acid dehydrogenase is inhibited.

BCAAs (leucine, isoleucine and valine) are essential amino acids important in gluconeogenesis.
The catabolic pathways of all three amino acids (refer to Figure 4.13) involve the same enzymes, namely branched chain amino acid transaminase and branched chain 2-ketoacid dehydrogenase. Each of the amino acids undergo a single transamination with BCAA aminotransferase with α -ketoglutarate as the amino acceptor, producing three α-keto acids which are then oxidised by α-keto acid dehydrogenase (BCKD), creating three different CoA derivatives. Interestingly, this BCKD complex is one of three dehydrogenase complexes that is associated with several cofactors, such as lipoic acid (Chang *et al.* 2002).

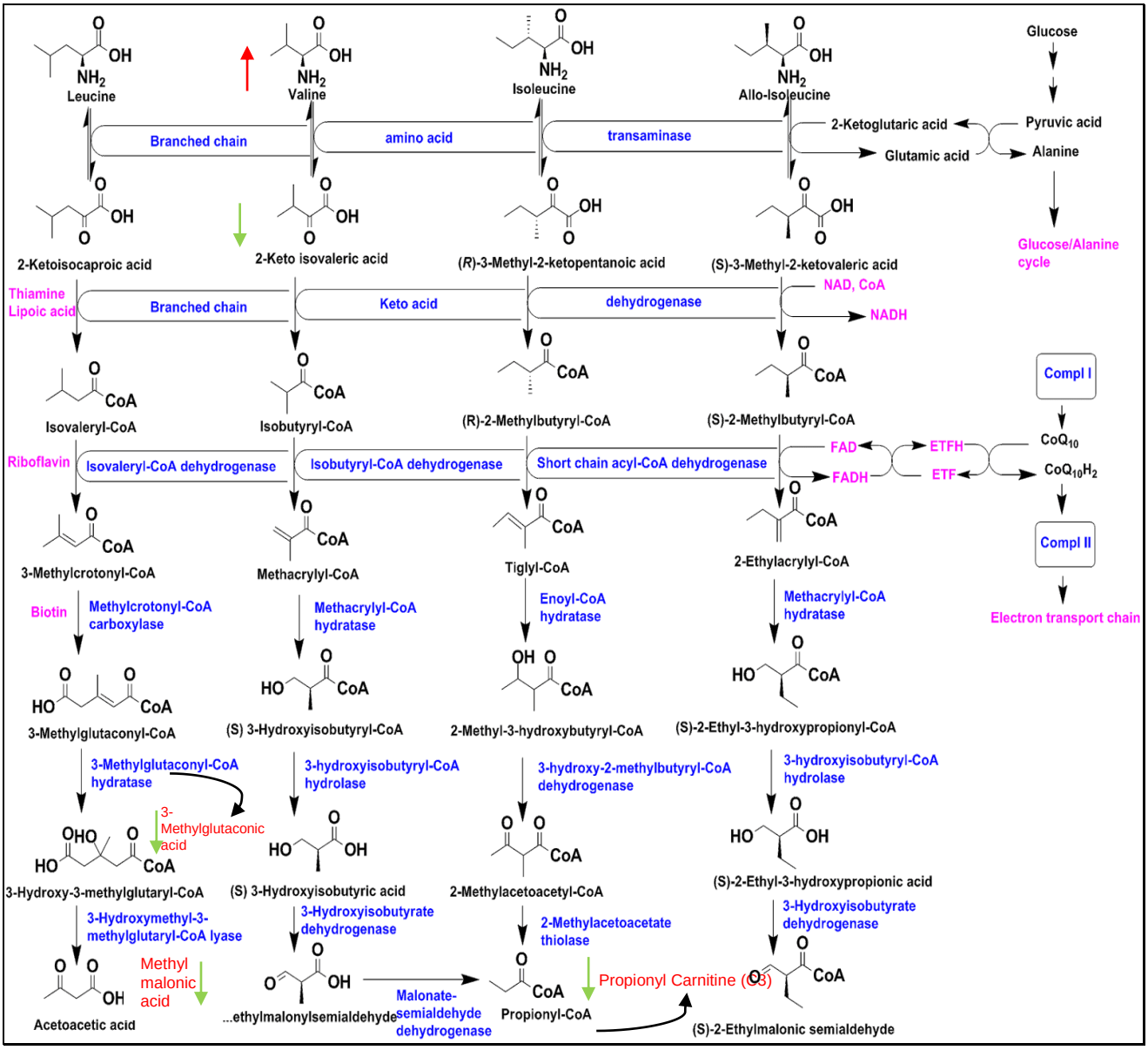

Figure 4.13: A schematic overview of the branched chain amino acid metabolism, associated intermediates and enzymes.

4.4.3 Amino acid metabolism: Sulphur-containing amino acids

As evidence of lipoic acid involvement increases, it also highlights the known affinity of sulphur for (heavy) metals (Sharma *et al.* 1998). It is therefore important to also evaluate the involvement of other sulphur containing compounds (such as amino acids). Amino acids containing sulphur are not as abundant in nature and therefore the metabolism thereof is in many ways a reservoir. Figure 4.14 displays an overview of the sulphur-containing amino acid pathways and the related findings of this study. The statistically significant compounds involved in this metabolism after nanogold treatment were methionine and choline (elevated) and pyroglutamate (decreased). Methionine, though not statistically elevated according to the t-test, still presented a significant effect size and therefore is of note in this discussion.

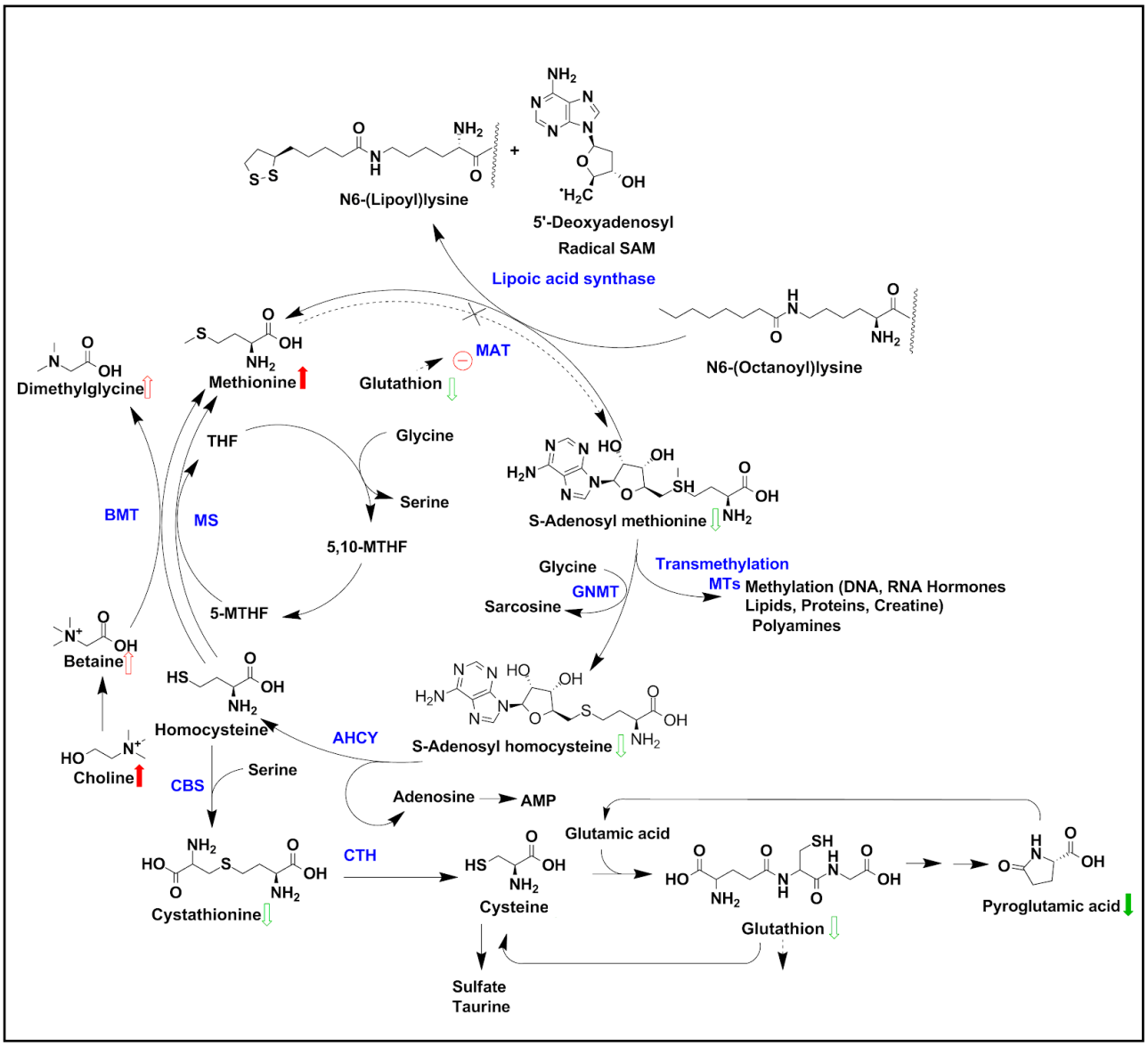

Figure 4.14: The metabolism of sulphur-containing amino acids, where MAT I/III= methionine adenosyltransferase, MTs = S -adenosylmethionine-dependent transmethylation reactions, GNMT = glycine methyltransferase, AHCY =S -adenosylhomocysteine hydrolase, BMT = betaine homocysteine methyltransferase, MS = 5-methyltetrahydrofolate homocysteine methyltransferase; CBS = cystathionine ß-synthase, CTH = cystathionine γ-lyase, AMP = adenosine monophosphate

The first step in methionine metabolism is the formation of S-adenosylmethionine (SAMe) in a reaction catalysed by methionine adenosyltransferase (MAT) (Finkelstein, 1990; Mato *et al.* 2002). This occurs mainly in the liver. SAMe donates a methyl group and takes part in three major pathways in the liver, namely: polyamine synthesis, transmethylation and transsulfuration (Lu and Mato, 2008).

During transmethylation, SAMe gives off its methyl group to various acceptor molecules, all of which the reactions are catalysed by methyltransferase (MTs) (Finkelstein, 1990).

The product of transmethylation is S Adenosylhomocysteine (SAH), which is then hydrolysed by a reversible reaction with SAH hydrolase, to create homocysteine (Hcy) and adenosine. Homocysteine and adenosine should be removed promptly as the failure to do so, would cause an accumulation of SAH (SAH inhibits the process of methylation to a great extent) (Ulrey *et al.* 2005). Hcy can be methylated to form methionine by either methionine synthase (MS) or betaine homocysteine methyltransferase (BHMT). The first enzymatic reaction requires sufficient levels of folate and vitamin B12 and the second requires betaine, a derivative of choline.

Homocysteine is remethylated by MS and this reaction requires methyltetrahydrofolate (5-MTHF), which is a product of 5,10-methylenetetrahydrofolate (5,10-MTHF) in a reaction catalysed by methylenetetrahydrofolate reductase (MTHFR). 5,10-MTHF is then gives off its methyl group to form THF and existing THF is converted to 5,10-MTHF.

Homocysteine can also be converted to cysteine while in the liver, by a reaction along the transsulfuration path. This reaction involves the combination of homocysteine with serine, which produces cystathionine, in a reaction catalysed by cystathionine β synthase (CBS), which requires vitamin B6 as a cofactor. Dissolution of cystathionine then occurs via another B6-dependent enzyme called cystathionase, which generates free cysteine used in GSH synthesis (Finkelstein, 1990). All mammalian tissues express MAT and MS, but BHMT is only located in the liver and kidneys (Lu and Mato, 2008). SAMe activates CBS by the inhibition of MS and MTHFR (Lu and Mato, 2008). Therefore, in the case of SAMe depletion, homocysteine is directed to be remethylated in order to regenerate SAMe, while with the presence of high levels of SAMe, the homocysteine will follow the transsulfuration pathway. In the case of cirrhosis, patients often display high levels of methionine (hypermethioninemia), which is related to the impairment of hepatic MAT activity (Mato *et al.* 2002). Mato *et al*. (1994) stated that this decreased MAT activity is partly responsible for decreased GSH level and to support this finding, the administration of SAMe to sufferers of liver cirrhosis have indeed increased the hepatic GSH level (Vendemiale *et al.* 1989)

Another key player in this part of the metabolism is glycine and the associated *glycine cleavage system*, which is NADH dependent. Glycine (GLY) is not an essential amino acid. It is easily produced by two pathways:
L-serine (SER) is converted to GLY by serine hydroxymethyltransferase (SHMT) and also GLY can be synthesised anew from carbon dioxide (CO_2) and ammonium (NH_4). Both these reactions however, are reversible (Fujiwara *et al.* 1984).

The glycine cleavage system contains the thiol-containing lipoic acid by way of its H-protein which is a carrier protein for the aminomethyl intermediate (Kochi *et al.* 1976). This protein is modified with lipoic acid and interacts with all other components in reductive methylamination (catalysed by the P-protein), methylamine transfer (catalysed by the T-protein) and electron transfer (catalysed by the L-protein).

This raises interest due to the possibility that lipoic acid among other sulfur-rich compounds readily bonded to the nanogold particles. No sizeable changes post intervention were detected with regards to this process, apart from changes to oxalic acid levels and though elevated levels of oxalic acid is expected with a disturbance in this system, contradictory results of decreased oxalic acid levels were observed. However given the numerous metabolic pathways contributing to glycine it is possible that mild changes regarding the associated metabolites could have been masked and this is mentioned to merely state this observation.

Several defects of the sulphur amino acid metabolism are known and are summarised in table 4.2.

Table 4.2: The relevant changes in metabolite levels in different disorders of sulphur amino acid metabolism.

Disorder	Methionine	Homocysteine	AdoMet	AdoHcy	Cystine	Cystathionine	Sulfocysteine
MAT deficiency	↑↑↑	n-↑	n	n	n	n	n
GNMT deficiency	↑↑↑	n-↑	↑↑↑	n	n	n	n
SAHH deficiency	n-↑↑↑	n-↑	↑↑↑	↑↑↑	n	n	n
CBS deficiency	n-↑↑↑	↑-↑↑↑	↑↑	↑↑	↓↓	n	n
CTH deficiency	n	n	n	n	n	↑↑↑	n

None of the known metabolic defects displays the exact same perturbations. The only valuable result obtained is the slight elevation of methionine with nanogold, which perhaps with prolonged exposure the closest resemblance can be found in the profile of a MAT deficiency. A MAT deficiency can be caused by genetic defects, but decreased glutathione concentrations and increased radicals also inhibit MAT. This inhibition occurs to facilitate increased lipoic acid, which is involved in the production of antioxidants and increases the formation of sulphur proteins that are involved in the electron transport chain.

4.5 Heavy metal poisoning:

Taking into consideration the most prominent results in this study, the evidence starts to correlate with other heavy metal findings, albeit most of the studies were not conducted at nanoform but produced a similar profile, which probes further questioning. It is also speculated then whether these particles possibly disassemble and breakdown, losing their stability obtained with citrate during synthesis.

Nanogold particles are marketed and sold as a stabilised citrate-gold complex (Sigma-Aldrich product no: 741949-777137), but it could be proposed that the citrate is easily displaced from this complex, due to bonds with higher affinity within the body. Modern studies indicate that transition metals act as catalysts in the oxidative reactions of biological macromolecules and therefore the toxic nature observed could be associated with oxidative tissue damage (Ercal *et al.* 2001). Redox-active metals, such as iron, chromium and copper, undergo redox cycling whereas redox-inactive metals, such as lead, mercury and cadmium cause depletion of antioxidants, more specifically the thiol-containing antioxidants (such as metallothionein) and enzymes (Lindeque *et al.* 2010). The elevated production of reactive oxygen species (ROS) such as hydroxyl radical (HO), superoxide radical (O^{2-}) or hydrogen peroxide (H_2O_2) could be due to either redox – active or redox-inactive metals (Ercal *et al.* 2001). This additional generation of ROS can overpower the cells' intrinsic antioxidant defences, and result in a condition known as “oxidative stress“. Cells under oxidative stress have decreased function due to lesions to lipids, proteins and DNA, caused by ROS. Therefore, it is suggested that metal-induced oxidative stress in cells can be partially responsible for the toxic effects of heavy metals. Ercal *et al*. (2001) also reported that many studies are devoted to determining the effect of antioxidant supplementation to counteract heavy metal exposure. The importance of using antioxidants in heavy metal poisoning is most definitely of note today and thus the biochemical mechanisms for metal-induced oxidative stress should be investigated further.

One of the earlier studies, is that of Kennedy and Lever (1972) who investigated complexes of pyridine thiols and some of their oxygen analogs, which were cadmium (II), nickel(II), mercury(II), platinum(II), bismuth(III) and tin(IV) and concluded that bonding occurred rather at the sulfur site than the nitrogen atom as expected. It also states that the direction of electron transfer is from sulfur to metal (Kennedy & Lever, 1972).

A more recent publication by Jan *et al*. (2015) describes the affinity for heavy metals for L-cysteine and related compounds due to the abundance of thiol groups and how effective L-cysteine is used in the removal of heavy metals such as mercury, cadmium, lead and copper, due to its highly reactive thiol side chain.

Rafati-Rahimzadeh *et al.* (2014) reported in their mercury poisoning studies that biological tissues such as hair and nails were tested for high levels of methyl mercury, since these samples contain sulfhydryl groups and mercury tends to bind to sulfur compounds. Research also mentioned by Rafati-Rahimzadeh *et al.* (2014) stated that esters of dimercaptosuccinic acid (DMSA) may be appropriate antidotes for heavy metal poisoning, since the sulfhydryl groups thereof bound tightly to heavy metal elements and mercury specifically have been successfully removed with DMSA from kidneys and bile, which further cements the finding that heavy metals tend to attach to sulfhydryl- groups and interact radically with sulfur-containing compounds overall.

According to Duruibe *et al*. (2007) the poisoning effects of heavy metals are due to their interference with the normal metabolic processes and when in the presence of stomach acid, these metals convert easily to their stable oxidation states (Zn2+, Pb2+, Cd2+, As2+, As3+, Hg2+ and Ag+) and bind to proteins and enzymes to form strong and stable chemical bonds. 25

As mentioned before the original element (hydrogen or other metal) on the protein or enzyme is substituted by the poisoning metal. In the case of enzymes the lock-and-key mechanism is disrupted and inhibits enzyme function and in the case of protein-metal bonds it acts as a new substrate and interacts with a metabolic enzyme, all leading to a deviation of the normal body biochemistry (Duruibe *et al.* 2007).

Chapter 5: Conclusion

Herewith, a final conspectus of the findings and the conclusions derived in answer to the questions raised previously in Section 2.6:

1. What is the overall effect of nanogold on the metabolome of rodents?
2. Which metabolic pathways are affected by nanogold (from a systemic point of view)?
3. Can the metabolic changes be related to toxicity?

The overall effect of a nanogold drug vehicle (as investigated with regards to the metabolome of rodents), is the notable change in several major metabolic pathways with altered concentration levels of numerous significant amino acids, acylcarnitines and organic acids after treatment . These affected metabolites play vital roles in their respective pathways and can lead to systemic consequence and produce a phenotype similar to that observed with heavy metal poisoning. The pathways linked to energy metabolism (glycolysis, Krebs-cycle and electron transport chain) were altered, indicating effect on mitochondrial function with a decrease in ATP production, which results in overall fatigue and (in severe circumstance) muscle involvement. An induced thiamine deficiency can occur with long term treatment due to the continuous inhibition of pyruvate dehydrogenase, which may have an impact on the cardiovascular and nervous system. The branched chain amino acid metabolism was also affected by nanogold intervention, with increased levels of valine and 2-OH-isovaleric acid, mimicking the profile of the inhibition of the enzyme branched chain 2-ketoacid dehydrogenase, which can lead to impaired liver and muscle function. It is apparent from the findings that the metabolism of sulphur-containing amino acids is affected, with the greatest influence on methionine which can impact the hepatic system.

The common thread in these affected pathways appears to be the metabolism of lipoic acid, which is a sulphur-rich compound, mainly present in the mitochondria and involved in five redox reactions within the human body. These reactions include four 2-Ketoacid dehydrogenase enzymes and the glycine cleavage system. Two of these enzymes (α-ketoglutarate dehydrogenase and pyruvate dehydrogenase) are native to energy metabolism, while the other three involve amino acid metabolism, branched chain ketoacid dehydrogenase and the glycine cleavage system (Mayr *et al.* 2014). Lipoic acid synthesis within the mitochondria occurs via a series of reactions along the fatty acid synthesis type II (FAS II), the first being the relocation of an octanoyl group to an acceptor protein, namely the glycine cleavage H protein, followed by lipoate synthesis by the transfer of two sulfhydryl groups to octanoic acid and a final transfer from the H-protein to 2-oxoacid dehydrogenases.

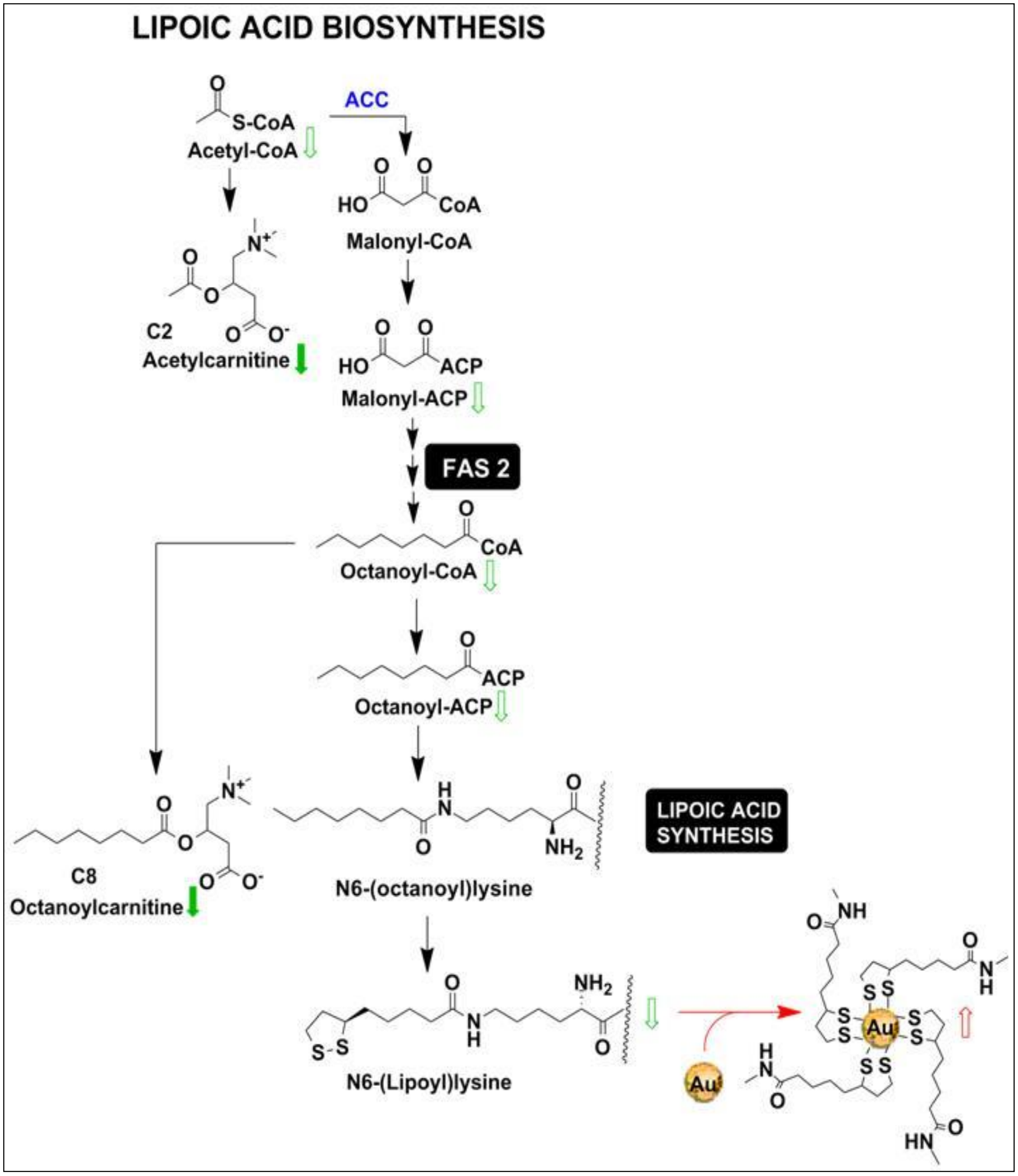

Figure 5.1: A possible mechanism for the inactivation of lipoic acid synthesis by nanogold binding.

The involvement of lipoic acid is supported by the knowledge of heavy metal affinity towards the sulphur active sites, displacing the original bond and causing an imbalance in the subsequent metabolism. Figure 5.1 provides a possible mechanism for the inactivation of lipoic acid synthesis by nanogold binding. Numerous studies surrounding this bonding of heavy metal with thiol-containing compounds exist (as discussed in Chapter 4) and the metabolic profiles obtained are very similar to the profile obtained here with nanogold. The closest related effect is that of arsenic poisoning.

Enzymes that were shown to be inhibited by arsenic include pyruvate dehydrogenase, 2-ketoglutarate dehydrogenase, branched chain 2-ketoacide dehydrogenase, glycine cleavage system and methyltransferases (the enzyme responsible for the transfer of the methyl group of S-adenosylmethionine (SAM)).

As it is evident that there are some relevant perturbations along certain metabolic pathways, pertaining to lipoic acid involvement, as an immediate consequence of nanogold intervention. Perhaps one should start assessing these findings from the knowledge that gold in essence is a heavy metal and that these perturbations caused by it in nanoform might still be directly linked to that fact. Bearing in mind a previously mentioned speculation of nanoparticles disassembling from the citrate in the solution and acting freely as gold atoms. Although there is no exclusivity to the nanogold-sulphur bond and the affinity between any sulphur-containing compound and a heavy metal is quite strong in general, the affinity of nanogold toward lipoic acid deserves attention.

Low concentrations of most heavy metals are essential to biological function, but the underlying mechanism of heavy metal poisoning is the fact that in higher doses these elements bind to unsuitable protein sites by displacing the original metals (Jaishankar *et al.* 2014), which in turn leads to the malfunctioning of cells and general symptoms of metal toxicity.

The metabolites highlighted in Chapter 4 thus provide some insight into the safety of nanogold particles as a potential drug delivery tool. The metabolism is affected in such a manner that there is strong evidence for possible toxicity, given the right set of variables including patient health, dose and exposure. Campion *et al*. (2013) researched novel ways to improve the detection of organ specific toxicity. The aforementioned article reviews the meeting held by the Northeast Society of Toxicology titled ‘Translational Biomarkers in Toxicology’ and how biomarkers are identified and validated. The traditional biomarkers in liver impairment, kidney malfunction and cardiovascular toxicity is being thought of as inadequate and Campion *et al.* (2013) emphasises the need for histopathology in addition as a true reflection of toxicity. The studies done by Rambanapasi (2015) which included the examination of tissues (heart, spleen, lungs, liver and kidney) and found no overt toxicity, with assessment of toxic biomarkers and general health indicators. Bioaccumulation, however was detected in most of the tissues, with the liver retaining the highest amount of nanogold (in µg). This bioaccumulation of the particles could clarify some of the lowered levels of metabolites found across the different time points of collection. Even though no hepatoxicity or nephrotoxicity was found by Rambanapasi (2015), the thiol-binding and lipoic acid involvement alone could induce toxicological effects similar to heavy metal poisoning.

I) Hypothesis:

The interaction of gold nanoparticles with sulphur-containing compounds will occur readily within the biochemistry of the body and intravenous administration of gold nanoparticles will negatively impact the metabolism of an animal system by suppressing the function of lipoic acid.

I) Critical assessment of study:

The study involved a once-off administration of nanogold, therefore increased exposure and dosage may lead to more elucidative results. Sample collection proved to be troublesome and many samples were excluded, due to insufficient volume or excess of debris. This should be addressed in further studies. Furthermore, though urine is a good matrix to identify any effect on the metabolome, it is an inceptive step in assessing the consequence of a nanogold vehicle and merely pointing to the areas of interest, thus tissue specific metabolic profiling is required.

II) Further studies:

The involvement of lipoic acid needs to be verified with histopathology and enzyme analysis, to eliminate circumstantial evidence If the hypothesis is valid and proven correct with long term experiment, then perhaps a study into most appropriate coatings of nanoparticles could be launched. More specifically, the potential of lipoic acid as a coating itself, could be investigated as its reaction with nanogold appears to be secure and the implementation thereof as a coating could greatly aid the therapeutic platform of gold nanoparticles.

Bibliography:

Abdelhalim, M.A.K. and Moussa, S.A.A., 2013. The gold nanoparticle size and exposure duration effect on the liver and kidney function of rats: In vivo. *Saudi journal of biological sciences*, *20*(2):177-181.

Agilent Technologies Inc. 2016 Fundamentals of Gas Chromatography: Hardware [PowerPoint Slides] Retrieved from https://www.agilent.com/cs/library/slidepresentation/public/5991-5423EN_Agilent_GC_Hardware_English_v2.pptx

Avila, M.A., Garcıa-Trevijano, E.R., Lu, S.C., Corrales, F.J. and Mato, J.M., 2004. Methylthioadenosine. *The international journal of biochemistry & cell biology*, *36*(11):2125-2130.

Bajak, E., Fabbri, M., Ponti, J., Gioria, S., Ojea-Jiménez, I., Collotta, A., Mariani, V., Gilliland, D., Rossi, F. and Gribaldo, L., 2015. Changes in Caco-2 cells transcriptome profiles upon exposure to gold nanoparticles. *Toxicology letters*, *233*(2):187-199.

Bathe, O. and Farshidfar, F., 2014. From genotype to functional phenotype: unravelling the metabolomic features of colorectal cancer. *Genes*, *5*(3):.536-560.

Bingol, K., 2018. Recent Advances in Targeted and Untargeted Metabolomics by NMR and MS/NMR Methods. *High-throughput*, *7*(2), p.9.

Brust, M., Walker, M., Bethell, D., Schiffrin, D.J. and Whyman, R., 1994. Synthesis of thiol-derivatised gold nanoparticles in a two-phase liquid–liquid system. *Journal of the Chemical Society, Chemical Communications*, (7):801-802.

Cajka, T. and Fiehn, O., 2015. Toward merging untargeted and targeted methods in mass spectrometry-based metabolomics and lipidomics. *Analytical chemistry*, *88*(1):524-545.

Cajka, T., Riddellova, K., Tomaniova, M. and Hajslova, J., 2011. Ambient mass spectrometry employing a DART ion source for metabolomic fingerprinting/profiling: a powerful tool for beer origin recognition. *Metabolomics*, *7*(4):500-508.

Calandra, P., Calogero, G., Sinopoli, A. and Gucciardi, P.G., 2010. Metal nanoparticles and carbon-based nanostructures as advanced materials for cathode application in dye-sensitized solar cells. *International Journal of Photoenergy*, *2010*.

Chang, C.F., Chou, H.T., Chuang, J.L., Chuang, D.T. and Huang, T.H., 2002. Solution structure and dynamics of the lipoic acid-bearing domain of human mitochondrial branched-chain α-keto acid dehydrogenase complex. *Journal of Biological Chemistry*, *277*(18):15865-15873.

Cho, W.S., Cho, M., Jeong, J., Choi, M., Han, B.S., Shin, H.S., Hong, J., Chung, B.H., Jeong, J. and Cho, M.H., 2010. Size-dependent tissue kinetics of PEG-coated gold nanoparticles. *Toxicology and applied pharmacology*, *245*(1):116-123.

Choi, J.E., Kim, S., Ahn, J.H., Youn, P., Kang, J.S., Park, K., Yi, J. and Ryu, D.Y., 2010. Induction of oxidative stress and apoptosis by silver nanoparticles in the liver of adult zebrafish. *Aquatic Toxicology*, *100*(2):151-159.

Clarke, C.J. and Haselden, J.N., 2008. Metabolic profiling as a tool for understanding mechanisms of toxicity. *Toxicologic Pathology*, *36*(1):140-147.

Conde, J., Larguinho, M., Cordeiro, A., Raposo, L.R., Costa, P.M., Santos, S., Diniz, M.S., Fernandes, A.R. and Baptista, P.V., 2014. Gold-nanobeacons for gene therapy: evaluation of genotoxicity, cell toxicity and proteome profiling analysis. *Nanotoxicology*, *8*(5):521-532.

Dang, V.T. and Werstuck, G.H., 2016. Metabolomics-based biomarkers of the pathogenesis of atherosclerosis. *Biomarkers Journal*, *2*(10).

De Jong, W.H. and Borm, P.J., 2008. Drug delivery and nanoparticles: applications and hazards. *International journal of nanomedicine*, *3*(2):133.

Dreaden, E.C., Alkilany, A.M., Huang, X., Murphy, C.J. and lystvet, M.A., 2012. The golden age: gold nanoparticles for biomedicine. *Chemical Society Reviews*, *41*(7):740-2779.

Dreher, K.L., 2004. Health and environmental impact of nanotechnology: toxicological assessment of manufactured nanoparticles. *Toxicological Sciences*, *77*(1):3-5.

Duruibe, J.O., Ogwuegbu, M.O.C. and Egwurugwu, J.N., 2007. Heavy metal pollution and human biotoxic effects. *International Journal of physical sciences*, *2*(5):112-118.

Ellinger, J.J., Chylla, R.A., Ulrich, E.L. and Markley, J.L., 2013. Databases and software for NMR-based metabolomics. *Current Metabolomics*, *1*(1):28-40.

El-Sayed, I.H., Huang, X. and El-Sayed, M.A., 2006. Selective laser photo-thermal therapy of epithelial carcinoma using anti-EGFR antibody conjugated gold nanoparticles. *Cancer letters*, *239*(1):129-135.

Engelking, L.R., 2010. *Textbook of Veterinary Physiological Chemistry, Updated 2/e*. Academic Press.

Ercal, N., Gurer-Orhan, H. and Aykin-Burns, N., 2001. Toxic metals and oxidative stress part I: mechanisms involved in metal-induced oxidative damage. *Current topics in medicinal chemistry*, *1*(6):529-539.

Ercal, N., Gurer-Orhan, H. and Aykin-Burns, N., 2001. Toxic metals and oxidative stress part I: mechanisms involved in metal-induced oxidative damage. *Current topics in medicinal chemistry*, *1*(6):529-539.

Finkelstein, J.D., 1990. Methionine metabolism in mammals. *The Journal of nutritional biochemistry*, *1*(5):.228-237.

Frens, G., 1972. Particle size and sol stability in metal colloids. *Kolloid-Zeitschrift und Zeitschrift für Polymere*, *250*(7):736-741.

Fujiwara, K., Okamura-Ikeda, K. and Motokawa, Y., 1984. Mechanism of the glycine cleavage reaction. Further characterization of the intermediate attached to H-protein and of the reaction catalyzed by T-protein. *Journal of Biological Chemistry*, *259*(17):10664-10668.

GAO, J., Huang, X., Liu, H., Zan, F. and Ren, J., 2012. Colloidal stability of gold nanoparticles modified with thiol compounds: bioconjugation and application in cancer cell imaging. *Langmuir*, *28*(9):4464-4471.

Gerber, A., Bundschuh, M., Klingelhofer, D. and Groneberg, D.A., 2013. Gold nanoparticles: recent aspects for human toxicology. *Journal of occupational medicine and toxicology*, *8*(1):32.

Ghosh, D. and Chattopadhyay, N., 2013. Gold nanoparticles: acceptors for efficient energy transfer from the photoexcited fluorophores. *Optics and Photonics Journal*, *3*(01):18.

Gioria, S., Lobo Vicente, J., Barboro, P., La Spina, R., Tomasi, G., Urbán, P., Kinsner-Ovaskainen, A., François, R. and Chassaigne, H., 2016. A combined proteomics and metabolomics approach to assess the effects of gold nanoparticles in vitro. *Nanotoxicology*, *10*(6), pp.736-748.

Halket, J.M., Waterman, D., Przyborowska, A.M., Patel, R.K., Fraser, P.D. and Bramley, P.M., 2004. Chemical derivatization and mass spectral libraries in metabolic profiling by GC/MS and LC/MS/MS. *Journal of experimental botany*, *56*(410):219-243.

Hanauer, M., Pierrat, S., Zins, I., Lotz, A. and Sönnichsen, C., 2007. Separation of nanoparticles by gel electrophoresis according to size and shape. *Nano letters*, *7*(9):2881-2885

Hau, J., 2008. Animal models for human diseases. In *Sourcebook of models for biomedical research* (p. 3-8). Humana Press.

Herizchi, R., Abbasi, E., Milani, M. and Akbarzadeh, A., 2016. Current methods for synthesis of gold nanoparticles. *Artificial cells, nanomedicine, and biotechnology*, *44*(2):596-602.

Hrycyna, C., 2009. CHM333 Lecture 31: Pyruvate Dehydrogenase Complex. [PowerPoint Slides] Retrieved: http://www.chem.purdue.edu/courses/chm333/Fall%202009/Lectures/Fall%202009%20Lecture%2031.pdf

Huang, X. and El-Sayed, M.A., 2010. Gold nanoparticles: optical properties and implementations in cancer diagnosis and photothermal therapy. *Journal of advanced research*, *1*(1):13-28.

Huang, X. and El-Sayed, M.A., 2010. Gold nanoparticles: optical properties and implementations in cancer diagnosis and photothermal therapy. *Journal of advanced research*, *1*(1):13-28.

Huang, X., Jain, P.K., El-Sayed, I.H. and El-Sayed, M.A., 2008. Plasmonic photothermal therapy (PPTT) using gold nanoparticles. *Lasers in medical science*, *23*(3):217.

Imbraguglio, D., Giovannozzi, A.M. and Rossi, A., 2013. Nanometrology.

Jain, S., Hirst, D.G. and O'Sullivan, J.M., 2012. Gold nanoparticles as novel agents for cancer therapy. *The British journal of radiology*, *85*(1010:101-113.

Jan, A., Azam, M., Siddiqui, K., Ali, A., Choi, I. and Haq, Q., 2015. Heavy metals and human health: mechanistic insight into toxicity and counter defense system of antioxidants. *International journal of molecular sciences*, *16*(12):29592-29630.

Kanani, H., Chrysanthopoulos, P.K. and Klapa, M.I., 2008. Standardizing GC–MS metabolomics. *Journal of Chromatography B*, *871*(2), pp.191-201.

Kennedy, B.P. and Lever, A.B.P., 1972. Studies of the Metal–Sulfur Bond. Complexes of the Pyridine Thiols. *Canadian Journal of Chemistry*, *50*(21):3488-3507.

Khan, I., Saeed, K. and Khan, I., 2017. Nanoparticles: Properties, applications and toxicities. *Arabian Journal of Chemistry*.

Kochi, H. and Kikuchi, G., 1976. Mechanism of reversible glycine cleavage reaction in Arthrobacter globiformis: function of lipoic acid in the cleavage and synthesis of glycine. *Archives of biochemistry and biophysics*, *173*(1):71-81.

Kodiha, M., Wang, Y.M., Hutter, E., Maysinger, D. and Stochaj, U., 2015. Off to the organelles-killing cancer cells with targeted gold nanoparticles. *Theranostics*, *5*(4):357.

Kogan, M.J., Bastus, N.G., Amigo, R., Grillo-Bosch, D., Araya, E., Turiel, A., Labarta, A., Giralt, E. and Puntes, V.F., 2006. Nanoparticle-mediated local and remote manipulation of protein aggregation. *Nano letters*, *6*(1), pp.110-115.

Kohlschütter, A., Behbehani, A., Langenbeck, U., Albani, M., Heidemann, P., Hoffmann, G., Kleineke, J., Lehnert, W. and Wendel, U., 1982. A familial progressive neurodegenerative disease with 2-oxoglutaric aciduria. *European journal of paediatrics*, *138*(1):32-37.

Koole, R., Groeneveld, E., Vanmaekelbergh, D., Meijerink, A. and de Mello Donegá, C., 2014. Size effects on semiconductor nanoparticles. In *Nanoparticles* (p13-51). Springer, Berlin, Heidelberg.

Lasagna-Reeves, C., Gonzalez-Romero, D., Barria, M.A., Olmedo, I., Clos, A., Ramanujam, V.S., Urayama, A., Vergara, L., Kogan, M.J. and Soto, C., 2010. Bioaccumulation and toxicity of gold nanoparticles after repeated administration in mice. *Biochemical and biophysical research communications*, *393*(4):649-655.

Lee, H., Lee, M.Y., Bhang, S.H., Kim, B.S., Kim, Y.S., Ju, J.H., Kim, K.S. and Hahn, S.K., 2014. Hyaluronate–gold nanoparticle/tocilizumab complex for the treatment of rheumatoid arthritis. *ACS nano*, *8*(5):4790-4798.

Leite-Silva, V.R., Le Lamer, M., Sanchez, W.Y., Liu, D.C., Sanchez, W.H., Morrow, I., Martin, D., Silva, H.D., Prow, T.W., Grice, J.E. and Roberts, M.S., 2013. The effect of formulation on the penetration of coated and uncoated zinc oxide nanoparticles into the viable epidermis of human skin in vivo. *European Journal of Pharmaceutics and Biopharmaceutics*, *84*(2):297-308.

Li, J.J., Hartono, D., Ong, C.N., Bay, B.H. and Yung, L.Y.L., 2010. Autophagy and oxidative stress associated with gold nanoparticles. *Biomaterials*, *31*(23):5996-6003.

Lin, L., Yu, Q., Yan, X., Hang, W., Zheng, J., Xing, J. and Huang, B., 2010. Direct infusion mass spectrometry or liquid chromatography mass spectrometry for human metabonomics. A serum metabonomic study of kidney cancer. *Analyst*, *135*(11):.2970-2978.

Lindeque, J.Z., Matthyser, A., Mason, S., Louw, R. and Taute, C.J.F., 2018. Metabolomics reveals the depletion of intracellular metabolites in HepG2 cells after treatment with gold nanoparticles. *Nanotoxicology*, *12*(3):251-262.

Liu, D., Yang, F., Xiong, F. and Gu, N., 2016. The smart drug delivery system and its clinical potential. *Theranostics*, *6*(9):1306.

Liu, D.C., Raphael, A.P., Sundh, D., Grice, J.E., Soyer, H.P., Roberts, M.S. and Prow, T.W., 2012. The human *stratum corneum* prevents small gold nanoparticle penetration and their potential toxic metabolic consequences. *Journal of Nanomaterials*, *2012*:7.

Liu, Z., Wang, L., Zhang, L., Wu, X., Nie, G., Chen, C., Tang, H. and Wang, Y., 2016. Metabolic Characteristics of 16HBE and A549 Cells Exposed to Different Surface Modified Gold Nanorods. *Advanced healthcare materials*, *5*(18):2363-2375.

Lu, S.C., Tsukamoto, H. and Mato, J.M., 2002. Role of abnormal methionine metabolism in alcoholic liver injury. *Alcohol*, *27*(3):155-162.

Lystvet, S.M., 2013. Emergent properties of protein-gold nanoconstructs for biomedical applications.

Mascarenhas, B.R., Granda, J.L. and Freyberg, R.H., 1972. Gold metabolism in patients with rheumatoid arthritis treated with gold compounds—reinvestigated. *Arthritis & Rheumatism: Official Journal of the American College of Rheumatology*, *15*(4):391-402.

Mayr, J.A., Feichtinger, R.G., Tort, F., Ribes, A. and Sperl, W., 2014. Lipoic acid biosynthesis defects. *Journal of inherited metabolic disease*, *37*(4):553-563.

National Nanotechnology Initiative, 2014. Official website of the United States National Nanotechnology Initiative. Available at https://www.nano.gov/. [Accessed 12 September 2018]

Oregan State University, 2008. [Lecture winter 08] http://oregonstate.edu/instruct/bb451/winter08/lectures/citricacidcycle.html

Rafati-Rahimzadeh, M., Rafati-Rahimzadeh, M., Kazemi, S. and Moghadamnia, A.A., 2014. Current approaches of the management of mercury poisoning: need of the hour. *DARU Journal of Pharmaceutical Sciences*, *22*(1):46.

Rambanapasi, C., 2015. *An assessment of the biodistribution, biopersistence and toxicity of gold nanoparticles* (Doctoral dissertation, North-West University (South Africa), Potchefstroom Campus).

Roberts, L.D., Souza, A.L., Gerszten, R.E. and Clish, C.B., 2012. Targeted metabolomics. *Current protocols in molecular biology*, *98*(1):30-2.

Roessner, U. and Beckles, D.M., 2009. Metabolite measurements. In *Plant metabolic networks* (p. 39-69). Springer, New York, NY.

Saha, P.P., Bhowmik, T., Dasgupta, A.K. and Gomes, A., 2014. Nano gold conjugation, anti-arthritic potential and toxicity studies of snake Naja Kaouthia (Lesson, 1831) venom protein toxin NKCT1 in male albino rats and mice.

Saraiva, C., Praça, C., Ferreira, R., Santos, T., Ferreira, L. and Bernardino, L., 2016. Nanoparticle-mediated brain drug delivery: overcoming blood–brain barrier to treat neurodegenerative diseases. *Journal of Controlled Release*, *235*:34-47.

Schnackenberg, L.K., Sun, J. and Beger, R.D., 2012. Metabolomics techniques in nanotoxicology studies. In *Nanotoxicity* (p.141-156). Humana Press, Totowa, NJ.

Scholz, M. and Selbig, J., 2007. Visualization and analysis of molecular data. In *Metabolomics* (p. 87-104). Humana Press.

Schymanski, E.L., Jeon, J., Gulde, R., Fenner, K., Ruff, M., Singer, H.P. and Hollender, J., 2014. Identifying small molecules via high resolution mass spectrometry: communicating confidence.

Seifuddin, F., Pirooznia, M., Judy, J.T., Goes, F.S., Potash, J.B. and Zandi, P.P., 2013. Systematic review of genome-wide gene expression studies of bipolar disorder. *BMC psychiatry*, *13*(1):213.

Sharma, S.S., Schat, H. and Vooijs, R., 1998. In vitro alleviation of heavy metal-induced enzyme inhibition by proline. *Phytochemistry*, *49*(6):1531-1535.

Sperling, R.A., 2008. Surface modification and functionalization of colloidal nanoparticles.
Steuer, R., 2007. Computational approaches to the topology, stability and dynamics of metabolic networks. *Phytochemistry*, *68*(16-18):2139-2151.

Strömme, J.H., Borud, O. and Moe, P.J., 1976. Fatal lactic acidosis in a newborn attributable to a congenital defect of pyruvate dehydrogenase. *Pediatric research*, *10*(1):62.

Tiwari, G., Tiwari, R., Sriwastawa, B., Bhati, L., Pandey, S., Pandey, P. and Bannerjee, S.K., 2012. Drug delivery systems: An updated review. *International journal of pharmaceutical investigation*, *2*(1), p.2.

Tomaszewska, E., Soliwoda, K., Kadziola, K., Tkacz-Szczesna, B., Celichowski, G., Cichomski, M., Szmaja, W. and Grobelny, J., 2013. Detection limits of DLS and UV-Vis spectroscopy in characterization of polydisperse nanoparticles colloids. *Journal of Nanomaterials*, *2013*, p.60.

Truong, L., Tilton, S.C., Zaikova, T., Richman, E., Waters, K.M., Hutchison, J.E. and Tanguay, R.L., 2013. Surface functionalities of gold nanoparticles impact embryonic gene expression responses. *Nanotoxicology*, *7*(2):192-201.

Turkevich, J., Stevenson, P.C. and Hiller, J., 1951. Synthesis of gold nanoparticles Turkevich method. *Discuss. Faraday Soc*, *11*:55-75.

Ulrey, C.L., Liu, L., Andrews, L.G. and Tollefsbol, T.O., 2005. The impact of metabolism on DNA methylation. *Human molecular genetics*, *14*(suppl_1):R139-R147.

Vendemiale, G., Altomare, E., Trizio, T., Le Grazie, C., Di Padova, C., Salerno, M.T., Carrieri, V. and Albano, O., 1989. Effects of oral S-adenosyl-L-methionine on hepatic glutathione in patients with liver disease. *Scandinavian journal of gastroenterology*, *24*(4):407-415.

Verzele, M., 1964. The choice of carrier gas in preparative gas chromatography. *Journal of Chromatography A*, *15*:482-487.

Vithiya, K. and Sen, S., 2011. Biosynthesis of nanoparticles. *International Journal of Pharmaceutical Sciences and Research*, *2*(11):2781.

Wang, B., Chen, N., Wei, Y., Li, J., Sun, L., Wu, J., Huang, Q., Liu, C., Fan, C. and Song, H., 2012. Akt signalling-associated metabolic effects of dietary gold nanoparticles in Drosophila. *Scientific reports*, *2*:563.

Wang, X., Wang, D., Wang, Y., Zhang, P., Zhou, Z. and Zhu, W., 2016. A combined non-targeted and targeted metabolomics approach to study the stereoselective metabolism of benalaxyl enantiomers in mouse hepatic microsomes. *Environmental pollution*, *212*:358-365.

Warrack, B.M., Hnatyshyn, S., Ott, K.H., Reily, M.D., Sanders, M., Zhang, H. and Drexler, D.M., 2009. Normalization strategies for metabonomic analysis of urine samples. *Journal of Chromatography B*, *877*(5-6):547-552.

Wilson, K. and Walker, J. eds., 2010. *Principles and techniques of biochemistry and molecular biology*. Cambridge university press.

Xu, Y. and Goodacre, R., 2012. Multiblock principal component analysis: an efficient tool for analyzing metabolomics data which contain two influential factors. *Metabolomics*, *8*(1):37-51.

Yan, D., Afifi, L., Jeon, C., Trivedi, M., Chang, H.W., Lee, K. and Liao, W., 2017. The metabolomics of psoriatic disease. *Psoriasis (Auckland, NZ)*, *7*:1.

Yeh, D.M., Huang, C.F., Chen, C.Y., Lu, Y.C. and Yang, C.C., 2008. Localized surface plasmon-induced emission enhancement of a green light-emitting diode. *Nanotechnology*, *19*(34):345201.

Yeh, Y.C., Creran, B. and Rotello, V.M., 2012. Gold nanoparticles: preparation, properties, and applications in bionanotechnology. *Nanoscale*, *4*(6):1871-1880.

Zhao, P., Li, N. and Astruc, D., 2013. State of the art in gold nanoparticle synthesis. *Coordination Chemistry Reviews*, *257*(3-4):638-665.

Annexure A: Repeatability

Herewith, a sample of the repeatability results obtained during the course of the study, from pooled samples from the urine collected. These results validated the precision and validity of the analytical aspects of the study. Statistical intervention performed here only included a pre-processing step where log scaling was performed and all the zeroes and problematic analytes were removed. A confidence interval of 80% was implemented and the variance fell within acceptable FDA guidelines (RSD ≤ 0.3).

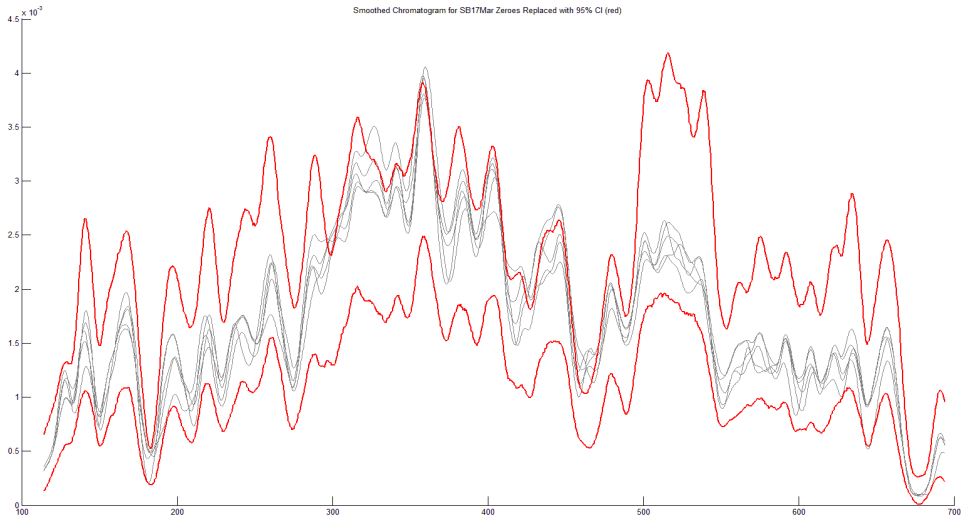

Zeroes replaced

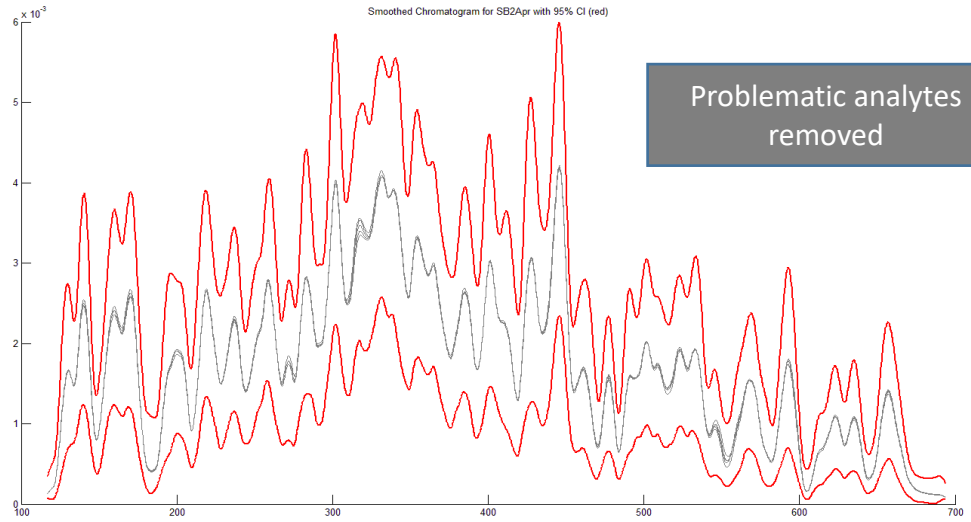

Problematic analytes removed

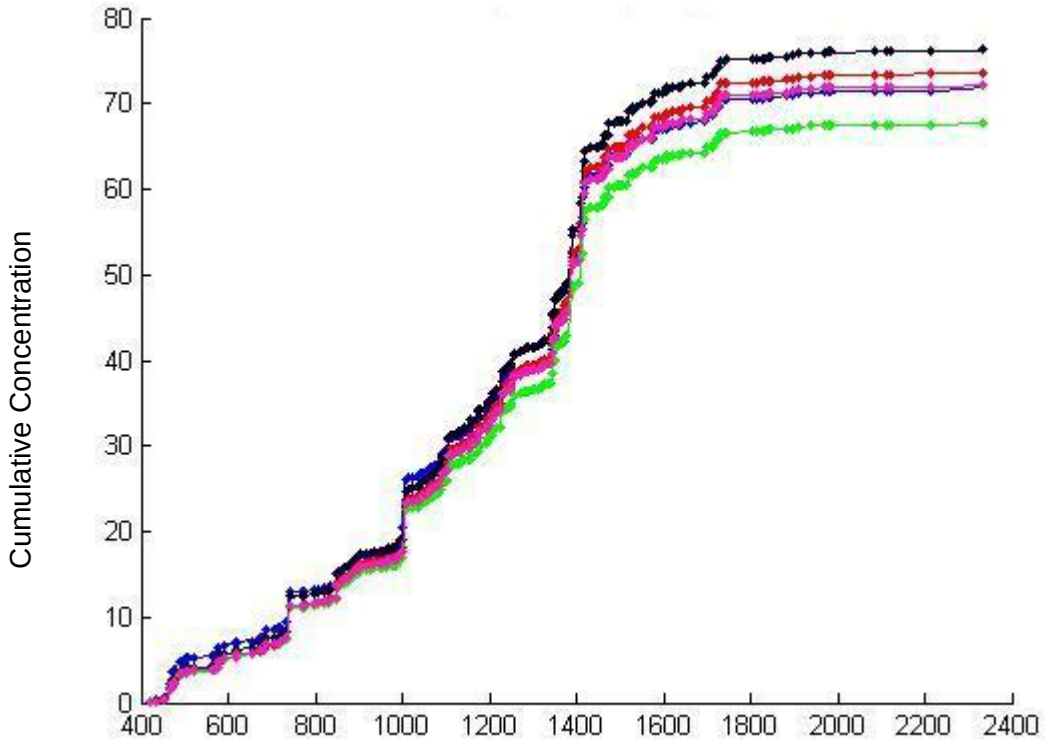

The dots in the above figure represent the cumulative concentrations at the associated retention time of each replicate. In other words, at every retention time its correlating concentration is added to the previous one, thus any error will be accumulated and carried over to all the succeeding retention times, thus seeming greater at later retention times. The lines lie in close proximity to another, thus indicating that the data and techniques were notably repeatable.

The scatter plot below is of coefficient variance plotted against metabolite mean values. The smaller the concentrations, the greater frequency of “noise” is expected. The higher concentrations are therefore of interest, to determine the actual degree of repeatability. The red line represents the 30% cut-off line for metabolite CV, established by the FDA. All the CV-values are scattered below the cut-off line, indicating satisfactory repeatability

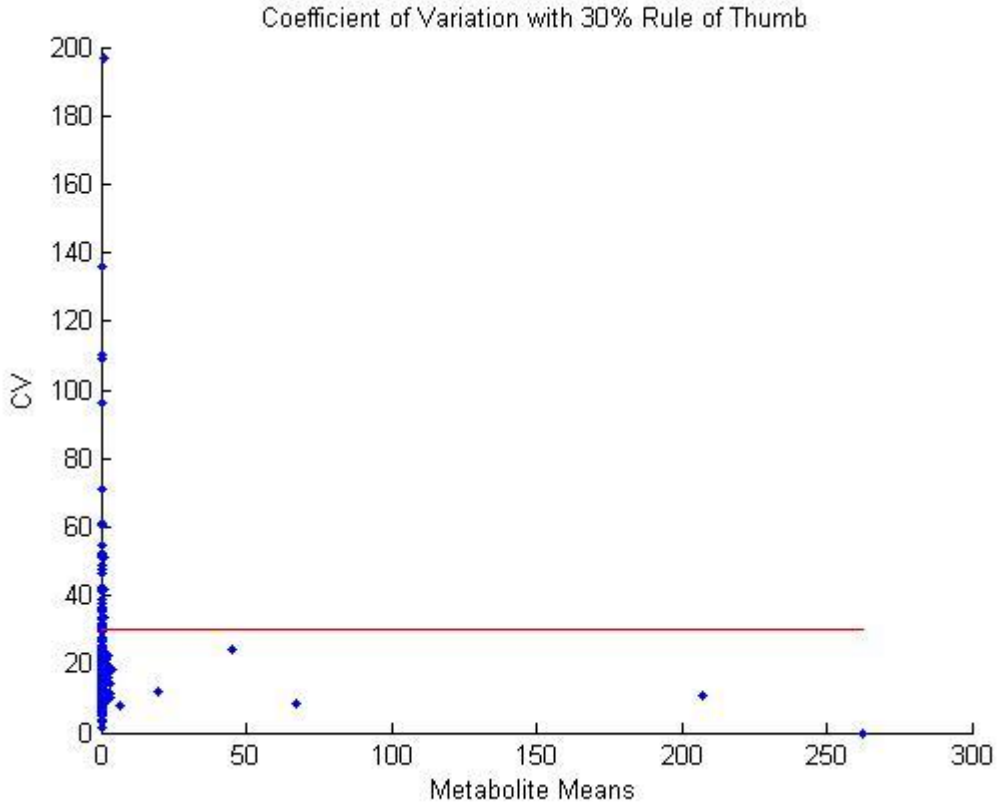

Annexure B: Synthesis of nanogold particles

Herewith, an excerpt (p.59 & 60) from the PhD thesis submitted by Dr Clinton Rambanapasi in 2015 describing the synthesis of the nanoparticles used in this study, by an adapted Turkevich-Frens method.

3.4. Experimental Section

4.1. Preparation of AuNPs and Dual-Radiolabeled AuNPs

Elemental gold (24 carat) was purchased from Cape Precious Metals Holding Pvt. Ltd., Johannesburg, South Africa. 1,5-[^{14}C] citric acid (concentration: 3.7 GBq/mL; specific activity: 2.07 GBq/mmol) was purchased from American Radiolabeled Chemicals, Inc. (St. Louis, MO, USA). Hydrochloric acid (HCl, 37%), nitric acid (HNO_3, 68%) (used to prepare aqua regia using an HCl:HNO_3 in a 3:1 ratio) and trisodium citrate ($Na_3C_6O_7H_5{\cdot}H_2O$), were all of analytical grade and purchased from Merck (Billerica, MA, USA). Deionized water (resistance >18 MΩ) was prepared by an in-house ultrapure water system (Merck Millipore, Billerica, MA, USA). All chemicals, except for the 1,5-[^{14}C] citric acid (deprotonated using NaOH to make trisodium citrate), were used as received without purification. All radioactive materials were produced and handled at the South African Nuclear Energy Corporation (Necsa, Pelindaba, South Africa) facilities and laboratories.

Two 5-mg samples of natural gold (^{197}Au) metal were weighed using an analytical balance (5-decimal place Mettler Toledo). One sample was used as natural gold, while the other sample (target) was irradiated in the SAFARI 1 20 MW research reactor situated at Necsa in a hydraulic position with a neutron flux of 0.5×10^{14} n·cm^{-2}·s^{-1} for 20 min to obtain ^{198}Au. Both Au samples were dissolved in aqua regia (5 mL) dried down (using heat) and reconstituted in 0.5–1 mL 0.005 N HCl to yield $HAuCl_4{\cdot}HAuCl_4$ and [^{198}Au]$HAuCl_4$-[^{198}Au]$HAuCl_4$ in 0.05 N HCl [45], the starting material in the synthesis of AuNPs. The activity of the [^{198}Au]$HAuCl_4$-[^{198}Au]$HAuCl_4$ was measured using a CRC-15R dose calibrator (Capintec Inc., Ramsey, NJ, USA). The radioactive $HAuCl_4$ sample was used to synthesize the dual-radiolabeled AuNPs. The activity concentration of 1,5-[^{14}C]trisodium citrate was determined by liquid scintillation. Three counting solutions were used to determine the activity concentrations of the 1,5-[^{14}C]trisodium citrate. These solutions were prepared using a standard containing 10 µL (37KBq) of 1,5-[^{14}C]trisodium citrate whose volume was made up to 1 mL (stock solution). Five, then and one hundred microliters of the stock solution were added to 20-mL glass vials containing 15 mL of the liquid scintillation cocktail (Bioscint). The activity measurements in the vials were 8491, 14,420 and 139,818 disintegrations per minute (DPM), respectively.

An adaptation of the method published by Turkevich, *et al.* [46] and Frens [47] was used to synthesize sterile radioactive and natural AuNPs. The volumes of the prepared solution of radioactive [^{198}Au]$HAuCl_4$-[^{198}Au]$HAuCl_4$ in 0.05 N HCl and the non-

59

radioactive $HAuCl_4$·$HAuCl_4$ in 0.05 N HCl were diluted to 25 mL using deionized water to make 1 mM solutions. Solutions of hydrogen chloroauric acid were heated to the boiling point with vigorous stirring, and the reducing agents were added to the solutions and boiled under reflux for a further 30 min. For the non-radioactive synthesis, 2.5 mL of 38.8 mM trisodium citrate were used as the reducing agent. For the dual radiolabel synthesis, 2.5 mL (38.8 mM) of solution containing 1,5-[^{14}C]trisodium citrate (1.52 MBq: 600 µL, 1.07×10^{-3} mmol) and non-labeled trisodium citrate (1.9 mL: 9.743×10^{-2} mM) were used as the reducing agent. Figure 4 shows the adapted method used to synthesize dual-radiolabeled [^{14}C]citrate-[^{198}Au]AuNPs.

4.2. Characterization of Dual-Radiolabeled AuNPs

Both the radioactive and non-radioactive AuNPs were characterized using the same techniques to assess the impact of using radioactive precursors in the quality attributes of AuNPs. With the exception of the UV/Vis spectra, the radioactive sample was analyzed after 10 half-lives (27 days), when the radioactivity of the samples was low enough to be safely cleared from Necsa laboratories and analyzed in non-radiological laboratories.

The hydrodynamic size (Z-average size) and polydispersity index (PDI) of the nanoparticles was acquired by dynamic light scattering with a Zetasizer Nano ZS (Malvern Instruments Ltd., Worcestershire, UK) operated in backscattering mode at 173° with a He–Ne laser beam (λ = 632.8 nm). For the zeta potential measurements, which were performed at 25 °C with a scattering angle of 90°, the particles were dispersed in aqueous solution with an average pH of 6.2. The experiment was done in triplicate, and the results were averaged.

The morphology and primary size distributions of AuNPs were determined using transmission electron microscopy (TEM) (FEI Tecnai G2, Eindhoven, The Netherlands). Specimens were prepared by drop casting of a 10-µL aliquot of a dilute NP solution on an Athene® grid (Plano GmbH, Wetzlar, Germany). At least 250 particles were used to determine the primary size distributions using ImageJ software (Version 1.48; National Institutes of Health, Bethesda, MD, USA).

UV/Vis spectra were recorded for both the radioactive and non-radioactive AuNP suspensions using a PerkinElmer LAMBDA 1050 UV/Vis/NIR spectrophotometer (Waltham, MA, USA). The spectra were also used to determine the concentration [48].

Annexure C: Comparison of TUS and creatinine normalization (GC T1)

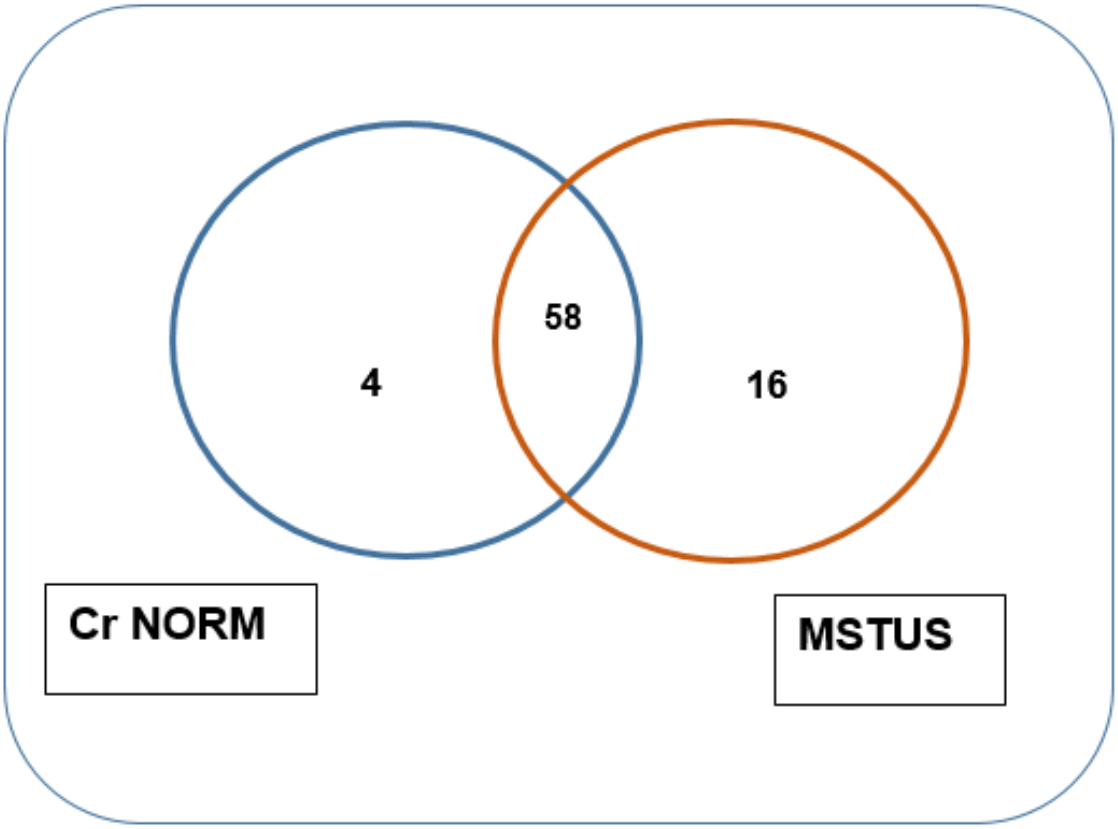

This relationship between MSTUS (Mass Spectrometry Total Useful Signal) and normalisation with creatinine is illustrated by the above Venn Diagram, indicating that regardless of normalisation method, the majority of VIP metabolites remain significant.

Annexure D: ICPLM Newsletter

A newsletter indicating the award received at the 14th International Conference of Paediatric Laboratory Medicine (2017) for a presentation given on partial of the work done herein.

Successful 14th International Congress of Paediatric Laboratory Medicine in Durban, South Africa – Record number of scholarships and merit awards, diverse global representation, novel scientific program, and charity for children

by Sharon M. Geaghan
on behalf of the IFCC Task Force on Paediatric Laboratory Medicine

Aerial view of the Durban, South Africa coastline *(courtesy of Grant Pitcher)*

The IFCC's Task Force on Paediatric Laboratory Medicine organized its 14th successful Congress in Durban, South Africa, proffering new levels of scholarship grants and research awards, while continuing to attract global delegate representation, offer scientific novelty in programming, and provide charity for local children. One of the Task Force Committee's primary goals was to insure the Congress would be accessible, particularly for African colleagues. The Congress received 120 registered participants, and approximately a quarter (of 74 delegates) were African. The delegates represented a diversity of scientific communities around the globe: Algeria, Australia, Bolivia, Canada, France, Germany, Greece, India, Italy, Japan, Lithuania, Netherlands, Nigeria, Norway, Oman, Pakistan, Poland, Qatar, Russian Federation, Saudi Arabia, Singapore, South Africa, Switzerland, Thailand, Turkey, United Arab Emirates, United Kingdom, and the United States.

Choir: The Key of Hope children's choir performed at the Opening Ceremony for the Paediatric Congress in Durban

Article continued on next page

Scholarship grants were key to insuring accessibility, and we are grateful to the Society for the Study of Inborn Errors of Metabolism (SSIEM) for their generous support of 22 educational grants. SSIEM, founded in 1963, aims to foster the study of inherited metabolic disorders. It has over 1400 members and is truly international, with representation from more than 75 countries. A registered charity in the UK, the SSIEM publishes The Journal of Inherited Metabolic Disorders (see ssiem.org).The Society also monitors training in pediatric metabolic medicine on behalf of the European Academy of Paediatrics. Dr. Timothy Lang was instrumental in securing the travel grants, € 500 each, which were allocated to support individuals with interest in inherited metabolic disease. After publicity and recruitment of candidates through calls for applications by the Task Force, the Organizing Committee was able to offer every applicant a grant this year.

IFCC Task Force for Pediatric Laboratory Medicine
L-R (front): Tim Lang, Vijay Grey, Tze Ping Loh, Magdalena Turzyniecka, Sharon Geaghan, Klaus Kohse; *L-R (back):* Martin Hersberg, Tahir Pillay

A larger number of monetary research prizes was a notable feature of this year's Congress, which included Best Poster prize for Corey Markus and team (Singapore, Australia) for *"Derivation of data-driven, outcome-based critical values"*; and second-place finalist Poster prize for Martin Hersberger and team (Switzerland) for *"Development of a LC-MS/MS Method for the Quantification of 16 Steroids in Plasma from Children"*.

Merit awards were also presented for five additional outstanding posters (in alphabetical order): Sibtain Ahmed (Pakistan) for *"Establishment of Reference Intervals of Thyroid Stimulating Hormone in Neonates-An Experience from Pakistan"*, Randa Alratrout (Saudi Arabia) for *"The Frequency of Inherited Metabolic & Endocrine Disorders in the Eastern and North-Western Jawf Provinces of Saudi Arabia: Four Years' Data from the Newborn Screening Department , Ministry of Health, Dammam"*, Marta Camilot (Italy) for *"1st and 99th percentiles of aminoacids and acylcarnitines measured in dried blood spots collected at two and four weeks of life from prematures and/or low birth weight newborns for extended newborn screening"*; Busadee Pratumvit (Thailand) for *"Close Correlation between Arterial and Central Venous Lactate Concentrations of Children in Shock: A Cross-sectional Study"*; and Natalia Simakova (Russian Federation) for *"Reference intervals for reticulocyte parameters of infants during their first year after birth using Sysmex XN-1000 hematology analyzer"*.

Of 52 accepted abstracts, seven were offered oral presentation The Best Oral Presentation prize (for investigators over 40 years of age) was awarded to Chris Vorster (South Africa) for *"Justification for and perceived barriers to the implementation of a newborn screening program for South Africa"*. The Best Oral Presentation prize (for young investigator, up to 40 years of age) was awarded to Sonja Bartlett (Canada) for *"A basic metabolomics investigation of the effect of nanogold based treatment: Potential applications/consequences in inborn errors of metabolism."* In total, monetary prizes were provided to nine winners at the Congress. Veteran judges noted an especially high quality of abstracts and posters for this Congress, combined with excellent oversight by Dr. Tze Ping Loh over the process and prizes.

Scientific programming focused on novel technologies and breaking news topics of paedatric interest, which included four distinguished plenary speakers in the following scientific realms: recent experience

Article continued on next page

SSIEM scholarship recipients gather for the Paediatric Congress

with the Ebola Virus in West Africa (Dr. Janusz Paweska), use of point of care to improve patient care (Dr. Sverre Sandberg), the microbiome in early life (Dr. Michael Surette) and the genetics of calcium metabolism disorders (Dr. Rajesh Thakker). Additionally, nine symposia featuring 32 speakers were offered in the general paediatric interest areas of newborn screening; endocrinology; panel discussion of critical values; reference intervals; next generation sequencing; nutrition and immunology; bone metabolism; select oral platform presentations; and general pediatric laboratory testing.

An initiative of this Congress's Organizing Committee was to identify an opportunity for charitable sponsorship to a local community of children, in keeping with the paediatric mission of the Task Force. Accordingly, Drs. Tahir Pillay and Sharon Geaghan arranged the opening ceremony to be graced by the Key of Hope Choir, a group of young girls and boys whose voices and joyful energy welcomed attendees and made spirits soar. In return for this gift, the Task Force donated to this meritorious organization, which helps children that have been orphaned by or otherwise affected by HIV and AIDS in South Africa. Specifically, over 1200 children are visited in their home every week, over 200 children are sent to school every year, and more than 300 children's rights cases are advocated for annually by this organization. For others who may wish to make their visit to South Africa into a lasting relationship, and might be interested in supporting a Durban-based fountain of goodwill and hope, please visit its website: https://keyofhope.org/.

Financial support for the Congress, a satellite meeting presented in advance of the IFCC WorldLab on a triennial basis, was independently recruited by the TF-PLM Committee members. The efforts once again resulted in excellent funding, and our gratitude extends to Platinum level sponsor, Alexion Pharmaceuticals; six Gold level sponsors (in alphabetical order): American Association of Clinical Chemistry (AACC), Roche Diagnostics, Canadian Society of Clinical Chemists (CSCC), Deutscheland Gesellschaft für Klinische Chemie und Laboratoriumsmedizin/German Society for Clinical Chemistry (DGKL), the Society for the Study of Inborn Errors of Metabolism (SSIEM), and the Swiss Society of Clinical Chemistry (SSCC); and Bronze level sponsor, Sarstedt. Additional sponsorships included the Royal College of

SSIEM scholarship recipients network during the Paediatric Congress

Article continued on next page

Pathologists (RCP), South African Medical Research Council (SAMRC) and the Federation of South African Societies of Pathology (FSASP).

Committee members include Chair, Michael Metz (AU) and Vice-Chair Timothy Lang (UK); Immediate Past-Chair Vijay Grey (CA); Past Past Chair Klaus Kohse (DE); and (in alphabetical order): Sharon Geaghan (USA); Martin Hersberger (CH); Patti Jones (USA); Tze Ping Loh (SG); Magdalena Turzyniecka (ZA) and Tahir Pillay (ZA).

For the magnificent programme design (Dr. Magdalena Turzyniecka) and core leadership for the Durban Symposium, the trio of Drs. Michael Metz, Tahir Pillay and Magdalena Turzyniecka are heartily thanked.

The 14th Congress met the longstanding mission statement of the IFCC Task Force on Paediatric Laboratory Medicine: *improving the diagnosis and management of patients from birth to adolescence*. Looking ahead three years to 2020, the TF-PLM will continue its mission in Seoul, South Korea.

14TH INTERNATIONAL CONGRESS OF PAEDIATRIC LABORATORY MEDICINE: TESTIMONIALS RECEIVED FROM SEVERAL AWARDEES *(excerpts)*

+++++

To have a conference of this magnitude in my own country was already an inspiration to me...The lectures were topical, vast and interesting and the presenters made an extra effort to engage and discuss which was refreshing. The intimate setting allowed for networking & open discussion outside the plenaries. In a short space of time a lot of ground was covered and it was interesting to see how far other countries have progressed ....I am grateful for the SSIEM travel bursary which has allowed me the opportunity to broaden my horizon and look to the future especially for my country & its health amongst our most vulnerable population. (Ashandree Reddy-ZA)

+++++

The XIV International Congress of Paediatric Laboratory Medicine (ICPLM) was a great experience and I am truly grateful for the SSIEM travel scholarship that made it possible for me to attend the conference .I have gained insights to improve laboratory service especially in children in my hospital and my country. I returned from the conference with a great deal of inspiration, enthusiasm and ideas to apply with pediatric laboratory service and expand my knowledge to laboratory professional personnel in the country. Thank you very much to give this great opportunity. (Best regards, Busadee Pratumvinit, MD-THAILAND)

+++++

Thank you again for this incredible opportunity to attend an international conference in paediatric laboratory medicine, specifically focused on inborn errors of metabolism, for which I have a particular passion. ....I thoroughly enjoyed all of the sessions at the ICPLM conference, as well as the opportunity to catch up with distant colleagues and to meet and interrogate the great minds in this field. The smaller numbers attending the conference meant that these individuals were more accessible to those of us that are junior and who would normally not have an opportunity to come close to them, let alone to sit at lunch with them! The conference was superbly organized, with all sessions running smoothly and to time. I thank you again for a most valuable experience. (Kind regards, Justine Cole-ZA)

+++++

...The congress had a lively opening ceremony where the Key of Hope children's choir entertained us with enthusiastic renditions of popular local songs. The children's smiling faces set the tone for the academic programme leaving delegates also smiling and satisfied with the intellectual content of the congress ...There was a small group of attendees which allowed registrars and other trainees greater opportunity to network more meaningfully with all categories of laboratory staff including consultants and experts in their fields. I wish to thank the organizers for a highly enjoyable programme, for reducing the registration fee for African delegates and SSIEM for granting me a travel grant despite being an older delegate. (Jocelyn Naicker-ZA)

+++++

I was the fortunate recipient of a travel scholarship from SSIEM....I would also like to take the opportunity to thank the Organising Committee for recruiting these world class speakers for the Congress....I was welcomed to an emotional opening ceremony, with an uplifting performance from the children's choir, Key of Hope. Key of Hope provides long term mentoring, allowing children to thrive as citizen's and potential leaders, to combat the future challenges Africa faces. We were then provided with stark evidence of the

tragic reality of life in Africa and risks healthcare workers face (both local and foreign), with Prof. Janusz Paweska opening plenary lecture discussing the ecological and epidemiological aspects of the recent Ebola outbreak in west Africa from 2013 to 2015...the work done by Prof. Janusz Paweska team gives hope to rapid and effective control of future viral outbreaks....I would like to thank the SSIEM for funding 22 travel scholarships, the largest number of scholarships awarded in the history of the ICPLM, of which I was fortunate enough to be granted one. I have retuned back Australia having made many wonderful new friends and fostering new collaborative partnerships into the future. (Corey Markus-AU)

+++++

How can you explain traceability in laboratory medicine to your clinician users?

by Graham Beastall
on behalf of the Joint Committee for Traceability in Laboratory Medicine

JCTLM
Accurate results for patient care

How can you explain traceability in laboratory medicine to your clinician users?

A recent article by Graham Jones in his local hospital journal provides one approach to answer this question.

Clinicians who use laboratory medicine services take it for granted that the laboratory provides 'the right result'. They believe that the result they get back from their laboratory is both accurate and capable of comparison with results obtained from other laboratories or retrieved from the medical/scientific literature. It comes as a shock to most clinicians to learn that for many results they receive there is significant between-method variability. In some cases, the variability may be such that clinical outcomes and even patient safety may be compromised if they compare the results that they get from their local laboratory with literature or clinical practice guideline results that were obtained using a different method.

Traceability in laboratory medicine (TLM) is the key to reducing between-method variability. IFCC is a founder member of the Joint Committee for Traceability in Laboratory Medicine (JCTLM), which "supports worldwide comparability, reliability and equivalence of measurement results in laboratory medicine, for the purpose of improving health care and facilitating national and international trade in *in vitro* diagnostic devices".

The website www.jctlm.org provides freely available resources to help laboratory medicine specialists to understand TLM and to train others to appreciate its importance. These resources take the form of webinars, PowerPoint presentations, symposia at scientific meetings and publications.

As part of the support provided to its users the clinical laboratory has a responsibility to alert clinicians to between-method variability and the pitfalls that could arise. At the same time clinicians can be reassured that there is a global effort to reduce the problem to make results more comparable. The article by Graham Jones from St Vincent's Hospital in Sydney, Australia provides an excellent template for communication with clinician users. Entitled 'Chemical Pathology – Getting the Right Answer' the article is written in non-technical language using examples that may be understood by clinicians and other healthcare professionals. Key references are included.

The article is published in the St Vincent's Clinic, Proceedings (Sydney) Volume 25, 1 December 2017. It may be downloaded here. The article may be reproduced or modified for local use as long as an acknowledgement is provided to the original publication. The article provides you with an opportunity to educate and support your clinical users.